



AALBORG UNIVERSITY  
DENMARK



REGION NORDJYLLAND

# Characterization of hypoxia- induced proteome changes & exosomes bystander effect in H69 small-cell lung cancer cells

Master in Medicine with Industrial Specialisation in Translational Medicine

Aalborg University and Aalborg University Hospital

---

Jorge Medina Fernández

MSc Programme: Medicine with Industrial Specialization in Translational  
Medicine

MSc Thesis title: Characterization of hypoxia-induced proteome changes &  
exosomes bystander effect in H69 small-cell lung cancer cells

MSc Thesis period  
19<sup>th</sup> of September of 2017 – 31<sup>st</sup> of May of 2018

Group  
9036

Thesis type  
Long MSc Thesis (2 Semesters)

Author  
Jorge Medina Fernández (Study Number: 20161060)

Main Supervisor  
Shona Pedersen, Associate professor, PhD

Co-supervisors  
Anders Askeland, PhD  
Jonas Ellegaard, PhD

Pages and words  
60 in total (25,259 words)/ 49 pages without appendixes

Appendix  
15 pages. From Appendix A to E

## Preface and Acknowledgements

This Master Thesis was made as a completion of the Master education in Medicine with industrial Specialisation in Translational Medicine. This master thesis has been elaborated under the supervision of Associate Professor, PhD, Shona Pedersen at the Department of Clinical Biochemistry, Aalborg University Hospital. I was engaged in researching and writing this Thesis from 28<sup>th</sup> of September 2017 to 31<sup>st</sup> of May 2018.

Several persons have contributed to this master thesis in different ways. I would therefore firstly like to thank my head supervisor Shona Pedersen and co-supervisors Anders Askeland and Jonas Ellegaard for their time, valuable input and support throughout the entire master period. Secondly, I would like to thank Ole Østergaard for performing the mass spectrometry analysis. And finally, I would like to thank my family and friends for their support and unconditional love throughout these two years studying at Aalborg University.

Aalborg University

May 2018

---

Jorge Medina Fernández

## Abstract

**Background:** small-cell lung cancer (SCLC) is a type of tumour which suffers from poor patient prognosis due to its aggressive and chemo-resistant profile. Therapeutic clinical advances during the last four-decades are almost non-existent. Previous research has found that hypoxia may play an essential role in this cancer, however, further research is required to understand its significance. Therefore, study of the implications of hypoxia in SCLC sound imperative. Additionally, extracellular vesicles (EVs), fundamental mediators in cancer communication has been placed in the spotlight due to its reprogramming abilities over other cells. We concluded that study of the effects induced by hypoxia together with the interplay orchestrated by EVs in SCLC is essential to further understand this complex disease. As a result, future innovative perspectives into research might bring further clinical outcomes to improve the lives of SCLC patients.

**Methods:** two separate experiments were conducted in this MSc Thesis. The hypoxia experiment, in which the cells were exposed to different oxygen conditions during 24h. Obtention of the EVs and the cell lysates was performed. Later, the exosomes generated from the hypoxia experiment were co-cultured with cells under normoxic conditions for 48h in what is addressed as the co-culture experiment. In this experiment analysis of the cell lysates was carried out. We used Nano-tracking analysis (NTA) for EVs characterization and tandem mass spectrometry (MS/MS) for analysis of all samples.

**Results:** regarding the hypoxia experiment we could observe an up-regulation of the metabolic profile of SCLC cells and an increased exosome production when hypoxic conditions take place. Furthermore, GPI and P4HA1 protein up-regulation were found. The hypoxic-EVs contained pro-carcinogenic proteins driving angiogenesis, metastasis, cell proliferation and motility, as well as, over-expression of specific pro-carcinogenic proteins like the ephrin receptor (EPH) and the high-mobility group protein A1 (HMGA1) when compared with normoxic-EVs. The hypoxic-exosomes bystander effect resulted in SCLC cell reprogramming towards an enhanced pro-carcinogenic phenotype including a decrease in apoptosis and programmed cell death, up-regulation of cell growth, proliferation and survival of cells, as well as, hypermethylation of the CpG islands and DDX6 over-expression.

**Conclusion:** hypoxia induces carcinogenesis and tumour progression in SCLC cells by direct effect when present in hypoxic tumours. Furthermore, hypoxia alters cell communication ability through EVs. And indirectly, hypoxia affects other SCLC cells through hypoxic-originated exosomes which carry the potential of inducing a pro-carcinogenic bystander effect.

**Key terms:** SCLC, hypoxia, extracellular vesicles, proteomics, reprogramming, in vitro

## Abbreviations

ABs - Apoptotic bodies	GOMF – Gene-ontology molecular function
ALIX - Programmed cell death 6-interacting protein	GPI - Glucose-6-phosphate isomerase
ANOVA - Analysis of variance	GSEA - Gene set enrichment analysis
ATP - Adenosine triphosphate	HCMDDB – The human cancer metastasis database
BCA - Bicinchoninic acid assay	HIF - Hypoxia-inducible factor
DDX6 - Probable ATP-dependent RNA helicase DDX6	HMGA1 - high mobility group AT-hook 1
DNA - Deoxyribonucleic acid	HRP - Horseradish peroxidase
DYNLL - Dynein light chain protein (DYNLL)	ILVs - Intraluminal vesicles
ECM – Extracellular matrix.	KEGG – Kyoto Encyclopedia of Genes and Genomes
ED-SCLC - Extensive-stage disease	LC – Liquid chromatography
EMT - Epithelial-mesenchymal transition.	LDH - Lactate dehydrogenase
EPH - Ephrin receptor proteins (EPH)	LD-SCLC - Limited-stage disease
ESCRT - Endosomal sorting complexes required for transport	LOX - Lysyl Oxidase.
EVs – Extracellular Vesicles.	MEA – Modular enrichment analysis
FBS – Fetal bovine serum	MMPs – Matrix metalloproteinases.
FDR – False discovery ratio	MS – Mass spectrometry
GO – Gene-ontology	MVBs – Multivesicular bodies.
GOBP – Gene-ontology biological processes	MVs – Microvesicles.
GOCC – Gene-ontology cellular components	NAD - Nicotinamide adenine dinucleotide
	NRAP – Nebulin-related-anchoring protein

NSCLC - Non-small cell lung cancer

NTA - Nanoparticle tracking analysis

P4HA1 - Prolyl 4-Hydroxylase Subunit  $\alpha$ -1

PBS - Phosphate-Buffered Saline

PCA - Principal component analysis

PM – Plasma membrane.

PMN - Pre-metastatic niche

PPI - Protein-protein interaction (PPI)

PSMD14 - 26S proteasome non-ATPase  
regulatory subunit 14 or Rpn11

RNA - Ribonucleic acid.

ROS - Reactive oxygen species.

SCLC - Small-cell lung cancer

SDS-PAGE - Sodium dodecyl sulfate-  
polyacrylamide gel electrophoresis

SEA - Singular enrichment analysis

TSG101 – Tumour susceptibility gene 101

UPS - Ubiquitin-Proteasome System

VEGF – Vascular endothelial growth factor.

VEGF(R) – Vascular endothelial growth  
factor (receptor)

VHL - Von Hippel-Lindau protein

WB – Western blot

## Table of Contents

Title page.....	i
Preface and Acknowledgements.....	ii
Abstract .....	iii
Abbreviations .....	iv
Table of Contents .....	1
1. Background.....	3
1.1. Small cell lung cancer .....	3
1.2. Hypoxia and cancer .....	3
1.2.1. Influence of hypoxia on chemotherapy .....	5
1.2.2. HIF-1 in small cell lung cancer .....	5
1.3. Extracellular vesicles .....	8
1.3.1. Biogenesis.....	8
1.3.2. Extracellular vesicles composition and cargo.....	9
1.3.3. Extracellular vesicles functions and utilities.....	10
1.3.4. Extracellular vesicles isolation methods and current limitations .....	10
1.3.5. Extracellular vesicles in cancer .....	11
1.3.6. Hypoxic extracellular vesicles in cancer .....	12
1.4. Proteomics .....	13
1.4.1. Proteomics, cancer and extracellular vesicles .....	14
2. Aim .....	15
3. Materials and methods .....	16
3.1. Pre-project: exosome isolation from plasma samples .....	16
3.2. Experimental design .....	16
3.2.1. Hypoxia experiment .....	16
3.2.2. Co-culture experiment .....	17
3.3. Procedures .....	18
3.3.1. Pre-analytical preparation.....	18
3.3.2. Cell culture .....	18
3.3.3. Cell isolation and lysis.....	19
3.3.4. Isolation of microvesicles and exosomes .....	19
3.3.5. Determination of particle concentration and size .....	20
3.3.6. Determination of protein concentration .....	20
3.3.7. Detection of CD9 and HIF-1 $\alpha$ proteins .....	21

3.3.8.	Sample preparation and protein discovery by LC-MS/MS analysis .....	22
3.4.	Statistical analysis.....	23
3.4.1.	General statistical analysis .....	23
3.4.2.	Proteomics data analysis.....	23
4.	Results .....	26
4.1.	Confirmation of extracellular vesicles isolation .....	26
4.2.	Hypoxia drives changes in extracellular vesicles.....	27
4.2.1.	Hypoxia and HIF-1 $\alpha$ content in extracellular vesicles .....	27
4.2.2.	Extracellular vesicles release is affected by hypoxic conditions .....	27
4.2.3.	Hypoxia drives changes in the extracellular vesicle protein composition .....	28
4.2.4.	Hypoxia drives protein profiles of microvesicles and exosomes .....	29
4.2.5.	Hypoxia drives microvesicles and exosomes proteome composition .....	30
4.3.	Cell lysate results.....	33
4.3.1.	Detection of HIF-1 $\alpha$ in cell lysate .....	33
4.3.2.	Effect of hypoxia on cells proteome expression .....	33
4.3.3.	Proteome composition of h-69 cancer cells cultured under different oxygenation conditions.....	34
4.4.	Co-culture experiment results .....	37
4.4.1.	Exosomes originated under hypoxic conditions induce proteome shift of SCLC cells when co-cultured .....	37
4.4.2.	Exosomes originated under hypoxic conditions induce changes in the proteome composition of SCLC cells when co-cultured .....	38
5.	DISCUSSION .....	42
5.1.	Hypoxia induces metabolic reprogramming increasing pro-carcinogenic pathways .....	42
5.2.	Cells under hypoxia shift their EV-packing and release modifying its communication and reprogramming abilities.....	44
5.3.	Hypoxic exosomes have an enhanced pro-carcinogenic bystander effect.....	45
5.4.	Study limitations.....	47
6.	Conclusion .....	48
7.	Future directions .....	49
8.	Bibliography .....	50



## 1. Background

### 1.1. Small cell lung cancer

Cancer accounts for 8.2 million deaths worldwide. Lung cancer alone accounts for 27% of the cancer-related deaths, making it the leading cause of cancer deaths worldwide <sup>1</sup> (Figure 1A).

Lung cancer can be divided into two major types including non-small cell lung cancer (NSCLC) and small-cell lung cancer (SCLC). SCLC being the most aggressive <sup>2</sup>. SCLC is divided into two stages; limited-stage disease (LD-SCLC, in which tumour has not metastasised yet) and extensive-stage disease (ED-SCLC, in which the tumour has metastasised to adjacent and distant tissues) <sup>3</sup>. Of all new lung cancer cases, SCLC accounts for 15 - 20% of them <sup>4</sup>. At the time of diagnosis, 70% of the patients are diagnosed as ED-SCLC, due to an aggressive fast-growing tumour progression and an early and intrusive metastatic dissemination <sup>5-7</sup>. SCLC has a poor survival rate when compared with any of the other primary lung cancers with a total survival below 2% <sup>8,9</sup> and a 20% and 7% at 1 and 5-year survival, respectively <sup>10-12</sup> (Figure 1B). SCLC results in approximately 250,000 deaths every year <sup>13</sup>.

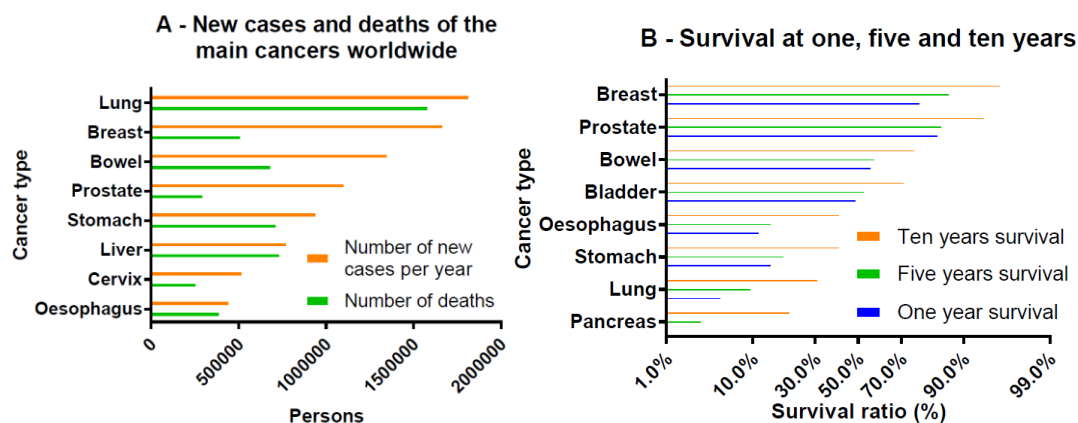


Figure 1. (A) Number of new cases and number of deaths of the main cancers worldwide (GLOBOCAN 2012) <sup>14</sup>. (B) Survival at one, five and ten years after first diagnose of cancers with the highest incidence and worse prognosis (2010 – 2011 England and Wales) <sup>15</sup>.

Current standard therapy for SCLC is a combination of cytotoxic drugs (cisplatin or carboplatin combined with etoposide) <sup>16</sup>. However, it has been found that SCLC cells can develop an enhanced DNA repair mechanism, impairing the effect of this treatment <sup>17,18</sup> and leading to chemo-resistance. Resistance to chemotherapy during treatment and the high incidence of relapse results in a fatal prognosis <sup>19</sup> of the patients with SCLC. One common feature of SCLC is its hypoxic core, which mediates in the recalcitrant issue of chemo-resistance, relapse and in the onset of a highly aggressive phenotype, causing SCLC to be one of the most lethal cancers worldwide <sup>20-22</sup>.

### 1.2. Hypoxia and cancer

A common factor of most tumours, and highly accentuated in SCLC, is hypoxia. Hypoxia is defined as a low level of oxygen. Hypoxic condition in tumours ranges between 1-2% oxygen compared to normoxic or *physoxic* conditions (physiological oxygenation levels in tissues) which are around 4-10% (e.g., lung 5,6%). Hypoxia normally occurs because of the accelerated proliferation and growth of the tumour, thus, increasing the oxygen demands by the cancer cells and therefore exceeding the available oxygen supply. This has consequences at many cellular

and molecular levels. For example, hypoxia activates many intracellular signalling pathways, the most notorious of which is the hypoxia-inducible factor (HIF) pathway. The HIF-1 pathway is implicated in the regulation of oxygen delivery and consumption. HIFs is a family of heterodimeric transcriptional regulators and includes HIF-1, 2 and 3. HIF-1 is formed by an oxygen-regulated  $\alpha$ -subunit and an oxygen-independently regulated  $\beta$ -subunit.

HIF-1 is a major transcription factor mediating the adaptation of cells to hypoxic environments, playing an essential role in physiological processes, and deeply implicated in cancer. Under normoxic conditions, HIF-1 is degraded, however, in hypoxia, accumulation of HIF-1 occurs. This leads to a series of pathway activations resulting in an enhanced and more aggressive carcinogenic phenotype (enhanced metastatic, angiogenic, invasive and proliferative potentials).

Degradation of HIF-1 takes place when the HIF-1 $\alpha$  subunit is hydroxylated by oxygen-dependent enzymes (prolyl hydroxylase domain protein 2 and Factor inhibiting HIF-1). After this, von Hippel-Lindau protein (VHL) binds to HIF-1 $\alpha$ -OH, causing ubiquitination and protein degradation by the proteasome<sup>23</sup> (Figure 2A). However, when there is lack of oxygen, the degradation of HIF-1 $\alpha$  is inhibited and as a result, accumulation of HIF-1 $\alpha$  takes place. If accumulation occurs, HIF-1 $\alpha$  translocates to the nucleus and dimerize with HIF-1 $\beta$  (Figure 2B). Hereafter, the dimer binds to the DNA and initiate gene transcription of molecules involved in carcinogenic pathways such as cancer progression and chemo-resistance (Figure 2B)<sup>24</sup>.

There are additional stimulus enhancing the production of HIF-1 in a hypoxia-independent way and consequently aggravating the cancer state<sup>25,26</sup>. This stimulus are common enhanced pathways in cancer (like nuclear factor kappa-light-chain-enhancer of activated B cells (NF- $\kappa$ B), phosphatidylinositol-4,5-bisphosphate 3-kinase, Protein kinase B, Mammalian target of rapamycin and mitogen-activated protein kinases). This stimulus increases the production of HIF-1 through overexpression of HIF-1 gene (Figure 2).

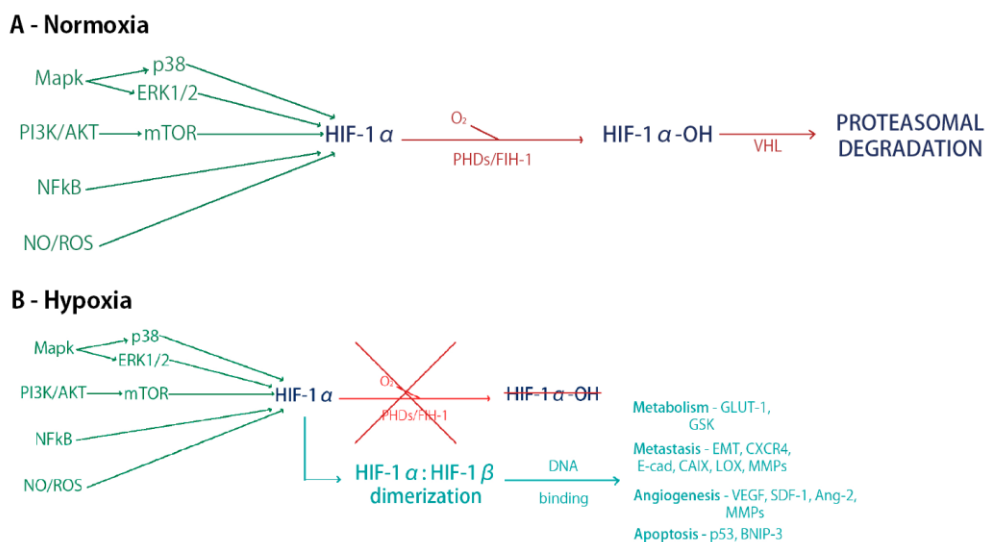


Figure 2. (A) Normoxic conditions lead to proteasomal degradation of HIF-1 by hydroxylation of the HIF-1 $\alpha$  subunit, binding of the VHL protein, and ultimately ubiquitination and degradation of HIF-1 $\alpha$  subunit. (B) In hypoxic conditions, the degradation of HIF-1 $\alpha$  subunit is inhibited and therefore dimerization with the HIF-1 $\beta$  subunit occurs leading to transcription of genes involved in carcinogenic pathways including metabolism, metastasis, angiogenesis and apoptosis<sup>26</sup>. PHD2 - Prolyl hydroxylase domain protein 2. FIH-1 - Factor inhibiting HIF-1. VHL - Von Hippel-Lindau protein (VHL). MAPK - Mitogen-activated protein kinases. p38 - Protein 38. PI3K/AKT - Phosphatidylinositol-4,5-

bisphosphate 3-kinase/ Protein kinase B. mTOR - Mammalian target of rapamycin. NF- $\kappa$ B - Nuclear factor kappa-light-chain-enhancer of activated B cells. NO/ROS – Nitric oxide/Reactive oxygen species. GLUT-1 - Glucose transporter 1. GSK - Glycogen synthase kinase. EMT - Epithelial-mesenchymal transition. CXCR4 - C-X-C chemokine receptor type 4. E-cad - Epithelial cadherin. CAIX - Carbonic anhydrase 9. LOX - Lysyl Oxidase. MMPs - Matrix metalloproteinases. VEGF – Vascular endothelial growth factor. SDF-1 - Stromal cell-derived factor 1. Ang-2 – Angiopoietin 2. p53 – Protein 53. BNIP-3 - BCL2/adenovirus E1B 19 kDa protein-interacting protein 3.

### 1.2.1. Influence of hypoxia on chemotherapy

Hypoxia-induced chemotherapy resistance has been known for several decades. Chemo-resistance to doxorubicin, etoposide, melphalan, doxorubicin, cisplatin, gemcitabine, docetaxel, etc. has previously been reported in many different tumour cell types due to hypoxia<sup>27–29</sup>.

Hypoxic tumours like SCLC shows a lack of drug bioavailability due to an impaired angiogenesis and the blockade of the necrotic tissue around the solid tumour. This blockage functions as a barrier and results in a reduced delivery of the cancer drug<sup>30</sup> (Figure 3). Also, inhibition of cell-death induced signals by hypoxia contributes to chemo-resistance.

Furthermore, hypoxia also induces cell differentiation known as epithelial-mesenchymal transition (EMT) in which, SCLC tumour cells, acquire an enhanced motility and plasticity<sup>31</sup>. It is fundamental to highlight the role that HIF-1 has in the adaptation of the cells to hypoxic environments and how this contributes to the chemo-resistance in lung cancer<sup>32,33</sup>. For instance, in 3 independent meta-analyses, HIF-1 overexpression decreased the overall survival of NSCLC patients<sup>34–36</sup>, establishing a link between HIF-1 overexpression with poor survival and chemoresistance in lung cancer. HIF-1 is not only involved in chemo-resistance, it also enhances and promotes many other carcinogenic phenotypes of SCLC cells<sup>37</sup>.

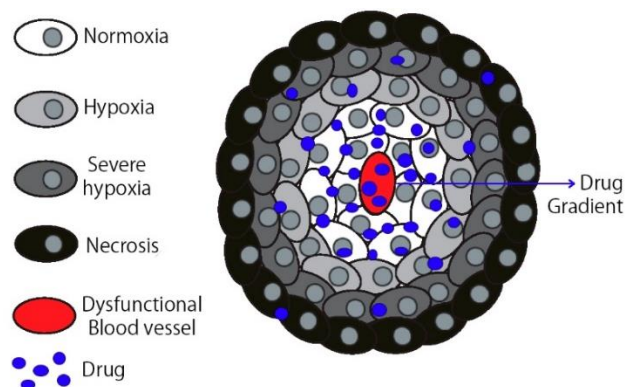


Figure 3. In hypoxia, the oxygen demand by SCLC cells is increased, therefore, enhancing tumorigenic properties which HIF-1 mediates. This figure is a representation of a dysfunctional blood vessel and the surrounding SCLC microenvironment of cells and the necrotic barrier. This barrier blocks the immune system, decreases drug effectivity by sealing the diffusion path the drug needs to reach the cancer, and isolates the cancer, facilitating cancer extravasation and metastasis.

### 1.2.2. HIF-1 in small cell lung cancer

Overexpression of HIF-1 has been found in a variety of cancers<sup>38,39</sup>. Cancers with higher hypoxic levels denoted a higher expression of HIF-1 and therefore an enhanced malignancy, including SCLC<sup>37,39–41</sup>. HIF-1 is implicated in many fundamental carcinogenic processes in SCLC including

angiogenesis via vascular endothelial growth factor (VEGF) <sup>42</sup>, metabolic reprogramming <sup>43</sup>, invasion <sup>43</sup>, metastasis <sup>25,44</sup> and in resistance to chemotherapy <sup>45</sup>.

One important feature in SCLC is an enhanced hypoxic microenvironment and characteristic hypoxic core. Therefore, accumulation of HIF-1 is greatly enhanced, which prompts the transcription of many genes that leads towards a more aggressive phenotype. One plausible reason of why SCLC is so aggressive, metastatic, invasive and prone to develop chemo-resistance may be its angiogenic potential. In SCLC, angiogenesis takes place through the transcription of VEGF gene which increases oxygen delivery by stimulating angiogenesis <sup>42</sup>. SCLC cells are known to proliferate in an uncontrolled way and the blood vessels formed are normally dysfunctional and unstructured. The aberrant vascularization leads to a vicious cycle of severe hypoxia and overproduction of HIF-1. This feedback-loop orchestrate the drive towards a highly aggressive carcinogenic phenotype in SCLC.

The aberrant vascularization in SCLC can also aid in progression and metastasis by helping the cancer cells to extravasate, migrate and invade other tissues<sup>46</sup>. In addition, HIF-1 modifies cell adhesion and motility through the transcription of genes encoding proteases that degrades (i.e., metalloproteinases - MMPs) <sup>47,48</sup> and remodels (i.e., lysyl oxidase - LOX) <sup>49</sup> the extracellular matrix (ECM) at the tumour site and at distant sites in order to facilitate further invasion of the tissue and metastasis <sup>50</sup> (Figure 4 and 5). Patients with higher expression of MMP-9 have a worse 5-year survival and therefore a bad prognosis <sup>48</sup>. This is why highly hypoxic tumours like SCLC are known to have a very aggressive profile with a highly metastatic and invasive potential resulting in a poor overall survival of the patients <sup>26,51</sup>.

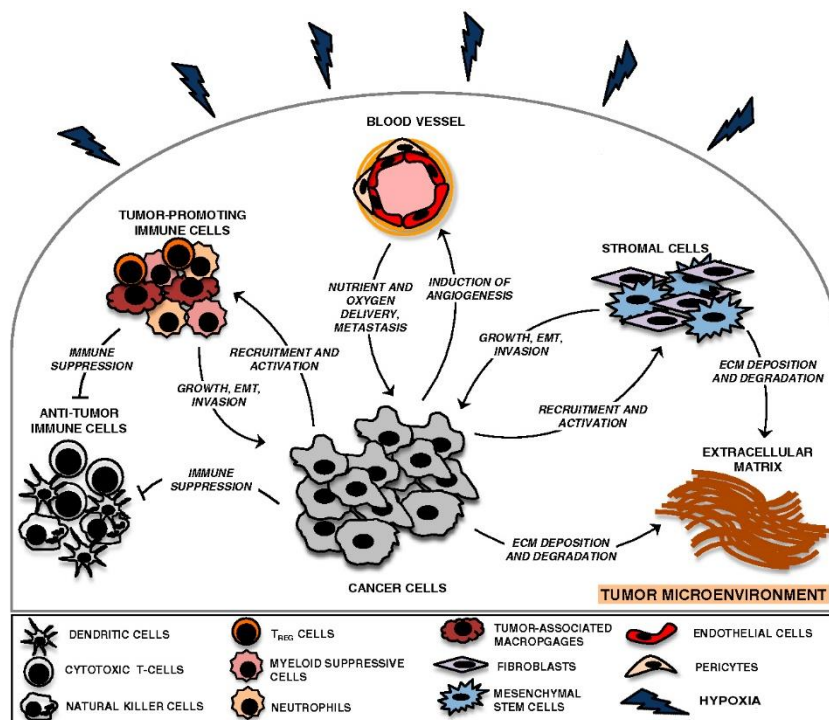


Figure 4. External stress conditions like hypoxia are known to be modulators in many pathways during cancer progression. In this figure, an illustration of the cross-talk between cancer cells and their tumour microenvironment under hypoxic conditions is displayed. Tumour cells mould their microenvironment to satisfy their own needs by

different communication pathways such as direct cell-to-cell contact, growth factors and extracellular vesicles (EVs). Tumour cells mediate suppression of anti-tumour cells, induction of angiogenesis, remodelling of the ECM and recruitment of other tumour promoting cells. In return, a favourable microenvironment for tumour progression and dissemination is set<sup>52</sup>.  $T_{REG}$  – Regulatory T-cells.

HIF-1 also plays a fundamental role in cell proliferation and cell survival of the cancer cells through growth factors that are regulated by HIF genes i.e., transforming growth factor alpha<sup>53</sup>, VEGF<sup>54</sup>, adrenomedullin<sup>55</sup> and erythropoietin<sup>56</sup>. This enhanced cell proliferation requires an increased consumption of energy, and thus, an augmented need for glucose. HIF-1 can induce metabolic reprogramming by upregulating glucose transporter genes (i.e., glucose transporter 1 and 3<sup>57</sup> and glycolytic enzyme (Figure 5). This promotes cell survival by blocking cell death, therefore avoiding apoptosis<sup>58</sup>.

Overall, HIF-1 mediates in a wide range of processes in cancer progression. The role of HIF-1 has been investigated, however, more detailed and comprehensive studies need to be carried out to fully understand the correlation between cancer, hypoxia and how HIF-1 mediates in these complex pathological responses. Proteins are fundamental mediators in all the previously described carcinogenic pathways. Understanding of the complete set of proteins of a cell in a specific moment of time (proteome) can be essential to comprehend pathological pathways and changes in the cellular phenotype. A shift in the proteome of SCLC cells can be the driving force behind these complex pathological responses that these cells portray under hypoxic conditions<sup>59</sup>. In addition, during the last decade, extracellular vesicles (EVs), a novel player in cancer has started to show its potential and their implication in many carcinogenic pathways. EV-secretion is known to be augmented in cancer and also during hypoxia<sup>60,61</sup>. Furthermore, there has been an increased interest towards EVs in the last years due to their ability to induce cell reprogramming in the recipient cells<sup>62–64</sup>. EV-research and their combination with modern high-throughput techniques like proteomics might reveal mechanisms and pathological pathways during cancer development and the link with hypoxia. As a result, this might unravel new therapeutic strategies in the incoming years, increasing the lifespan of patients.

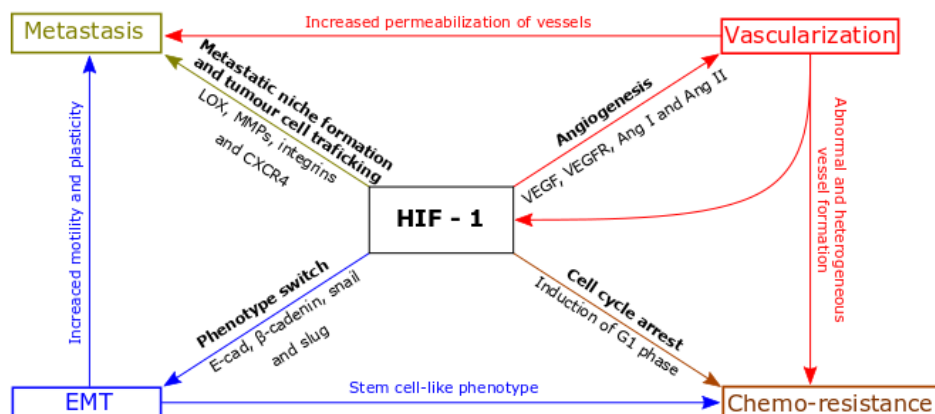


Figure 5. Hypoxia is the power driving tumour progression and metastasis. Hypoxia stimulates angiogenesis through VEGF, Ang-1 and Ang-2. LOX facilitates cancer cells to leave the primary tumour site, as well as MMPs, CXCR4 and integrins. SCLC cells also undergo epithelial-mesenchymal transition (EMT) acquiring increased motility properties and therefore decreasing the expression of adhesion molecules. This all results in enhancement of chemoresistance and metastatic potential of the cancerous cells<sup>26</sup>. LOX – Lysyl Oxidase. MMP – metalloproteinases. CXCR4 – Chemokine receptor type 4. VEGF(R) – Vascular endothelial growth factor (receptor). Ang – Angiotensin. E-cad – Epithelial-cadherin.

### 1.3. Extracellular vesicles

EVs are small lipid-bilayer membrane-enclosed sacs that originate in the cells and play a major role in intercellular communication<sup>65,66</sup>. These vehicles carry a rich cargo of DNA, ribonucleic acid (RNA), proteins, lipids and metabolites; resembling the parental cell of origin<sup>67,68</sup>. They are released into the extracellular space in physiological and pathological conditions<sup>69,70</sup>. EVs can be divided into 3 sub-types: exosomes, microvesicles (MVs) and apoptotic bodies (ABs) (Figure 6 and Table 1). The term EVs will be used throughout this MSc thesis to include exosomes and MVs as there is no gold standard to achieve a complete isolation of these two subpopulations. The size, biogenesis, cargo and densities of EVs are different. Exosomes are the smallest in size (30 – 150 nm), followed by MVs (50 – 2,000 nm) and ABs (50 – 5,000 nm)(Table 1)<sup>71</sup>.

*Table 1. Comparison of exosomes, microvesicles and apoptotic bodies physical properties, biogenesis origin and suggested markers for its isolation and characterization. MVBs – Multivesicular bodies. PM – Plasma membrane. HSP70 – Heat-shock protein 70. ARF6 - ADP-ribosylation factor 6. ALIX - Programmed cell death 6-interacting protein. TSG101 – Tumour susceptibility gene 101 protein. CD40 - Cluster of differentiation 40.*

	Exosomes	Microvesicles	Apoptotic bodies
<b>Intracellular origin</b>	MVBs	PM	PM
<b>Size</b>	30 – 150 nm	50 – 1,000 nm	50 – 5,000 nm
<b>Suggested markers</b>	ALIX, TSG101, tetraspanins, HSP70	ARF6, CD40, selectin, integrin	DNA and histones
<b>Density</b>	1.13 – 1.19 g/cm <sup>3</sup>	Unknown	1.16 – 1.28 g/cm <sup>3</sup>
<b>Composition</b>	RNA, DNA, proteins, lipids	Exosome-like.	Nuclear fractions and cell organelles

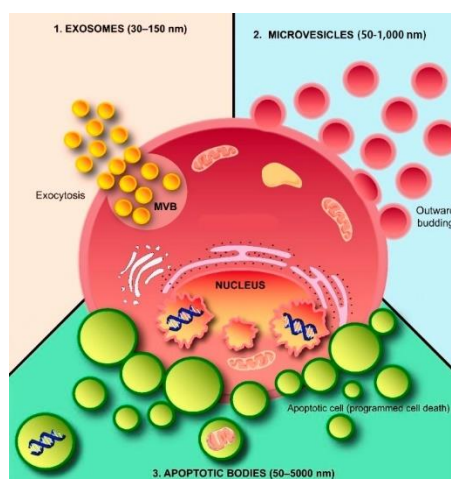


*Figure 6. Exosomes are produced within multi-vesicular bodies (MVB), have a size of 30 - 150 nm and are released by exocytosis. Microvesicles are produced by outward budding of the plasma membrane (PM) and have a size ranging from 50 – 2,000 nm. Lastly, apoptotic bodies are generated as sacks containing cell products during its programmed cell death (apoptosis) and have a size of 50 – 5,000 nm<sup>71</sup>.*

#### 1.3.1. Biogenesis

Exosomes are assembled through the accumulation of endosomal membranes forming intraluminal vesicles (ILVs) by the assistance of tetraspanin-enriched microdomains (Tetraspanin-enriched microdomains, including CD9 and CD63, suggested markers in Table 1)



within larger multivesicular bodies (MVBs). These ILVs originate with the help of the endosomal sorting complexes required for transport (ESCRT) machinery comprising ESCRT-0, 1, 2 and 3 which plays a role in the ILVs specific cargo loading and pinching off. After the formation of MVBs, these can then travel to lysosomes and be degraded or to the plasma membrane (PM) with which they will fuse with the help of RAB proteins and Tetraspanin-enriched microdomains to be released into the extracellular space as exosomes. However, an ESCRT-independent pathway involving lipid rafts has recently been discovered <sup>68</sup>.

Opposed to exosomes, MVs are assembled and secreted by outward protrusion of the PM (Figure 7). Flippases creates an imbalance in the phosphatidylserine ratio of the PM forcing it to curve and engulf the cargo that the microvesicles will transport. Then, a cascade of reactions catalysed by different enzymes and involving the cytoskeleton leads to actomyosin contraction and subsequent pinching off the microvesicle. It has recently been discovered that ectosomes are also produced while lipid asymmetry is maintained, suggesting that an ESCRT-dependent pathway might also take place in the biogenesis of MVs <sup>72</sup>.

ABs formation follows a multiple step cell dismantling processes to avoid leaking of dangerous components into the surrounding tissues. ABs externalize phosphatidylserine as an “eat me signal” that facilitates further phagocytosis. Hereafter, actin restriction rings formation results in the blebbing and pinching of the AB that later will be phagocytosed <sup>73</sup>.

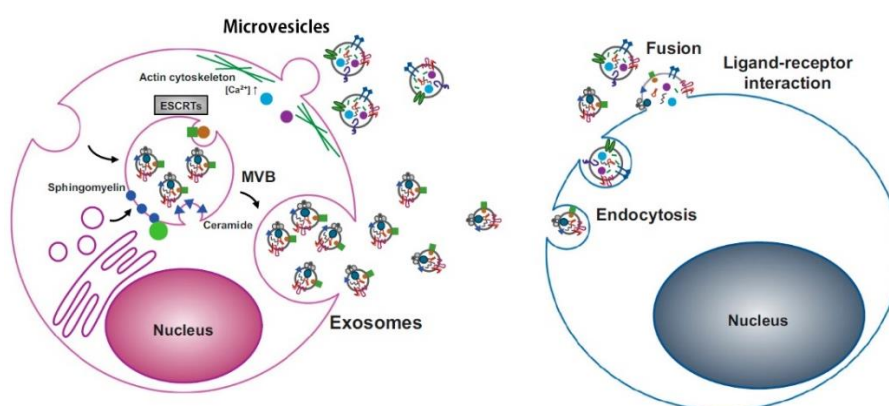


Figure 7. EVs biogenesis and uptake. Microvesicles are originated by outward protrusion of the PM and their uptake is by PM fusion as a result of the ligand-receptor interaction. Exosomes are originated by sphingomyelin/ceramide imbalance (lipid rafts) or by the aid of the ESCRT machinery and they are up-take by endocytosis by the recipient cell <sup>74</sup>. ESCRTs - endosomal sorting complexes required for transport. MVB – multivesicular body.  $[Ca^{2+}]$  – calcium +2 ion.

### 1.3.2. Extracellular vesicles composition and cargo

Exosomes and microvesicles transport endosomal and cytosolic cargos, while apoptotic bodies transport cell waste and debris <sup>75</sup>. Exosomes contain proteins from their biogenesis (TSG101 and ALIX) (Table 1), membrane transport and fusion, adhesion, tetraspanins (CD9, CD63 and CD81), heat shock proteins (HSP) and other lipid-related molecules. Exosomes are known to contain a set of specific cell-type proteins <sup>76</sup>. The cargo of MVs is similar to exosomes, however, is not as well defined as in the case of exosomes (Figure 8). MVs contain a different set of biogenesis-specific markers. Although the cargo of EVs reflects the cell of origin, it has been found that enrichment with some specific proteins and nucleic contents happens, suggesting an unknown sorting mechanism of their cargo <sup>68,77</sup>.

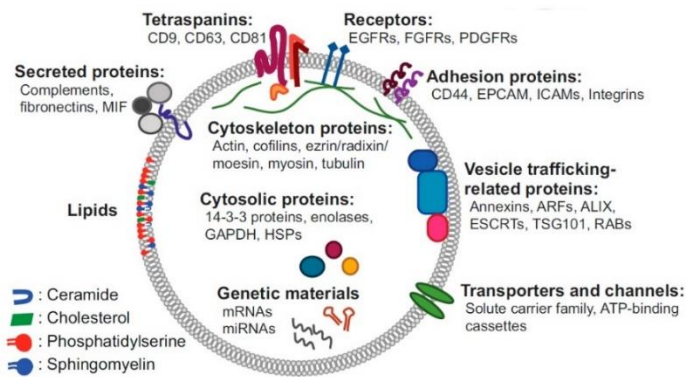


Figure 8. Overall composition of EVs, including main proteins, nucleic acids and lipids divided into functional groups <sup>74</sup>. MIF - macrophage migration inhibitory factor. HSP – heat shock proteins. GAPDH - glyceraldehyde 3-phosphate dehydrogenase. EPCAM - epithelial cell adhesion molecule. ICAM - intercellular adhesion molecule. ARF - ADP-ribosylation factor. ALIX - ALG-2-interacting protein X. ESCRT - endosomal sorting complexes required for transport. TSG101 - tumour susceptibility gene 101. ATP - adenosine triphosphate.

### 1.3.3. Extracellular vesicles functions and utilities

The main function of EVs is to serve as transport vehicles containing diverse cargos and mediate in intercellular communication. It is known that cells modify the cargo contained in EVs depending on extracellular stressors like heat shock, hypothermia, hypoxia, oxidative stress and infectious agents. EVs do not only serve as transporters, they can also interact with the recipient cell by direct interaction with the receptors on the surface of target cells, thus, activating intracellular pathways. Also, EVs can be internalised, release and transfer their cargos (endocytosis) or fuse with the plasma membrane of the recipient cell <sup>78,79</sup>.

Apart from the physiological function <sup>70</sup>, EVs have been suggested and used as diagnostic biomarkers as they are present in many body fluids <sup>80</sup>. In regards to cancer, tumour cells are known to secrete an increased amount of EVs and these might play an essential role in carcinogenesis <sup>81</sup>. However, to be able to use these newly discovered tools, isolation and characterization of subpopulations and sub-types need to be carried out.

### 1.3.4. Extracellular vesicles isolation methods and current limitations

There are many possibilities when it comes to EVs isolation <sup>82</sup> including centrifugation, filtration and immunoaffinity methods <sup>83</sup>. In addition, some kits have already been commercialised for the isolation of exosomes. Differential ultracentrifugation is the most widely used method for the isolation of EVs subpopulations, however, co-isolation of different EV-subpopulations is unavoidable. To improve the outcome of this issue, researchers recur to filtration methods or differential ultracentrifugation using density gradient centrifugation (utilizing sucrose or iodixanol gradients, also known as OptiPrep™) which isolates exosomes by their buoyant density. Another available option is immunoaffinity methods using different markers, however, no specific marker for exosomes or microvesicles have been found yet (current markers used specified in Table 1) and non-specific binding can make the results interpretations misleading.

Isolation and characterization of EVs remain a limiting problem for using EVs as a diagnostic tool. Exosomes and MVs overlap in size <sup>84</sup>, hindering this task. This fact complicates the research and the clinical applications of EVs. Therefore, a robust and specific method needs to be found to isolate EVs, as well as specific markers for the different EVs sub-populations. This will facilitate



the research, and make it possible to broadly use EVs as biomarkers in fields like cancer, in which a need for biomarkers is greatly demanded <sup>85</sup>.

### 1.3.5. Extracellular vesicles in cancer

Cancer cells are known to secrete an increased amount of EVs <sup>81</sup>. Therefore, a higher amount of circulating EVs are found to be correlated with a bad prognosis in cancer patients <sup>86</sup>. The analysis of the cargos of the EVs from cancer patients resulted in the discovery of many proteins and RNAs already known for their role in cancer progression and development. The transfer of the cancer-specific EV cargo has shown to contribute to the shift of the recipient cells phenotype towards tumour development <sup>77</sup> and aid in the metastatic processes <sup>87,88</sup> (Figure 9). For instance, carcinogenic-functional receptors like epidermal growth factor receptor from highly aggressive cancer cells towards non-aggressive cancer cells has been observed <sup>89</sup>.

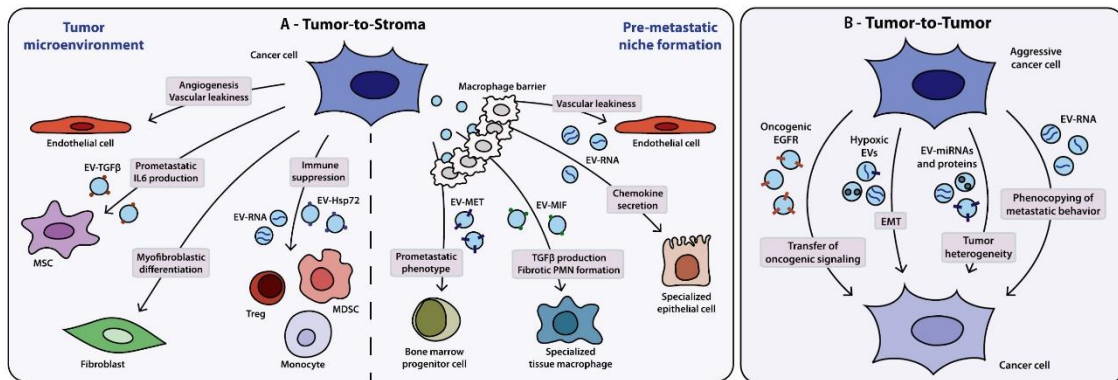


Figure 9. EV-mediation in cancer. (A) Tumour cells and stromal cells exchange extracellular vesicles (EVs) carrying cargos that can modify the function of the recipient cells. Tumour-derived EVs can contribute to the shift in the phenotype of the recipient cells, therefore aiding tumour cells to achieve their survival. (B) Tumour cells can affect other cancer cells by EVs. Highly aggressive cancer cells are known to enhance aggressiveness of other tumour cells through EVs. TGF - transforming growth factor. MSC - mesenchymal stem cell. Treg - regulatory T cells. MDSC - myeloid-derived suppressor cell. PMN - pre-metastatic niche. EGFR - epidermal growth factor receptor. EMT - epithelial-mesenchymal transition. miRNA - microRNA.

EVs play a crucial role in angiogenesis, a critical pathway involved in many carcinogenic functions. Different cancer types have shown to transfer oncogenes, mRNAs or other pro-angiogenic molecules through EVs targeting epithelial cells, thereby, stimulating angiogenesis by activation of VEGF <sup>90,91</sup> (Figure 9). Furthermore, EVs expressing transforming growth factor β has shown to trigger myofibroblastic differentiation inducing angiogenesis and tumour growth <sup>92</sup>. Also, this transforming growth factor β bound to membrane induces secretion of IL-6 by mesenchymal stem cells promoting metastasis <sup>93</sup> (Figure 9). One fascinating ability of cancer-derived EVs is their capability to form the pre-metastatic niches (PMNs) <sup>87</sup>. Comparison between highly and poorly metastatic cancer cells derived-EVs has shown a completely different profile of proteins. Furthermore, EVs can travel to the preferred metastatic sites (in which the cancer type normally metastasizes, also known as primary site), rearrange the ECM and increase the permeability of the surrounding vascular epithelium. This facilitates the process of metastasis and future growth of the cancer cells <sup>87</sup>. Contributing to the fact of selective metastasis, EVs contain specific adhesion molecules that facilitate metastasis towards the primary or specific metastatic sites <sup>94</sup>.

Cancer cells interact with their microenvironment through EVs and modify it to facilitate their own progression and invasiveness <sup>95</sup>. Tumours are known to generate EVs containing matrix-

degradative enzymes (MMP2 and MMP9) known to promote tumour growth and metastasis by degrading and re-modelling the ECM in the surrounding and distant tissue <sup>96,97</sup>. Additionally, chemotherapy is known to induce a survival signal for cancer cells, increasing their EVs release containing ECM-degradative enzymes, to facilitate cell migration and metastasis as a strategic getaway towards survival <sup>98</sup>.

Apart from metastasis, another characteristic of cancer cells is their ability to escape immune surveillance and their resistance to treatment. Cancer-derived EVs are able to suppress the immune surveillance by impairing the function of natural killer cells and CD8+ cells by the downregulation of receptors that mediates in the cell stimulation while promoting the expansion of T regulatory cells <sup>99,100</sup> (Figure 9). This function is correlated with a worse prognosis of the patient <sup>101</sup>. Evidently, EVs has the potential to “educate” immune cells towards a pro-tumour phenotype aiding in evasion of the immune surveillance <sup>102,103</sup>. For instance, micro-RNAs contained in EVs have been reported to polarize macrophages towards a pro-tumorigenic phenotype <sup>103</sup> (Figure 9). These striking getaway strategies that cancer cells-derived EVs portray are not unique and similar ones are displayed in drug resistance.

One of the major challenges in cancer treatment is the development of multidrug resistance against chemotherapy. Multidrug resistance in cancer cells is caused by various mechanisms which allow them to resist cytostatic and cytotoxic effects of applied drugs, and EVs are known to play an important role in it <sup>104,105</sup>. EVs can bind to the drug, reducing the drug available to bind the cancer cell surface <sup>106</sup>. Also, the release of the chemotherapeutic compound out of the cells by EVs has been discovered for many drugs <sup>107–110</sup>. Furthermore, increased in chemo-resistance, proliferation, viability and a decrease in apoptosis was found when co-culture of exosomes derived from chemo-resistant cancer cell lines were cultured with chemo-sensitive cells <sup>109</sup>. Additionally, acquisition of cross-resistance by chemo-sensitive cells from chemo-resistant cells by EV-transfer of functional p-glycoprotein (P-gp) has been described <sup>111</sup>.

#### 1.3.6. Hypoxic extracellular vesicles in cancer

Specific sets of proteins driving carcinogenic characteristics are packed in exosomes under stress conditions, like hypoxia. For example, within hypoxic conditions, EVs are highly enriched in hypoxia-regulated proteins and RNA, which are capable of inducing vascular permeability in lung cancer <sup>112</sup>. Furthermore, hypoxic-EVs enhance tumour growth, angiogenesis, proliferation and metastasis when compared with a normoxic tumour-derived EVs <sup>113</sup>, thereby, contributing to the fast onset of the aggressive carcinogenic phenotype, reducing the life-span of the patients <sup>114,115</sup> (Figure 10). Hypoxia and EVs have been independently well studied in the scope of cancer, however, further research is needed considering these two main players in cancer progression.

EVs have tumor-promoting effects through a wide variety of mechanisms (Figure 10). Particularly, many features regarding tumour progression, invasiveness and metastasis are only observed in EVs secreted by some types of tumours, and further studies are needed to prove the varied functions of EVs in more carcinogenic cell lines. The release of EVs and their interaction with other cells and the tumour microenvironment is a suitable model to describe and explain many of the unknown mechanisms involved in the progression, chemo-resistance development and generation of metastases in cancer patients. The role of EVs in these pathological pathways has not been broadly addressed. Particular cargo contents might be used as potential predictive biomarkers. However, the EV cargo is still not well defined and specific

isolation of MVs and exosomes is problematic due to the overlap in size, a lack of specific markers, and a need for an isolation gold-standard method still ballast the research within this area. Many questions regarding the role of EVs in cancer remain unsolved and additional research is required worldwide towards a better comprehension of EVs in cancer and how hypoxia as an external stressor might mediate in this response. To aid in this, high-throughput methods like mass-spectrometry (MS) proteomic analysis might be the key to overcome these limitations. The sensitivity, resolution and capacity to detect vast numbers of proteins by MS is unmatched by any other method and its development towards even more complex and better instruments and databases is inexorable.

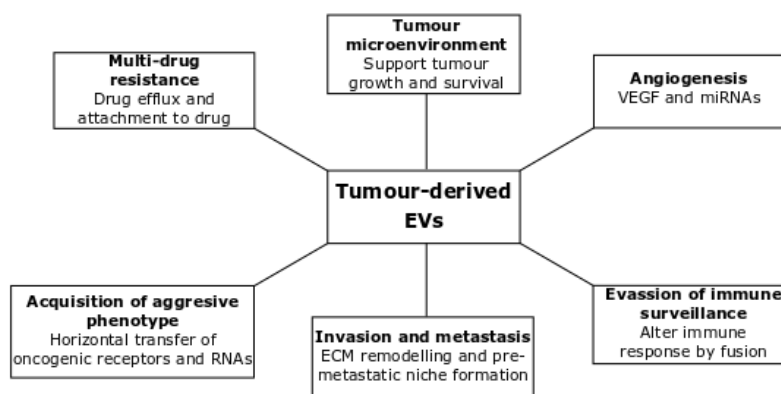


Figure 10. Summary of pathways affected by tumour-derived EVs. Tumour-derived EVs play a fundamental role in angiogenesis, evasion of immune cell surveillance, metastasis and invasiveness of other tissues, drive multi-drug resistance, interact with the tumour microenvironment and mediate in the acquisition of many carcinogenic aggressive phenotypes. This is achieved by transfer of bioactive functional cargos. Thus, having a deep impact on tumour progression <sup>116</sup>. VEGF – vascular endothelial growth factor. ECM – extracellular matrix.

#### 1.4. Proteomics

Proteins are the building blocks of the living organism and are made of amino acids. They differ greatly in their properties like function, stability, three-dimensional structures, and are considered the final gene products. The term proteome indicates the total assortment of proteins produced at a certain time expressed by a cell, tissue or organism. Proteins functions as mediators in most of the cellular processes in a direct form or through interactions with other biomolecules. Therefore, protein profiles can accurately represent a disease state <sup>117</sup>. Contrarily, alterations in gene expression do not always have direct functional consequences and might not reflect protein expression nor activity, because of a broad range of possible post-translational modifications, epigenetic regulations and non-coding RNAs <sup>118</sup>. That is why proteomics is answering questions that transcriptomics (the study of the sum of all RNA transcripts) and genomics (the study of the complete set of DNA, including all genes) have been unable to.

Two main strategies in MS-proteomics are top-down proteomics, which analyses intact proteins, and bottom-up proteomics, which analyses peptides in proteolytic digests. During the last decades, the most widely used approach has been bottom-up proteomics due to its capability of analysing many samples of a wide range of complexity, making it the ideal suit for discovery-driven proteomics in many fields like cancer and EVs research. Unlike bottom-up, top-down proteomics still suffers from technical limitations and is a more challenging approach due to the complexity of the data that can be extracted. Following bottom-up proteomic strategy, once the proteins have been extracted from the biological source, they are digested into peptides or

separated in a gel and digested (in-gel digestion). They can then be separated by different methods like liquid chromatography (LC) and then analysed by MS. The peptide ions are fragmented and their sequence can be deduced from their mass and charge ratio <sup>119</sup>. Hereafter, highly valuable quantitative information can be extracted.

#### 1.4.1. Proteomics, cancer and extracellular vesicles

Proteomics represents a comprehensive tool for the identification of biomarkers and discovery of therapeutic targets in cancer <sup>120</sup>. Biomarkers are a biological indicator of the pathological status and progression and represent a powerful tool for monitoring the course of the disease and assessing the efficacy and safety of novel therapeutic agents <sup>121,122</sup>. The study of these proteins in cancer and their interactions is known as oncoproteomics, a branch of the proteomic studies.

MS-proteomic analysis has also aided to broaden our knowledge in fields of EV-composition in the last years, especially bottom-up proteomics. The EV-proteome contains a wide variety of proteins and other components, so, to help researchers, databases containing information regarding EVs composition have been created. ExoCarta <sup>123,124</sup>, containing a database of the proteins, RNA and lipids found in exosomes, Vesiclepedia <sup>125</sup>, a composition compendium of all EV proteins and EVpedia <sup>74,126,127</sup>, an EV-proteome, transcriptome and lipidome database of all life forms.

EVs carry in carcinogenic settings, very specific proteins, normally in minute amounts, responsible for inducing and driving many pathological mechanisms in cancer. Bottom-up proteomics has during the last decade enabled the identification and quantification of EV-proteomes and multitude of cellular proteomes in cancer. Oncoproteomics has the potential to bring further understanding of the pathways driving pathogenesis in cancer cells and EVs in hypoxic conditions. This will help to understand the complexity of carcinogenesis and cancer progression in this very particular setting. Therefore, investigating highly-hypoxic cancers which develop aggressive and chemo-resistant phenotypes like in the case of SCLC might improve the prognosis of patients with SCLC.

## 2. Aim

Proteins constitute an essential part of cells in every single organism and therefore the change in the cell's proteome is an invaluable source of information regarding pathological and physiological states. In cancer, a shift in the proteome occurs, which drives the behaviour of the cell to characteristic aggressive and pro-carcinogenic phenotypes. In SCLC, hypoxic conditions might contribute to develop an aggressive and chemo-resistant phenotype. Proteome changes are one of the most reliable fingerprints to trace and understand complex biological responses. Cancer cells are not individual entities, communication between them takes place, and this communication is fundamental to understand the whole context of the pro-carcinogenic and chemo-resistant phenotype of cells. One way of communication that cells have is through EVs, as they can carry complex sets of molecules, induce changes and pass functional structures to the recipient cells in a fast and shielded way.

The aim of this MSc thesis is to characterize the changes in the cells and the EV-proteome of SCLC cell line under different oxygenation conditions. We have examined whether:

- Hypoxia induces proteome changes in H69 SCLC cells towards an enhanced pro-carcinogenic functionality, therefore, shifting its phenotype.
- Hypoxia drives changes in the EV-release and the EV proteome composition.
- Hypoxia-altered exosomes induce changes through the bystander effect on other SCLC cell phenotype and pro-carcinogenic ability.

### 3. Materials and methods

#### 3.1. Pre-project: exosome isolation from plasma samples

Before starting the project, different EV-isolation methods and purification techniques, as well as, western blot were performed to provide insight into the different methods and techniques and to carry out the validation and optimization of the WB (Appendix A) for CD9 and HIF-1 $\alpha$  proteins. Plasma samples from MyVes study (ethical approval no.: N-20140055) were used. These studies were conducted complying with the Declaration of Helsinki<sup>128</sup>. Exosome isolation from plasma samples was performed using qEV Original size exclusion chromatography columns (iZON Science, Christchurch, New Zealand) and a ME™ kit (New England Peptide, Inc., Gardner, Massachusetts, United States, Cat. #ME-020p-kit). The procedure was performed following the manufacturer protocol. After the collection of the exosomes, Bicinchoninic acid (BCA) Assay (Pierce™ BCA Protein Assay Kit, Cat. #23225) was performed for each of the EV-isolates to quantify the total protein concentration (further described in the Determination of protein concentration section). Isolates were kept at -80°C. Then, western blot was performed for CD9 and HIF-1 $\alpha$  protein marker (further described in the detection of CD9 and HIF-1 $\alpha$  proteins section).

#### 3.2. Experimental design

In this MSc thesis, two main experiments were conducted; an experiment in which the cells were exposed to different oxygen conditions (hypoxia experiment) during 24h and another experiment in which the exosomes generated from the previous experiment were co-cultured with cells under normoxic conditions for 48h (co-culture experiment) (Figure 11).

##### 3.2.1. Hypoxia experiment

Three different oxygenation conditions were used in this experiment. Normoxic cell culture under *in vitro* conditions (20% oxygen, denoted N20), normoxic physiologic conditions (5% oxygen, denoted H5) and hypoxic physiologic conditions (1% oxygen, denoted H1).

Before starting the hypoxia experiment, the SCLC cell line was cultured in the required amount (further details in the Cell Culture section). The cells were then seeded using EV-depleted media (further described in the Cell culture section). Three different conditions, each one consisting of quadruplets was set in an incubator or an oxygen-regulated chamber (XVIVO SYSTEM, Biospherix®, New York, New York, United States Mod. G300C). The cells were then incubated for 24h in the three different conditions.

After incubation, isolation of the different samples containing cells, MVs and exosomes was performed by differential ultracentrifugation. Subsequently, the isolates were aliquoted to different analyses and stored at -80°C until further use. Triplicates of each isolate from each condition were sent to mass spectrometry analysis at Statens Serum Institut (Copenhagen, Denmark). The exosome and microvesicle samples were also analyzed by nanoparticle tracking analysis (NTA) (triplicates) and western blot (quadruplets). The cell lysates were also analyzed by MS (triplicates for each condition) and western blot (one sample per condition).

### 3.2.2. Co-culture experiment

In this experiment, the exosomes obtained from the hypoxia experiment were co-cultured with the SCLC cell line in normoxia for 48h. The exosomes obtained after the hypoxia experiment were then analyzed by NTA to determine the particle concentration in order to load the same particles/cell ratio. After the co-culture process, the cells were isolated following the same procedure as performed in the hypoxia experiment and frozen. Cell samples were obtained in triplicates for each condition and the isolates were aliquoted to different analysis (MS and western blot) and stored at -80°C until further use. Cell-isolates triplicates from each condition were sent to mass spectrometry analysis at Statens Serum Institut (Copenhagen, Denmark).

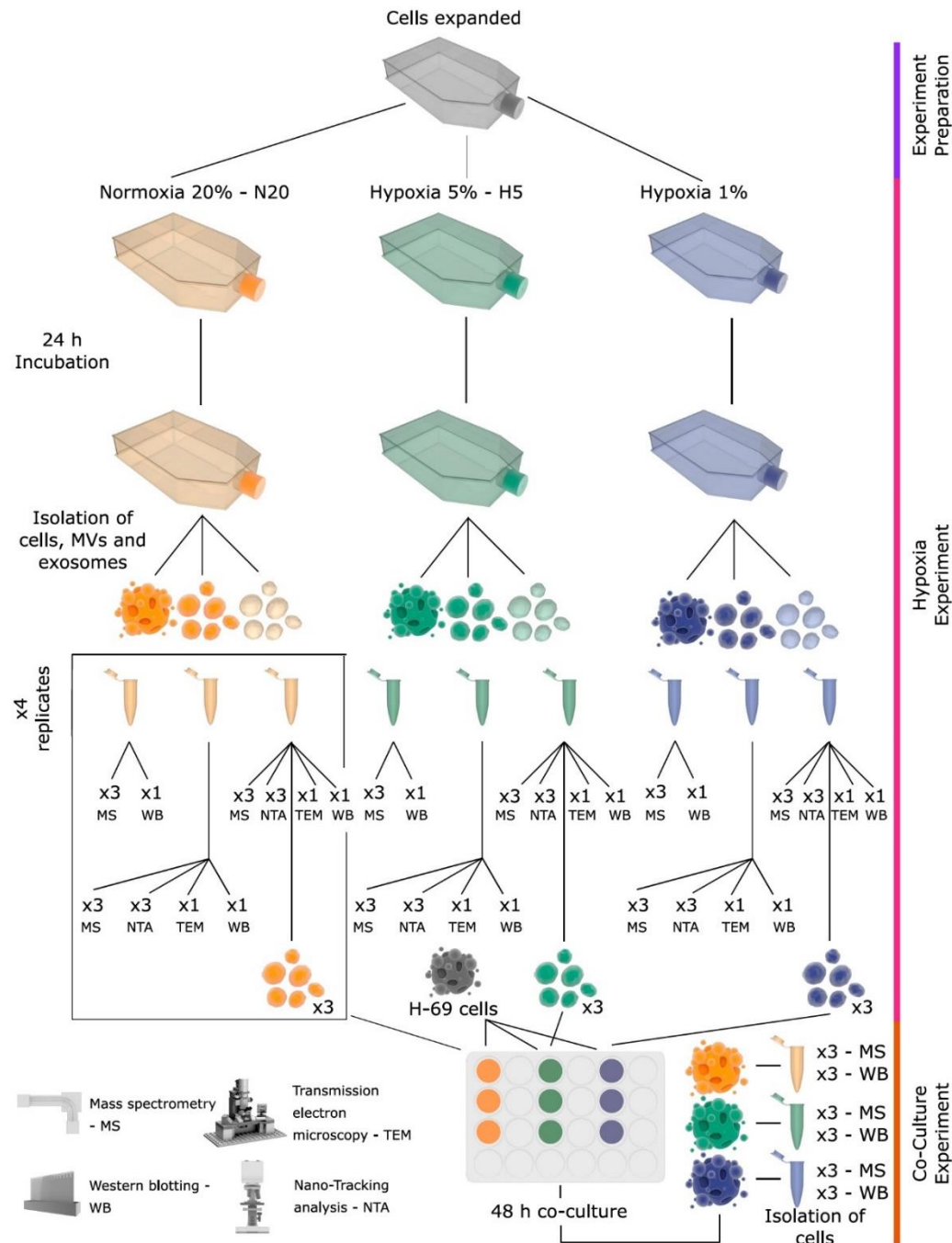


Figure 11. Scheme of the hypoxia and co-culture experiments. In this graph, the main steps to obtain the samples and the analysis performed are illustrated. MVs – microvesicles.



### 3.3. Procedures

#### 3.3.1. Pre-analytical preparation

The experiments were conducted on cells with only one passage. All the cells were previously cryo-preserved before using them in the experiments. The cells were cultured for a minimum of 5 days before starting the experiments and a maximum of 7 days. This ensured same conditions for all the cells and helped to make sure cells were in enough numbers before starting the experiments.

#### 3.3.2. Cell culture

##### 3.3.2.1. *H69 cell line culture*

The human SCLC cell line H69 (Sigma, Inc., San Luis, Missouri, United States, Cat. #91091802-1VL, Lot #14G006) used was obtained from the European Collection of Authenticated Cell Culture. The H69 cell line was originally obtained from the pleural fluid of an untreated 55-year-old Caucasian male diagnosed with SCLC. H69 cells were grown in suspension as spherical floating cell aggregates in Greiner CELLSTAR® T-75 flasks (Greiner Bio-One, Kremsmünster, Austria – Cat. #82050-856). Cells were cultured in RPMI 1640 (Gibco™, Thermo Fisher, Waltham, Massachusetts, United States, Cat. #21875034, Lot #1892413) complemented with 10% fetal bovine serum (FBS – Thermo Scientific, Thermo Fisher, Waltham, Massachusetts, United States, Cat. #10500064, Lot #42A1374K) and 1% penicillin/streptomycin antibiotic solution (Sigma-Aldrich, Darmstadt, Germany, Cat. #P4333-100ML, Lot #077M4780V). The cells were maintained at 37°C, 5% CO<sub>2</sub> and 20% O<sub>2</sub>.

The cells were subcultured when reaching a confluency level of 300,000 cells/mL (culture range: 75,000 – 300,000 cells/ml) accordingly to the manufacturer.

##### 3.3.2.2. *Preparation of exosome-depleted media*

For the hypoxia and the co-culture experiment, EV-depleted media was used during the incubation processes. To avoid contamination from the FBS EVs, the FBS was centrifuged for 23h at x 100,000 g in an Avanti J-30I centrifuge (Beckman Coulter Inc., Brea, California, United States, Cat. #363121) using a JA-30.50 Ti rotor (Beckman Coulter Inc., Brea, California, United States, Cat. #363420). The collected supernatant (EV-depleted FBS) was used to make EV-depleted media (Figure 12).

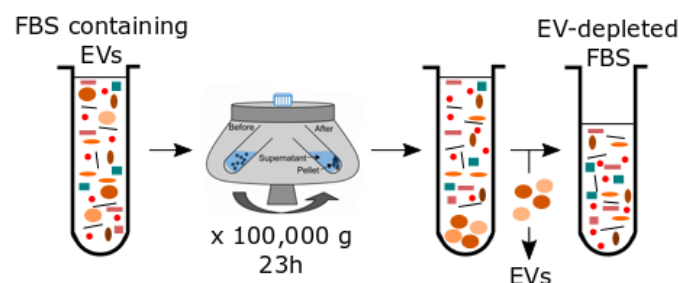


Figure 12. Scheme describing the preparation of the EV-depleted fetal bovine serum (FBS).



### 3.3.2.3. *Cell counting, viability and cryopreservation*

For counting cells and checking their viability, a solution of trypan blue (Sigma, Inc., San Luis, Missouri, United States, Cat. #T8154-20ML, Lot #RNBG1730) was added (1:1:1 cells: trypan blue: media ratio). Counting was performed using a haemocytometer and a microscope (Nikon, Minato, Tokyo, Japan, Cat. #E100) using x10 magnification.

For cryo-preservation of the cells, the cell's media was replaced with media containing 5% of dimethyl sulfoxide (DMSO - Fisher BioReagents™, Thermo Fisher, Waltham, Massachusetts, United States, Cat. #BP231-100). The cells then were stored in an insulated box of expanded polystyrene filled with paper (this ensures a freezing ratio of 1°C/min to ensure optimal cell viability) at -80°C for 24h and then transferred to a -196°C freezer until further use. Thawing and seeding were performed by instant warm up at 37°C in a water bath, centrifugation and resuspension in new warm media.

### 3.3.3. *Cell isolation and lysis*

After the incubation process, isolation of cells was conducted to further investigate the cell lysate by MS and western blot (WB). Centrifugation of the whole sample was performed at 300 x g for 10 minutes at 4°C to isolate the cell pellet. The supernatant was removed for further centrifugation steps and the cell pellets were kept at -80°C before further usage.

A different approach was taken when lysating the cells for MS (described in section 3.3.8.1.). In this section, cell lysis for WB analysis was performed using Radioimmunoprecipitation assay buffer (Pierce™, Thermo Fisher, Waltham, Massachusetts, United States, Cat. #89901, Lot #MF157162) with added protease inhibitors (Pierce™, Thermo Fisher, Waltham, Massachusetts, United States, Cat. #88666, Lot #QE20063010). Each sample received lysis buffer according to the number of cells present (100 µL of lysis buffer/1,000,000 cells). Then, the cells were incubated with the lysis buffer for 5 minutes, followed by 10 sonication cycles (Ultrasonic cleaner - Marshall Scientific, Hampton, Vermont, United States, Cat. #2510) of 10 seconds, with 50% amplitude and 1-minute rest between cycles. Subsequently, cells were incubated (on ice) for 5 minutes and further centrifuged (microcentrifuge - Eppendorf® Minispin®, Sigma-Aldrich, Darmstadt, Germany Cat. #Z605220) at 13,000 x g for 5 minutes. Following this, the supernatant was collected for western blot analysis.

### 3.3.4. *Isolation of microvesicles and exosomes*

In the hypoxia experiment, after the isolation of the cells, further isolation of microvesicles and exosomes was conducted by using the supernatant from the cells isolation. Centrifugation to remove dead cells and cell debris was performed at 2,000 x g for 30 min at 4°C (Figure 13). The resulting pellet was discarded, and the supernatant was further centrifuged using an LKB 2331 Ultraspinn 70 ultra-centrifuge with the RP70P rotor at 20,000 x g for 30 min at 4°C (Figure 13). The pellet containing microvesicles was washed in phosphate-buffered saline (PBS) citrate (in-house made, Appendix B). Centrifugation to wash the pellet was performed with the same settings using a Heraeus multifuge 3SR (Kendro Laboratory Products, Asheville, North Carolina, United States, Cat. #75004375). The supernatant obtained from the first ultracentrifugation was subsequently centrifuged using an LKB 2331 Ultraspinn 70 ultra-centrifuge with the RP70P rotor at 100,000 x g for 60 min at 4°C to obtain the exosomes (Figure 13). The pellet obtained was

washed in PBS citrate using the same centrifuge and settings. After obtaining the samples, cryopreservation of the isolates was performed using liquid nitrogen (snap-freeze). Part of the EV-isolates were kept in the fridge (4°C) for NTA analysis, performed in the following 48h post isolation, therefore ensuring the EV-sample quality <sup>129</sup>.

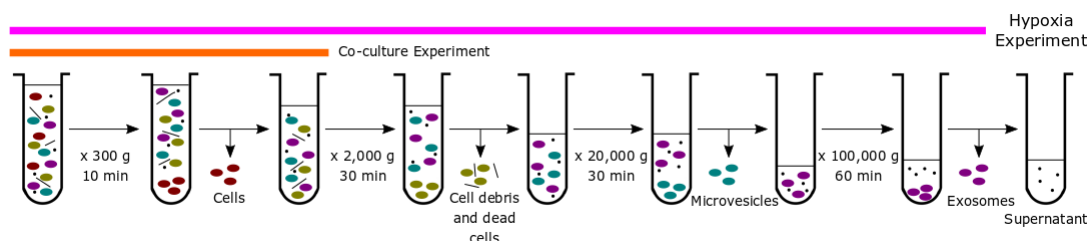


Figure 13. This scheme represents the isolation of cells, microvesicles and exosomes of the samples after the hypoxia and co-culture experiments.

### 3.3.5. Determination of particle concentration and size

NTA was carried out to assess the concentration of particles per sample. Once the particle concentration was assessed, an equal number of exosomes/cell was loaded in every replicate of the co-culture experiment. The concentration of MVs and exosomes in each oxygenation condition and their size distribution data was also obtained.

Particle concentration and size were measured with a NanoSight LM10 instrument (Nanosight, Malvern Panalytical, Salisbury, United Kingdom), equipped with a 405 nm blue laser and an EM-CCD camera (DL-658-OEM-630, Ser. #DL-00910, Andor™, Belfast, United Kingdom). As an internal control across experiments and to ensure the accuracy of the analyses, we performed measurements of 0.1 µm silica microspheres (Polysciences, Hirschberg an der Bergstrasse, Germany) immediately before analyzing the samples by NTA. Exosomes and microvesicles were pre-diluted in filtered DPBS (previously analyzed to ensure it was particle-depleted) to achieve a concentration within the  $10^8$ – $10^9$  range for optimal NTA analysis. The video acquisitions were performed with NTA software (Malvern Panalytical, Salisbury, United Kingdom, v3.0), using a camera level 13 for exosomes and 11 for microvesicles and silica beads. 5 videos of 30 seconds were captured per sample. For the analyses, the camera threshold was set to 3, blur set to automatic, and pixel maximum jump distance to 11.4– 12.9.

### 3.3.6. Determination of protein concentration

All samples were up-concentrated before protein quantification by using Amicon® Ultracel® - 100K centrifugal filter units (Millipore Corporation, Burlington, Massachusetts, United States, Cat. #UFC510096, Lot #R6JA92066).

To load an equal amount of protein in western blot, protein concentration was measured using BCA protein assay according to manufacturer's protocol (Pierce™ BCA Protein Assay Kit, Cat. #23225). Hereafter, measurement of the absorbance with a FLUOstar OPTIMA microplate reader (BMG Labtech, Ortenberg, Germany) at 562nm and calculation of the concentration of the unknown samples was performed using the software OPTIMA (V2.20R2) and MARS Data Analysis Software (V2.00) from BMG Labtech.

### 3.3.7. Detection of CD9 and HIF-1 $\alpha$ proteins

Western blot was performed to validate the isolation of EVs (CD9 marker) and the different oxygenation (HIF-1 $\alpha$  marker) incubation conditions of the hypoxia experiment. Samples (plasma samples, exosomes, microvesicles and cell lysate) containing 5 $\mu$ g protein with 5 $\mu$ L loading buffer were heated-up (95°C) prior to loading. The protein amount of the isolates was below the detection limit of the BCA (Appendix A) in most of the samples, therefore, loading of 20 $\mu$ L of the isolates and 5 $\mu$ L loading buffer was performed. Controls were also loaded with 5 $\mu$ L of loading buffer (Table 2).  $\beta$ -actin was used as a loading control to normalize the amounts of the proteins of interest in the samples. Two different ladders were used for WB: a chemiluminescent ladder used for the WB optimization (Precision Plus Protein™ WesternC Standards, Bio-Rad, Hercules, California, United States, Cat. #161-0376) and a dual color visible ladder for sample analysis (Bio-Rad, Hercules, California, United States, Cat. #161-0374). The proteins were separated by sodium dodecyl sulfate-polyacrylamide gel electrophoresis (SDS-PAGE) using Mini-PROTEAN® TGX™ 4-15% gradient pre-cast gels (Bio-Rad, Hercules, California, United States, Cat. #4561083). Then, the proteins were transferred to Amersham™, Hybond™ 0.2  $\mu$ m Polyvinylidene fluoride (PVDF) blotting membranes (GE Healthcare, Little Chalfont, United Kingdom, Cat. #10600021, Lot #A11706264).

After protein transfer, blocking of the membranes with skim milk powder (5% (w/v)) dissolved in blocking solution (Sigma-Aldrich, Darmstadt, Germany Cat. #70166-500G, Lot #BCBT8091) (PBS buffer with Tween 20 0.1% (Bio-Rad, Hercules, California, United States, Cat. #170-6531))) was carried out for 60 min at room temperature to avoid unspecific binding of the antibodies.

The primary antibodies (Anti-CD9, HIF-1 $\alpha$  and  $\beta$ -actin) were diluted (Table 3) in 2.5% (w/v) skim milk/PBS and incubated with the membrane overnight at 4°C. The next morning, the membranes were washed three times with washing solution, incubated with peroxidase-conjugated secondary antibodies (Table 3) for 2 hours at room temperature and again, washed. When using the chemiluminescent ladder, its HRP-conjugated was also added (Precision Plus Protein™ StrepTactin-HRP Conjugate, Bio-Rad, Hercules, California, United States, Cat. #1610381, Lot #D034351C). After this, detection of the immunoreactive bands was performed by using enhanced chemiluminescence (ECL) technique adding Lumi-light western blotting substrate (Roche, Basile, Switzerland, Cat. #12015200001). The chemiluminescence-signals were visualized using a Syngene PXi 4 imaging system (Syngene, Cambridge, United Kingdom) equipped with GeneSys software (Syngene, Cambridge, United Kingdom, v1.5.4.0).

Table 2. Controls used for western blot.

CONTROL	INFORMATION
CD9 – platelet lysate – 1:100 dilution	In-house made (Appendix C)
HIF-1 $\alpha$ – 1:4 dilution	HeLa + CoCl <sub>2</sub> lysate (Santa Cruz Technology, Dallas, Texas, Cat. #sc-24679, Lot #H1408)

Table 3. Primary and secondary antibodies used and their optimized concentrations. HRP - Horseradish peroxidase.

PRIMARY ANTIBODY	SECONDARY ANTIBODY
Mouse Anti-human CD9, Clone M-L13 (BD pharmingen, Franklin Lakes, New Jersey, United States, Cat. #555370, Lot #6138551) – 1:500 dilution	Polyclonal goat anti-mouse HRP, polyclonal (Dako, Santa Clara, California, United States, Cat. #P0447, Lot #2005443) – 1:30,000 dilution
Anti HIF-1 alpha purified from rabbit, polyclonal (Novus Biologicals, Littleton, Colorado, United States, Cat. #NB100-479, Lot #AL-4)– 1:1,000 dilution	Rabbit IgG HRP Linked F(ab') <sub>2</sub> from donkey, polyclonal (Sigma-Aldrich, Darmstadt, Germany Cat. # NA9340-1ML, Lot #5205500) – 1:30,000 dilution
Anti-β-actin antibody produced in mice, monoclonal (Sigma, Inc., San Luis, Missouri, United States, Cat. #A5441-100UL, Lot #116M4801V) – 1:5,000 dilution	Polyclonal goat anti-mouse HRP, polyclonal (Dako, Santa Clara, California, United States, Cat. #P0447, Lot #2005443) – 1:30,000 dilution

### 3.3.8. Sample preparation and protein discovery by LC-MS/MS analysis

#### 3.3.8.1. Sample preparation for MS analysis

Cell samples from the two experiments conducted were thawed, washed with PBS twice and mixed with a pre-heated (99°C) lysis buffer containing guanidinium hydrochloride and sonicated for 2 min at 50% amplitude with cycles of 1 second on, 1 second off). Protein concentration of all the samples (cell lysate, MVs and exosomes) was measured by Pierce™ Coomassie (Bradford) Protein Assay Kit (Thermo Fisher, Waltham, Massachusetts, United States, Cat. #23200) to calculate the amount of digestion product required for each sample and to load same amount of proteins into the MS-spectrometer.

In-solution digestion of the samples (cell lysates, MVs and exosomes) was performed using the endoproteinase LysC (1:300 LysC:protein ratio) for 1h and trypsin (1:100 trypsin:protein ratio) incubation overnight. Trifluoroacetic acid quenching was used to stop the digestion process. Following this, centrifugation took place at 1,000 rpm for 5 min and collection of the supernatant. Hereafter, the samples were ready to be loaded in the Sep-Pak column for further desalting, concentration and washing with trifluoroacetic acid. After this, the samples were stored at 4°C until analysis. In this study, bottom-up proteomics using MS coupled with liquid-chromatography (LC) was used.

#### 3.3.8.2. Mass spectrometry. LC-MS/MS analysis and protein identification

Peptides were loaded onto an Acclaim PepMap C18 precolumn (300 µm inner diameter, 5 mm long, 5 µm particle size, Dionex, Sunnyvale, California, United States). The peptides were then separated using an Acclaim PepMap100 C18 analytical column (75 µm inner diameter, 150 mm long, 3 µm particle size, Dionex, Sunnyvale, California, United States) by a 90-minute gradient. An Ultimate 3000 nano-LC system (Dionex, Sunnyvale, California, United States) was connected to a Q Exactive™ HF-X Hybrid Quadrupole-Orbitrap™ Mass Spectrometer (Thermo Fisher Scientific, Waltham, MA). For ionization of the peptides, the MS was equipped with a nano-electrospray (Proxeon, Odense, Denmark) (flow rate was 200 nL/minute). Record of the full scan (250 - 1,800 mass/charge [m/z]) to obtain MS data was performed in the Orbitrap with 240,000 resolution at 400 m/z. MS/MS data was recorded in data-dependent mode in parallel, fragmenting the 5 most abundant ions (charge +2 or higher) by induced dissociation in the HyperQuad mass filter.

The recorded raw files were analysed using MaxQuant version 1.6.1.0<sup>130</sup> for peptide quantitation. For protein identification the Andromeda search engine<sup>131</sup> was used against the Homo sapiens UniProt reference proteome (last version: 2018-03-13) including 71,599 entries (proteome ID: UP000005640) and a FASTA-file containing common contaminants. To increase the identified peptides, the match between runs (MbR) setting was activated. This setting allows using a recorded MS/MS spectrum for a feature (a certain m/z at a certain retention time (RT)) to be transferred to the same feature recorded in another sample if the same feature was observed and no MS/MS spectrum was triggered. This increases the number of identified peptides in each sample. Additionally, label-free quantitation values were determined to enable comparison of the protein intensities across all the samples.

To estimate false positive peptide spectral matches, MaxQuant was programmed to filter the proteins found to < 1% False Discovery Rate (FDR) using target-decoy strategy<sup>132</sup>. All protein tables were filtered to eliminate the identifications from the common contaminants and reverse database.

### 3.4. Statistical analysis

#### 3.4.1. General statistical analysis

Data obtained from the different analysis was collected in Excel (Microsoft Corporation, Albuquerque, New Mexico, United States, v2016) and analysed by SPSS (IBM, Armonk, North Castle, New York, United States, v25). The graphs and charts were made using GraphPad Prism (GraphPad Software, California, United States, v7.0).

Besides general proteomic analysis, comparison of all NTA samples was performed by SPSS, using independent sample t-tests. Before T-testing, normality (Saphiro-Wilkis;  $p > 0.05$ ) and homogeneity (Levene's test;  $p > 0.05$ ) was tested (Appendix D). None of the datasets contained non-normalized or non-homogenous datasets. Statistical significance ( $P < 0.05$ ) was represented by an asterisk (\*).

#### 3.4.2. Proteomics data analysis

In this study, label-free quantitation values could be used as the experimental design allows meeting the assumption that the protein variability between EVs-subpopulations samples and between cell lysate samples is not high.

The output data from Max Quant was then analysed with Perseus (v1.5.6.0, 1.5.8.5, v 1.6.1.3 and v1.6.3.1) to interpret the protein quantification. First, the data was filtered for reverse hits, contaminants and protein identification by site. Second, log2 transformation of the data was performed. Hereafter, imputation was performed in all the samples except in the cell lysate from the hypoxia experiment. Imputation was performed by assuming that the proteins absent are in fact present in the samples, however, they are found in concentrations below the detection limit of the MS, therefore, imputation was required to fix these missing values. As imputation, even if performed correctly, introduces bias<sup>133,134</sup>, its use was limited to the samples in which the missing values impaired the performance of further proteomic analysis. Therefore, imputation was avoided in the cell lysate samples from the hypoxia experiment as the missing values were much lower compared with other samples.

Different filtration for valid values was then applied depending on the samples (Table 4). Filtration for valid values was set to “70% in at least one group” in the cell lysates as they contained a bigger proteome and “50% in at least one group” was applied to MVs and exosomes as they had a smaller proteome. Annotations from Gene Ontology and KEGG pathways were added to ease the results interpretation of high-throughput proteomic data obtained with Perseus. Principal component analysis (PCA) was used to investigate the variance in protein expression and abundance across the samples. Analysis of variance (ANOVA) test and T-test were then performed to look for the significant protein expressions across the samples. Fisher exact test and hierarchical clustering analysis were carried out using the ANOVA significant proteins found. Fisher Exact Test was carried out to prove a non-random functional group linkage. T-test analysis was aided with volcano plots for its visualization (Table 4).

Table 4. Datasets analysis criteria and statistical analysis basis.

Experiment	Sample type	Imputation	Valid values	ANOVA (post hoc)	Fisher exact test	T-test/ Volcano
<b>Hypoxia Experiment</b>	Cell lysate	NO	70% at least in one group	FDR = 0.05	FDR = 0.05	FDR = 0.05
	Microvesicles	YES	50% at least in one group	p = 0.01	p = 0.02	p = 0.01
	Exosomes	YES	50% at least in one group	p = 0.01	p = 0.02	p = 0.01
<b>Co-culture Experiment</b>	Cell lysate	YES	70% at least in one group	p = 0.01	p = 0.01	p = 0.01

#### 3.4.2.1. Bioinformatic analysis

To better comprehend the functional differences of the different protein expression patterns among the samples, varied bioinformatic tools were used. These bioinformatic methods of enrichment analysis were applied through specific software and database/web resources; singular enrichment analysis (SEA) using the search tool for the retrieval of interacting genes/proteins (STRING, a biological database containing known and predicted PPI and providing functional enrichment using GO and KEGG) <sup>135</sup> and FunRich <sup>136</sup>, gene set enrichment analysis (GSEA) using Perseus <sup>137,138</sup> and modular enrichment analysis (MEA) using DAVID <sup>139,140</sup> (a database that provides functional interpretation of protein lists aiding for its visualization and annotation).

Venn diagrams were constructed using FunRich <sup>136</sup> to illustrate how the identified proteins were distributed compared to Exocarta <sup>123,124</sup>, EVpedia <sup>127,141</sup>, HypoxiaDB <sup>142</sup>, the human cancer metastasis database (HCMDB) <sup>143</sup>, and self-curated databases containing a list of proteins involved in motility, angiogenesis, proliferation and SCLC protein markers (Table 5). (Attached excel file: Self-curated databases, proteomic data and miscellaneous).

Table 5. Databases used, and the information contained within them.

Databases		Information provided
Gene-Ontology (GO) <sup>144</sup>	Biological processes (GOBP)	Sets of molecular events relevant to the functioning of living organisms
	Cellular components (GOCC)	Components of a cell or derived from the extracellular surroundings
	Molecular function (GOMF)	Fundamental functions carried out by a gene or protein
Kyoto Encyclopedia of Genes and Genomes (KEGG) <sup>145</sup>	KEGG pathways	Integrated networks of pathways involving cellular biomolecules
Exocarta <sup>123,124</sup>	TOP 100 proteins	List of the most common 100 proteins found in exosomes
EVpedia <sup>127,141</sup>	TOP 100 proteins	List of the most common 100 proteins found in human cell-derived EVs
HypoxiaDB <sup>142</sup>	Up-regulated proteins	A database of hypoxia up-regulated proteins
The human cancer metastasis database (HCMDB) <sup>143</sup>	Metastatic proteins	47 proteins related to metastasis and invasiveness in SCLC
Self-curated databases	SCLC markers	63 marker proteins of SCLC
	Motility	1424 protein related to motility in cancer from different research papers
	Proliferation	2005 proteins linked to proliferation in cancer from different research
	Angiogenesis	557 proteins related to angiogenesis in lung cancer from different research papers



## 4. Results

To establish the influence of hypoxia among SCLC cells and EVs and the effect of EVs over SCLC cells, two different experiments were conducted. The hypoxia experiment in which different oxygenation conditions were set to look at the direct influence of oxygen levels among cells and EV-release and cargo composition. And the co-culture experiment, in which the effect of the produced EVs under different oxygenation conditions over SCLC cells was investigated.

First, we investigated if different oxygenation conditions drive changes in the EV-release by measuring particle concentration and size. Second, we looked if hypoxia drives changes in the composition of the EVs and cells by proteome analysis. Finally, we examined whether the exosomes derived from the different oxygenation conditions have any bystander effect among SCLC cells when co-cultured, to determine this, proteome analysis was also performed.

### 4.1. Confirmation of extracellular vesicles isolation

To investigate whether we isolated EVs (MVs and exosomes); WB for the CD9 marker was carried out. However, no results apart from the positive control were visible (Figure 14). One feasible explanation for these results might lay in the low amount of protein loaded in the WB, (below the required protein concentration estimated in the optimization ( $> 20 \mu\text{g}$ )), therefore, hindering the detection of CD9. Despite of not finding surrogate proteins of EV-isolates, NTA found particles in high amounts and the proteomic analysis was able to find many EV-related functional enriched groups, both indicative of presence of EVs in the samples (Figure 16 and 22).

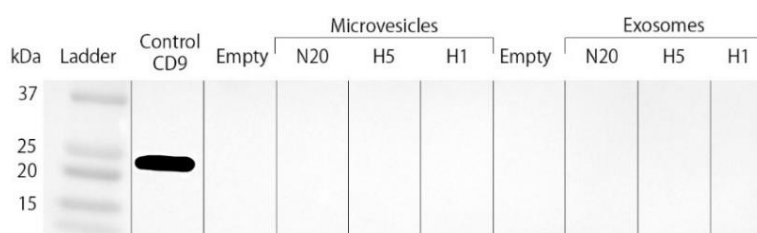


Figure 14. WB targeting CD9 protein in EV-isolated samples. Only the positive control was detected. N20 – Normoxia 20% oxygen. H5 – Hypoxia 5% oxygen. H1 – Hypoxia 1% oxygen.

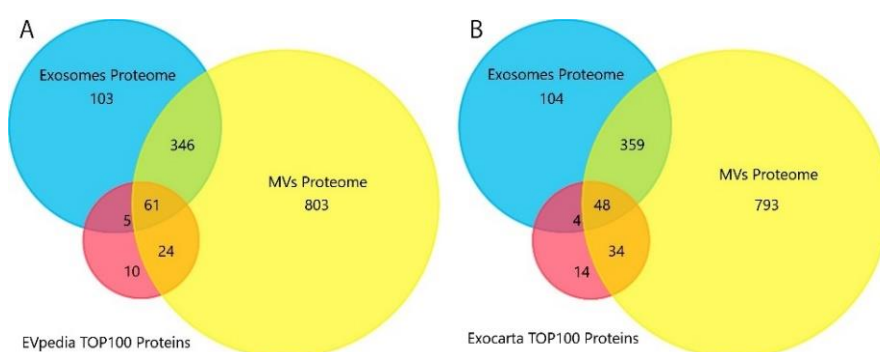


Figure 15. (A) Exosomes and MV proteomes comparison with the TOP 100 most commonly found proteins from the EVpedia database. (B) Exosomes and MV proteomes comparison with the TOP 100 most commonly found proteins from the Exocarta database.

To further investigate the EV-isolation, a comparison of the identified proteins in the microvesicles and exosomes samples against EVpedia TOP100 (Figure 15A) and Exocarta TOP101 (Figure 15B) databases was performed. This was carried out to see if these samples contained



common EVs proteins. Many of the proteins from Exocarta and EVpedia were found in both, MV and exosomes proteome (61/100 in EVpedia and 48/100 in Exocarta). In total, 90% and 86% proteins were matched in both EV-subpopulations in each one of the databases, respectively (Figure 15A and 15B). Therefore, suggesting the isolation of EVs.

## 4.2. Hypoxia drives changes in extracellular vesicles

WB was carried out to detect a specific hypoxia-related protein, HIF-1 $\alpha$ . Secondly, to examine whether hypoxia drives changes into the EV-concentration and EV-size, analysis of these were carried out by NTA. Thirdly, MS analysis determined whether hypoxia induce functional changes into the EV-proteome.

### 4.2.1. Hypoxia and HIF-1 $\alpha$ content in extracellular vesicles

WB analysis was performed to see if HIF-1 $\alpha$  forms part of the cargo of EVs under hypoxic conditions and if its concentration increases under hypoxic conditions. When WB was performed, none of the EV samples showed any detectable amount of HIF-1 $\alpha$  protein. The positive control was successfully identified (Figure 16A). This might suggest that HIF-1 $\alpha$  is not packed in the EVs or it might also be because low protein concentrations were loaded, resembling the same issue as with CD9 WB. Other logical explanation is the fast degradation of HIF-1 $\alpha$  protein, because of its extremely short half-life, therefore, making its discovery intricate. HIF-1 $\alpha$  detection is an issue that many other research groups faced before and still drags the research within this area<sup>23,146</sup>. However, when comparing the identified proteins in each of the different conditions of the two EV-subpopulations against the HypoxiaDB up-regulated proteins, we could see an increase in the hypoxia-related proteins in the hypoxic samples compared to the ones cultured under normoxia for both EV-subpopulations (Figure 16B). Therefore, proving the successful influence of the different oxygen conditions over the proteome composition of EVs regarding hypoxia-related protein content.

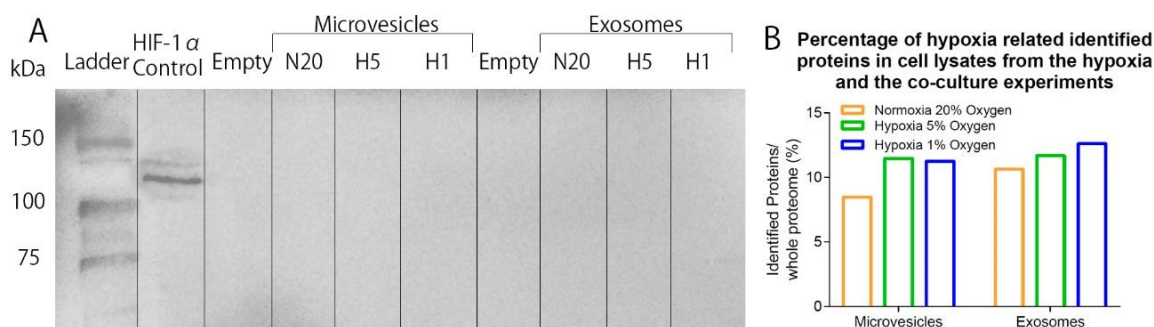


Figure 16. (A) WB targeting HIF-1 $\alpha$  in EV-isolated samples. Only the positive control was detected. (B) Protein identification against HypoxiaDB up-regulated proteins.

### 4.2.2. Extracellular vesicles release is affected by hypoxic conditions

MVs and exosome concentration (Figure 17) and particle size (Figure 18) was investigated by NTA analysis to see if oxygen levels have any influence over EV-release. The particle concentration found in MV samples ranged between  $0,68 - 2,30 \times 10^{10}$  particles/mL (Figure 17B) and exosome samples ranged between  $0,75 - 2,69 \times 10^9$  particles/mL (Figure 17A). No statistical significance has been found when comparing particle concentrations from the different conditions in MV and exosome samples, however, a trend is clearly visible. In the MV isolates, when the oxygen levels are reduced, the concentration of MVs diminishes (Figure 17B), while in

the exosome group concentration increases when hypoxia is aggravated (Figure 17A). Therefore, we can observe an opposite tendency in the production of EVs in both groups (Figure 17). Hypoxia might have some influence in the release of EVs.

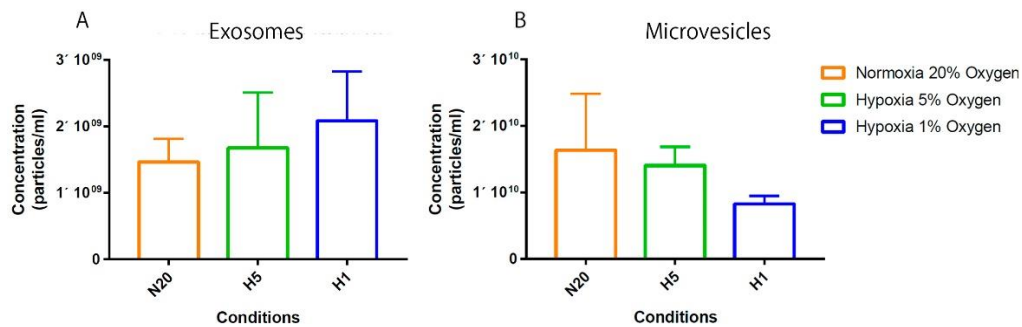


Figure 17. Comparison of (A) exosomes and (B) microvesicles production under different oxygen concentrations (N20 = 20% oxygen; H5 = 5% oxygen; H1 = 1% oxygen).

When comparing mean and mode size of MVs (Figure 18A and 18C) and exosomes (Figure 18B and 18D) a trend towards a larger size in MVs as the hypoxia is enhanced is found. Statistical significant ( $p < 0.05$ ;  $p = 0.037$ ) data was obtained when comparing the mode size of 20% oxygen and 1% oxygen groups (Figure 18C). However, no differences were found in the exosomes and the MVs mean size comparison.

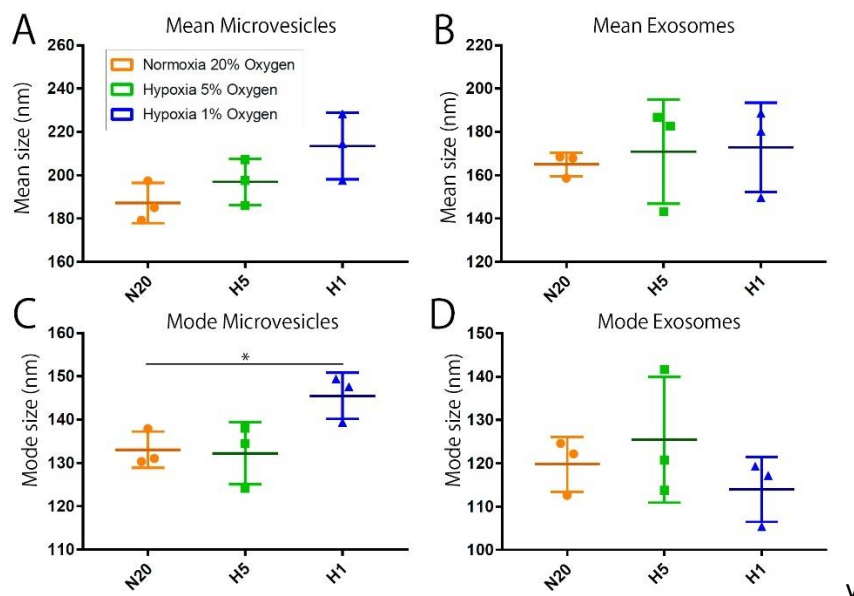


Figure 18. Comparison of mean (A and B) and mode size (C and D) distributions in microvesicles (A and C) and exosomes (B and D). N20 = 20% oxygen; H5 = 5% oxygen; H1 = 1% oxygen. \* = statistical significance. Statistical significance found when comparing N20 Vs H1 mode size of MVs ( $p < 0.05$ ;  $p = 0.037$ ).

#### 4.2.3. Hypoxia drives changes in the extracellular vesicle protein composition

MS analysis was performed to further understand the cargo contained within SCLC cell-derived EVs and investigate the possible influence of hypoxia in the protein composition of EVs. A total of 1,234 proteins were identified in the MVs samples while 515 proteins were identified within the exosomes samples. The proteins identified in the MVs and exosomes samples shared 407 proteins while expressing 827 and 108 unique proteins respectively (Figure 19A). Exosomes shared 79% of its proteome with MVs, and MVs shared 33% of its proteome with exosomes.

Assuming that some contamination across the two EV-subpopulation is present as ultracentrifugation is unable to perfectly isolate MVs and exosomes, we can suggest that even MVs and exosomes have a completely different biogenesis, they resemble each other's composition at some extent. Additionally, we saw that the proteome of MVs is larger than the one contained within exosomes.

Of all the 1,234 proteins identified in the MVs samples, 341 were shared proteins among the different cell culture conditions (Figure 19B). The culture conditions contained 1,054 (558 unique proteins), 397 (29 unique proteins) and 622 (149 unique proteins) proteins for the N20, H5 and H1 conditions, respectively (Figure 19B). In contrast, from the 515 proteins identified within the exosomes samples, 289 of those were shared within the three different sample conditions (N20, H5 and H1) (Figure 19C). The culture conditions contained 446 (124 unique proteins), 391 (36 unique proteins) and 322 (0 unique proteins) proteins, respectively (Figure 19C). The EV-samples from hypoxic conditions had a lower amount of proteins, expressing a smaller proteome and a reduced composition in unique proteins when compared with the EV-samples from normoxia conditions.

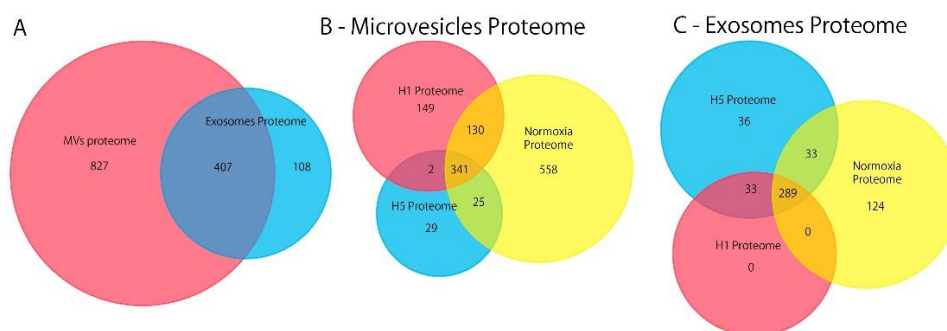


Figure 19. Venn diagrams representing the number of proteins identified in the extracellular vesicle samples obtained from cell culture under normoxia 20% (N20, hypoxia 5% (H5) and hypoxia 1% oxygen (H1) conditions. (A) MV and Exosome proteomes. (B) Microvesicle proteome divided into the three conditions (N20, H5 and H1). (C) Exosomes proteome divided into the three conditions (N20, H5 and H1).

#### 4.2.4. Hypoxia drives protein profiles of microvesicles and exosomes

To examine what kind of carcinogenic functions the identified proteins are involved in, comparison of the proteins against angiogenesis, metastasis and invasiveness, motility and SCLC specific biomarkers self-curated databases (Figures 20A, 20B, 20C and 20D, respectively) was performed. MVs samples express a higher number of proteins driving the main characteristics of the aggressive phenotype when compared with exosomes (Figure 20). However, when the proteins driving each carcinogenic phenotype found in each EV-subpopulation are compared against their own proteome, same protein enrichment is found for MVs and exosomes (Appendix E.1, Figure 2).

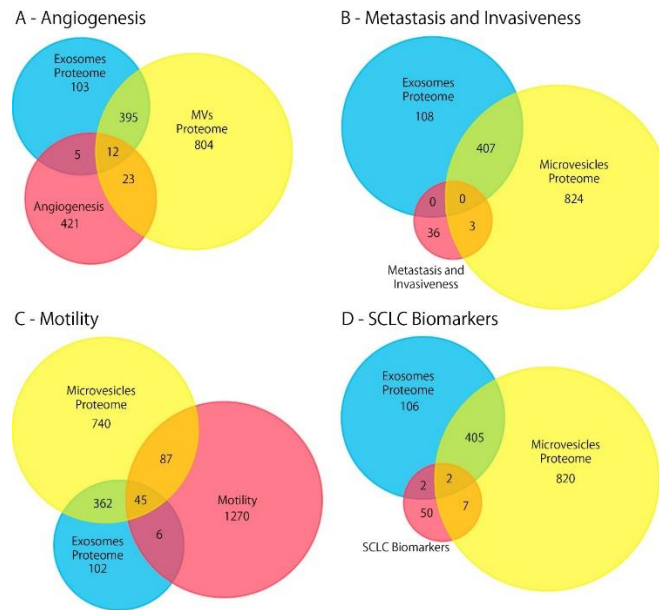


Figure 20. Venn diagrams representing proteins identified in the microvesicle and the exosome samples compared with self-curated databases including proteins driving (A) angiogenesis, (B) metastasis and invasiveness (C) motility and (D) SCLC specific biomarkers.

Also, comparison of the hypoxic and normoxic proteome of MVs and exosomes against the databases was performed. We found that the MV-hypoxic proteome conserved proteins regarding angiogenesis, metastasis and invasiveness and motility even though the proteome is reduced compared with the normoxic one (Figure 21). Therefore, hypoxic MVs are richer in pro-carcinogenic protein content when compared with normoxic MVs (Figure 21). To further investigate how hypoxia drives changes into the cargo of EVs and what implications this might have at a functional cellular level, specific comparison of the protein abundances needs to be considered.

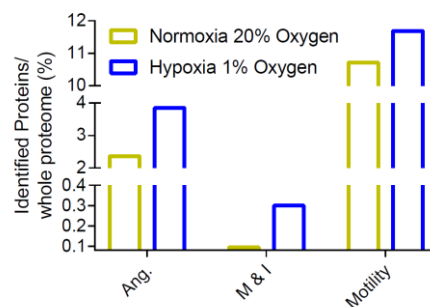


Figure 21. Comparison of the angiogenic, metastatic and invasive and motility proteins identified in the hypoxia and normoxia samples of MVs.

#### 4.2.5. Hypoxia drives microvesicles and exosomes proteome composition

Comparison of protein abundances across the different oxygenation conditions for MV and exosome samples showed three different protein expression patterns grouped according to their oxygenation level (Figure 22). This suggest that some proteins were differently packed in EVs under the three oxygenation conditions and that their expression patterns are driven by oxygen levels. This is true for both MVs (Figure 22A) and exosomes (Figure 22B).

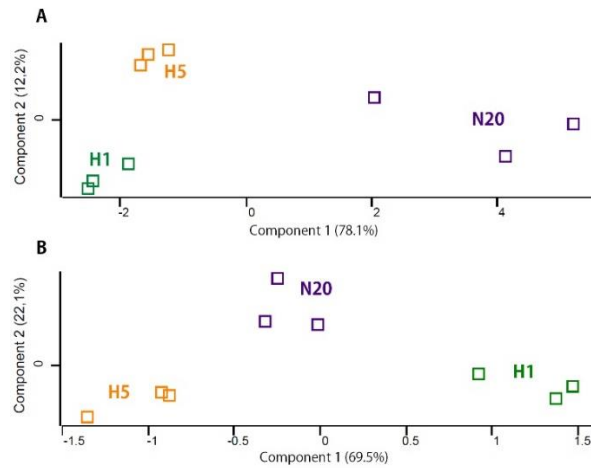


Figure 22. (A) Principal component analysis (PCA) representing protein expression between normoxia 20% (N20), hypoxia 5% (H5) and hypoxia 1% oxygen (H1). (B) PCA representing protein expression between normoxia 20% (N20), hypoxia 5% (H5) and hypoxia 1% oxygen (H1). MV – microvesicle. EXO – exosome.

ANOVA ( $p = 0.05$ ,  $S0 = 0$ ) was then performed to look at the differences between the protein abundances of different oxygenation conditions for MV and exosome samples. A total of 76 and 39 proteins were differentially expressed when comparing the different oxygenation conditions in MV and exosome samples, respectively (Appendix E1.1.). To better visualize these differences, hierarchical clustering of these proteins was performed. 4 clusters were visible in both, MVs (Figure 23A) and exosomes (Figure 23B). The clusters grouping resemble the oxygenation conditions, therefore, confirming the power of oxygen towards inducing a specific functional proteome shift.

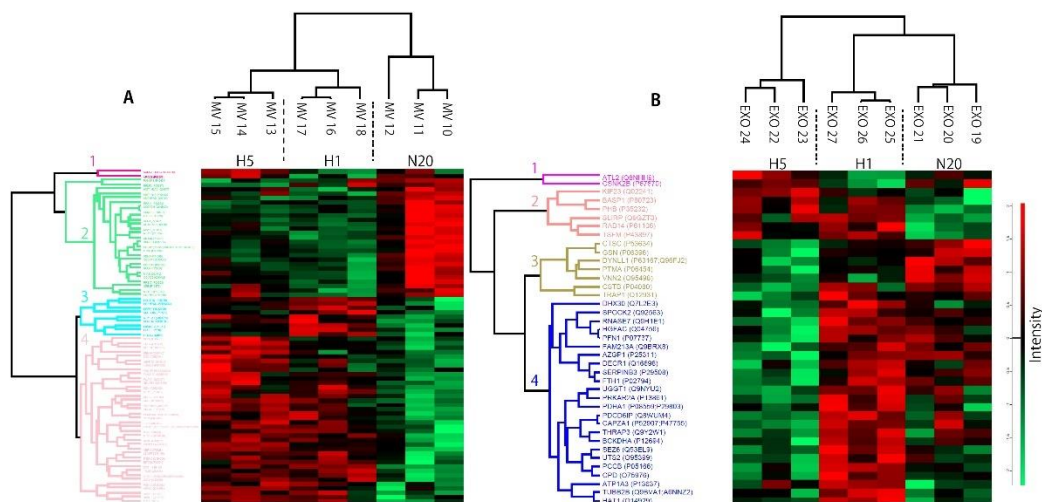


Figure 23. Hierarchical clustering analysis of significant (ANOVA) proteins extracted from (A) microvesicles and (B) exosomes.

When the clusters were analysed by STRING (SEA), different enrichments were found (Appendix E.1.2., Table 5 and 6). Proving that there are more pathways involved in these protein clusters. The enrichment groups detected proved that our samples contained EVs:

- The Extracellular exosome function (GOCC) was found in both, MVs cluster two and exosomes cluster three. This is an additional proof that we isolated the EVs correctly, even though, WB analysis was unable to find CD9 protein.

The most relevant functional enrichment groups found in STRING were:

- In the MV-STRING analysis (Appendix E.1.2., Table 5), clusters two and four showed enrichment while cluster one and three did not. In cluster two, ribosomal proteins were found to be highly expressed in normoxic conditions while underexpressed in hypoxia. Regarding cluster four, a wide variety of functional enrichments are found, but all fall within the same group of proteins, the ephrin receptor proteins (EPH), highly expressed in hypoxia compared with normoxia and profoundly implicated in carcinogenesis (Figure 23A).
- Regarding exosomes (Appendix E.1.2., Table 6), clusters one and two showed no functional enrichment. In cluster three, functional enrichment suggests that there is a positive regulation of apoptosis-related signalling pathways (GOBP) in normoxia, while it is downregulated in the hypoxic conditions (Figure 23B). Additionally, Dynein light chain protein (DYNLL) was found, which are involved in transport, motility and regulation of the nitric oxide synthase (NOS) activity.

Using STRING, protein-protein interaction (PPI) networks of the different clusters were obtained, graphically representing the linkages between all the proteins of the 4 clusters together from microvesicles and exosomes (Appendix E.1.4., Figure 3).

Using DAVID, 32 and 18 clusters were found within the MV and exosome significant proteins, respectively (Appendix E.1.3, Table 7). The clusters containing essential information were the following:

- Regarding MVs, only the first cluster was significantly enriched. The results from DAVID-MV resemble the ones obtained in STRING analysis, in which EPH receptor activity and nucleotide binding were found enriched.
- Regarding exosomes, enrichment of the oxidoreductase activity, acting on the aldehyde or oxo group of donors, disulphide as acceptor GOMF pathway was enriched.

To further look at where the functional differences between groups were, independent samples T-test ( $p = 0.01$ ,  $S0=0.1$ ) was performed (Appendix E.1.5., Table 8 (MV) and 9 (exosomes)). No enrichment groups were found in STRING and DAVID within the significant proteins. The main idea that can be

extracted when comparing the significant protein functions is that most of the proteins up-regulated in normoxic conditions are normally implicated within tumour suppression pathways, or were found in benign tumours, while the proteins over-expressed in hypoxic conditions (H5 and H1) were normally correlated with bad prognosis of the patient and cancer progression. Comparison of MVs N20 and H5 conditions found that receptor-like protein 2 and fatty acid binding protein 7 are highly expressed in normoxic conditions, while collagen 5 alpha-1, high mobility group AT-hook 1 (HMGA1) and cysteine and glycine-rich protein 1 were found to be up-regulated under hypoxic conditions.



### 4.3. Cell lysate results

#### 4.3.1. Detection of HIF-1 $\alpha$ in the cell lysate

To determine the effect of the hypoxic settings during the hypoxia experiment, detection of the specific protein HIF-1 $\alpha$  by WB was carried out. However, no detectable levels of the protein were identified apart from the positive controls (Figure 24). This might be due to a low protein concentration loading and the short half-life of HIF-1 $\alpha$  or to the fact that this protein is hard to detect due to its fast degradation as stated before.

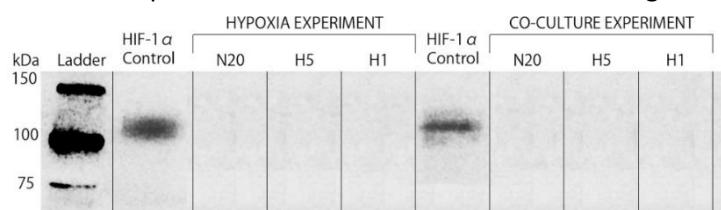


Figure 24. Western blot of the cell lysates from the hypoxia and the co-culture experiment targeting HIF-1 $\alpha$  protein.

To further determine the influence of hypoxia in the cell lysate proteome, comparison of the proteins identified against the up-regulated proteins from the HypoxiaDB was performed. This was carried out to determine whether the different oxygenation conditions do in fact have any effect on the regulation of the hypoxic related proteins within the cell's proteome (Figure 25A). Furthermore, to examine if the exosomes originated under different oxygenation conditions induce any substantial shift over the hypoxic-proteins of the co-cultured cells, comparison of the cell lysate proteome against HypoxiaDB up-regulated proteins was performed (Figure 25B). Statistical significant data is obtained when comparing the number of proteins identified within the proteome of normoxic and hypoxic conditions of cell lysates in the hypoxia experiment ( $p < 0.01$ ) and the co-culture experiment ( $p = 0.03$ ) (Figure 25C). Therefore, proving the effect of the hypoxic setting over the cells proteome and the potential of exosomes reprogramming the cell resembling the parental cell conditions, in our case inducing up-regulation of the hypoxia-related proteins (Figure 25).

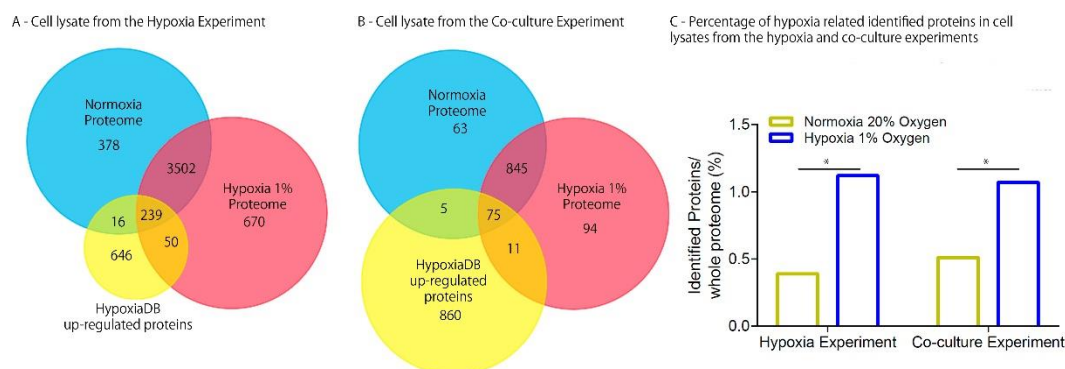


Figure 25. Comparison of the identified proteins in the cell lysates from (A) the hypoxia experiment and (B) the co-culture experiment against the up-regulated proteins from HypoxiaDB. (C) Comparison of the hypoxia up-regulated proteins found in (A) ( $p = 0.01$ ) and (B) ( $p = 0.03$ ). \* = statistically significant.

#### 4.3.2. Effect of hypoxia on cells proteome expression

A total of 4,832 proteins were identified in the cell lysate samples from the hypoxia experiment, of which, 3,644 were shared proteins between the different cell culture conditions. The proteins identified in the different conditions were: 3,963 (319 unique proteins), 3,901 (257 unique proteins) and 4,256 (612 unique proteins) proteins for the N20, H5 and H1 conditions, respectively (Figure 26). H1 condition expresses a bigger proteome than cells cultured under normoxic and hypoxia physiologic conditions.

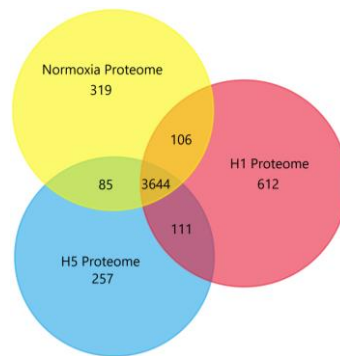


Figure 26. Venn diagrams representing the number of proteins identified in the hypoxia experiment cell lysates under normoxia 20% (N20, hypoxia 5% (H5) and hypoxia 1% oxygen (H1) conditions.

We performed a comparison of the different cell lysate proteomes identified against angiogenesis, motility, cell proliferation and metastasis self-curated databases (Figure 27). The hypoxic proteome (H1, 1% oxygen) includes a larger number of the proteins driving angiogenesis, metastasis and invasiveness, motility and proliferation pathways in carcinogenesis when compared with the normoxic proteome (Figure 27). Finding more proteins related to these mechanisms suggest that these pathways might be enhanced under hypoxia.

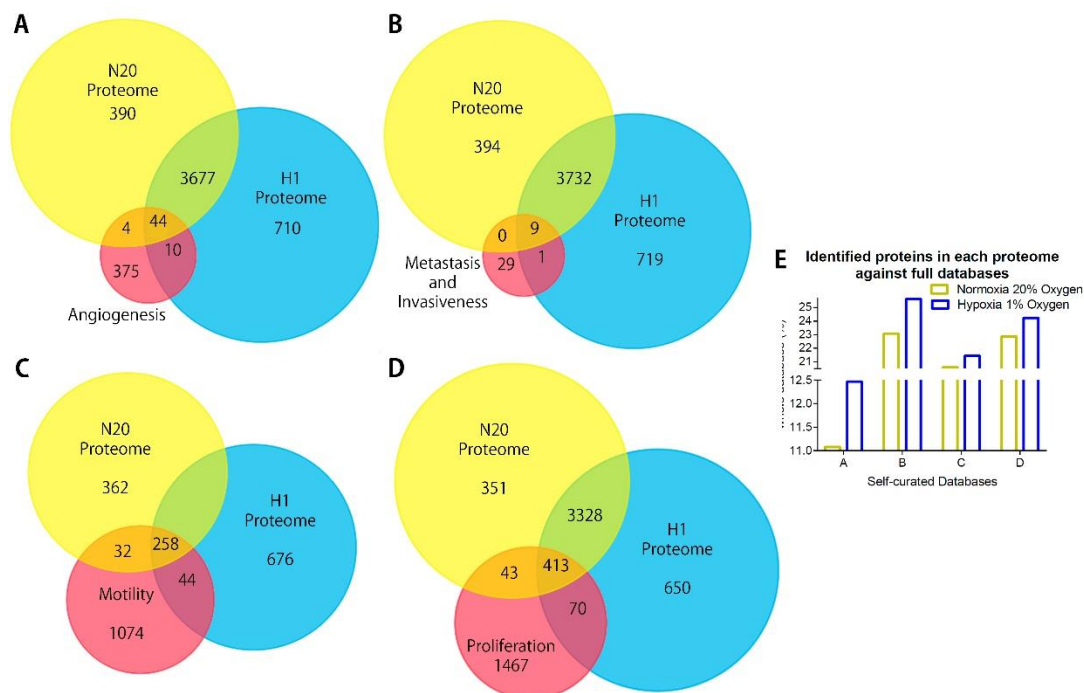


Figure 27. Venn diagrams representing the proteins identified in the normoxic (N20) and the hypoxic (H1) conditions are compared with self-curated databases. These databases include proteins driving (A) angiogenesis, (B) metastasis and invasiveness, (C) motility and (D) cell proliferation. (E) Comparison of the percentage of the common proteins within the database and the normoxia and hypoxia proteomes from graphs (A), (B), (C) and (D).

#### 4.3.3. Proteome composition of h-69 cancer cells cultured under different oxygenation conditions

Comparison of protein abundances across the three conditions (N20, H5 and H1) revealed differences in protein expression according to the different oxygenation conditions (Figure 28). This confirms that oxygen levels induce a proteome shift in H69 cell line, therefore, expressing a different protein profile.



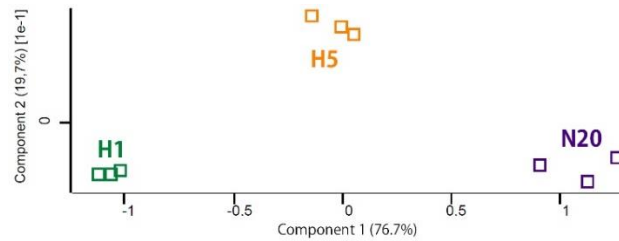


Figure 28. PCA between normoxia 20%, hypoxia 5% and hypoxia 1% oxygen conditions.

ANOVA (FDR = 0.05, 250 randomizations, S0 = 0) was performed to look at the differences between the functional protein groups in different oxygenation conditions. Significant differences in the expression of 23 proteins was found (Appendix E.2.1.). Fisher exact test showed an enrichment of 11 functions (Table 6) within these 23 proteins. Therefore, a common linkage between the proteins and their related functions was found. Most of the functions are related to metabolic processes, especially glucose, showing a shift in the metabolic response of the cells when hypoxic conditions take place.

Table 6. Fisher exact test functional enriched results by GSEA (gene set enrichment analysis). GOBP – Go-term biological processes. GOMF – Go-term molecular functions. KEGG – KEGG pathways. False discovery ratio (FDR) – Benjamini-Hochberg.

FISCHER EXACT TEST ENRICHED FUNCTIONS		FDR
GOBP	Gluconeogenesis	0.0017
	Hexose biosynthetic process	0.0034
	Monosaccharide biosynthetic process	0.0069
	Cellular carbohydrate biosynthetic process	0.0157
	Alcohol biosynthetic process	0.0157
	Glucose metabolic process	0.0063
	Hexose metabolic process	0.0134
	Small molecule biosynthetic process	0.0034
GOMF	Catalytic activity	0.0008
KEGG	Alanine, aspartate and glutamate metabolism	0.0168
	Glycolysis/Gluconeogenesis	0.0004

To better visualize the expression differences across these 23 proteins, hierarchical clustering of these proteins was performed (Figure 29). Proteins were grouped within three main clusters (Figure 29). The 3 samples of each oxygenation condition (N20, H5 and H1) were separated according to similar patterns in protein expression. This means that the oxygen levels drive the expression of these proteins, therefore, inducing specific changes in H69 cells proteome.

Functional enrichment (GSEA, FDR = 0.05) of the clusters from the hierarchical analysis was performed, showing an upregulation of the glycolysis/Gluconeogenesis KEGG pathway (Figure 29, cluster 2). This finding confirms the Fisher exact test results. No enrichment was found in cluster 1 and 3 (Figure 29). If we take into consideration the Fisher exact test and the hierarchical analysis results, we can see that hypoxia shifts the protein profile of H69 cells enhancing its metabolism, especially the glucose-related pathways. Therefore, inducing a metabolic reprogramming of the cell towards energy generation due to an increased energy demand to sustain their enhance pro-carcinogenic phenotype.

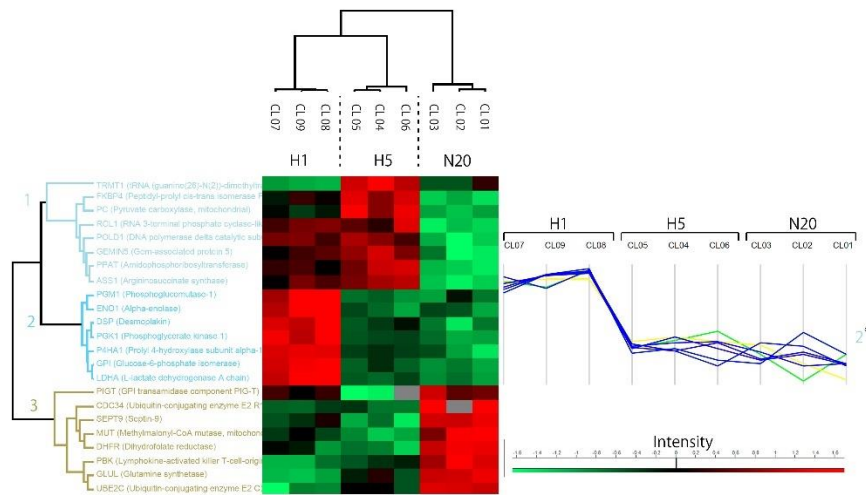


Figure 29. Hierarchical clustering analysis representing significant proteins extracted from ANOVA statistical analysis and the protein profile of the proteins contained within the GSEA enrichment found (Glycolysis/Gluconeogenesis (KEGG pathway)) - GSEA (FDR = 0.012).

Furthermore, when the clusters were analysed by STRING (SEA) and DAVID (MEA, 10 clusters found), different functional groups resembling the ones found in the Fisher exact test and GSEA showed up. Suggesting that there are more pathways involved behind these proteins:

- STRING (Appendix E.2.2., Table 10):
  - In cluster one, biosynthesis of amino acids and their metabolism is enhanced in hypoxic conditions (KEGG Pathway).
  - In cluster two, enhanced production of exosomes (GOCC), enhanced glycolysis/ gluconeogenesis and other metabolic processes regarding synthesis of amino acids, proteins and diverse energy molecules (GOBP and KEGG).
  - In cluster three, glyoxylate and dicarboxylate metabolism, involved in the biosynthesis of carbohydrates from fatty acids (KEGG Pathway).
- DAVID (Appendix D, E.2.3., Table 11):
  - In cluster one, an enrichment of the glycolysis/Gluconeogenesis (KEGG Pathway) and glycolysis (GOBP) were found.
  - In cluster two, glucose metabolic process (GOBP) and gluconeogenesis (GOBP) enrichments were found. These reiterative findings confirm the glucose metabolic enhanced activity portrayed by cells grown under hypoxic conditions.

Using STRING, a protein-protein interaction (PPI) network of the different clusters was obtained, graphically representing the linkages between proteins of the three different clusters alone (Appendix E.2.4., Figure 4), as well as, all the proteins of the 3 clusters together (Appendix E.2.4., Figure 5). This can depict the proteins involved within the same functional enriched category. The richest PPI occurs in cluster two, in which 5 proteins are related to most of the categories found within that cluster, indicating a close functional linkage (Appendix E.2.4., Figure 4B).

To further look at where the functional differences between groups were, independent samples T-test (FDR = 0.05, 250 randomizations, S0 = 0.1) was performed (Appendix E.2.5.). Hereafter, visualization with volcano plots (FDR = 0.05) was performed (Figure 30). The volcanos represent on the left side, in blue, the down-regulated proteins and on the right side, in red, the up-regulated proteins of N20 (Figure 30A against H1 and 30B against H5) and H5 (Figure 30C against H1). As it can be seen in the volcano plots, the largest amount of

significant proteins is contained within the N20 Vs H1 (Figure 30A) and N20 Vs H5 conditions (Figure 30B). This fact reconfirms the idea that a major shift in the proteome occurs when hypoxic conditions take place (Figure 30).

Independent analysis of the up-regulated and down-regulated proteins was performed for each volcano plot by STRING (Appendix E.2.6., Table 12). This revealed that most of the pathways identified fall again within the metabolic processes, with a predominance of glycolysis, gluconeogenesis and carbon metabolism (GOBP and KEGG Pathway) when comparing N20 Vs H1 (Figure 30A). No enrichment was found when comparing N20 Vs H5, despite of the high amount of significant proteins found. When the different hypoxic conditions (H5 Vs H1) were examined, an enhancement in glycolytic processes and nicotinamide adenine dinucleotide (NAD) metabolic process (GOBP) was found increased in H1 when compared with H5 (Figure 30C), suggesting that as hypoxic conditions are worsen, glucose-related metabolic processes are progressively increased.

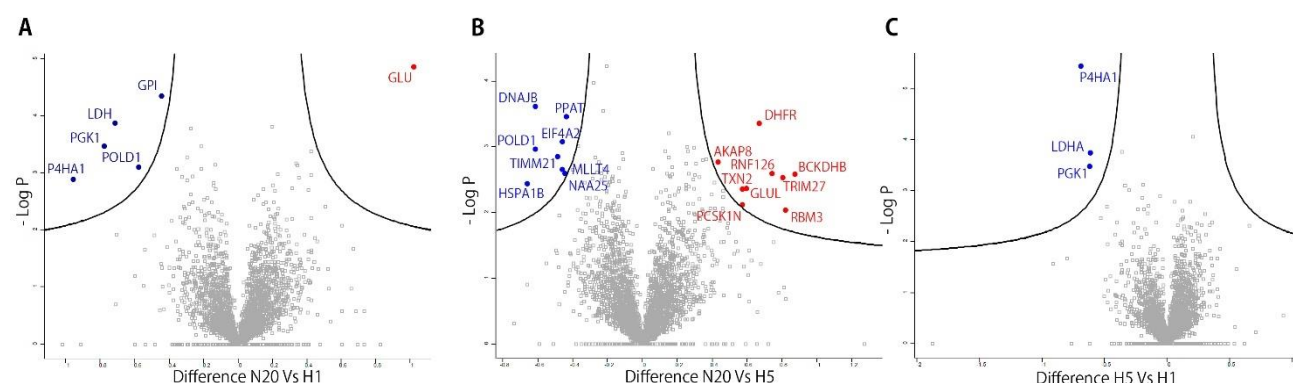


Figure 30. Volcano plots representing (A) N20 Vs H1 (B) N20 Vs H5 and (C) H5 Vs H1 proteins expressions. Blue – up-regulated proteins of the main condition (first in the comparison). Red – down-regulated proteins of the main condition (first in the comparison). FDR = 0.05.

#### 4.4. Co-culture experiment results

##### 4.4.1. Exosomes originated under hypoxic conditions induce proteome shift of SCLC cells when co-cultured

To investigate whether the exosomes originated under different oxygenation conditions when co-cultured can induce significant proteome changes with functional pro-carcinogenic consequences in H69 cells, MS analysis was performed. A total of 1,117 proteins were identified in the cell lysate samples when co-cultured with exosomes. 887 proteins were shared across the different cell culture conditions. The proteins identified were: 988 (49 unique proteins) for N20, 1,025 (50 unique proteins) for H5 and 985 (24 unique proteins) proteins for H1 condition (Figure 31). The cells co-cultured with exosomes from H1 condition had a higher amount of proteins expressed and contained a higher amount of unique proteins, therefore, expressing a bigger proteome than the cells cultured with normoxic and hypoxic-physiological condition-derived exosomes (N20 and H5) (Figure 31). This resembles the results obtained in the cell lysate from the hypoxia experiment, in which the H1 condition expressed a larger proteome.

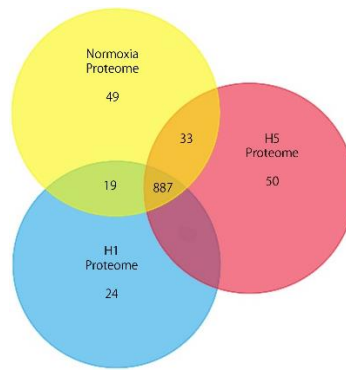


Figure 31. Venn diagrams representing the amount of proteins identified in the cell lysates co-cultured with exosomes from normoxia 20% (N20), hypoxia 5% (H5) and hypoxia 1% oxygen (H1) conditions.

Comparison of the different normoxia and H1 conditions cell proteome against angiogenesis, motility and cell proliferation self-curated protein databases was carried out (Figure 32). Co-culture of cells with exosomes from H1 conditions express a larger number of proteins driving the main characteristics of the aggressive carcinogenic phenotype (Figure 32). These results also match the results obtained from the proteomic analysis of the cell lysate from the hypoxia experiment, therefore, we can see that exosomes originated under hypoxic conditions might be behind this proteome shift towards a more enhanced pro-carcinogenic phenotype.

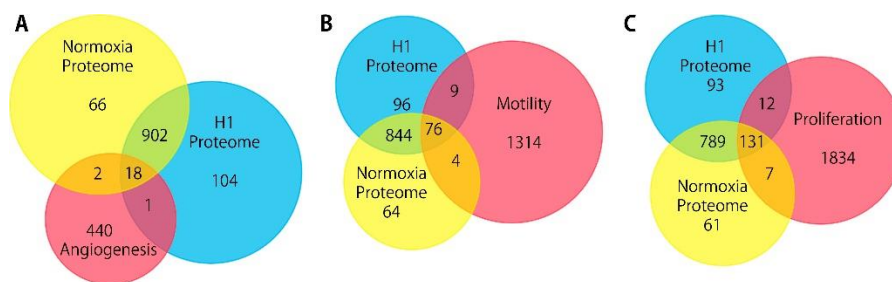


Figure 32. Venn diagrams of the proteins identified in the cell lysate of H69 cells co-cultured with exosomes from normoxic (N20) and hypoxic (H1) condition compared against self-curated databases including proteins driving (A) angiogenesis, (B) motility and (C) cell proliferation are represented.

#### 4.4.2. Exosomes originated under hypoxic conditions induce changes in the proteome composition of SCLC cells when co-cultured

When comparing the protein abundances across the cells co-cultured with exosomes from the three conditions (N20, H5 and H1), three different protein expression groups were found, resembling the different origin of the exosome (Figure 33). This indicates that the pro-carcinogenic profiles expressed by cells are highly affected by exosomes and that exosomes induce similar changes in the recipient cell mimicking the parental cell response towards hypoxia.

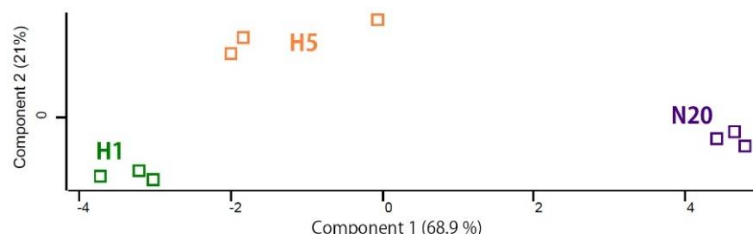


Figure 33. PCA representing protein expression of H69 cell lysate. These cells were co-cultured with exosomes originated under normoxia 20% (N20, including CL01, CL02 and CL03), hypoxia 5% (H5, including CL04, CL05 and CL06) and hypoxia 1% oxygen conditions (H1, including CL07, CL08 and CL09). CL – cell lysate.

To elucidate which proteins are involved in this proteome shift and if they have any pro-carcinogenic influence, ANOVA ( $P = 0.01$ ,  $S0 = 0$ ) was performed. 34 significant proteins were found (Appendix E.3.1.). Fisher Exact Test ( $P = 0.02$ ) showed an enrichment of 10 functions (Table 7). Most of the enriched functions were related to negative regulation of immune cells (GOCC), apoptotic (GOBP) and cell death processes (GOBP) (including kinase regulator activity linked with necroptosis, GOMF). This can be translated into an increase in the survival response of the cells. Additionally, histidine metabolism (KEGG pathways) is present, suggesting another linkage with metabolic implications.

Table 7. Fisher exact test functional enriched results by GSEA (general set enrichment analysis). GOBP – Go-term biological processes. GOCC – Go-term cellular compartment. GOMF – Go-term molecular functions. KEGG – KEGG pathways.

FISCHER EXACT TEST ENRICHED FUNCTIONS		p-value
GOBP	Regulation of protein tyrosine kinase activity	0.000569
	Regulation of gastrulation	0.00531
	Negative regulation of fibroblast proliferation	0.00531
	Negative regulation of programmed cell death	0.00762
	Negative regulation of apoptosis	0.00762
GOCC	Phagocytic cup	0.00326
	Platelet alpha granule	0.00531
	Cytoplasmic membrane-bounded vesicle	0.00725
GOMF	Kinase regulator activity	0.00877
KEGG	Histidine metabolism	0.00326

Within these 10 functional groups, a total of 34 proteins were differentially expressed when comparing the different co-culture conditions with exosomes originated under various oxygenation conditions. To better visualize these differences, hierarchical clustering of these proteins was performed (Figure 34). Three main clusters are visible, matching the exosome groups with which the cells were co-cultured with (Figure 34). This indicates that the exosomes shift the proteome of the cells resembling their provenance. Therefore, the oxygenation conditions in which the exosomes were produced can also provide exosomes with the ability to reprogramme the cell resembling the parental cell.

Functional enrichment (GSEA,  $FDR = 0.1$ ) of the clusters was performed, showing an upregulation of the vesicle membrane GOCC in cluster 2 (Figure 34). No significant enrichment was found in cluster 1 and 3 (Figure 34).

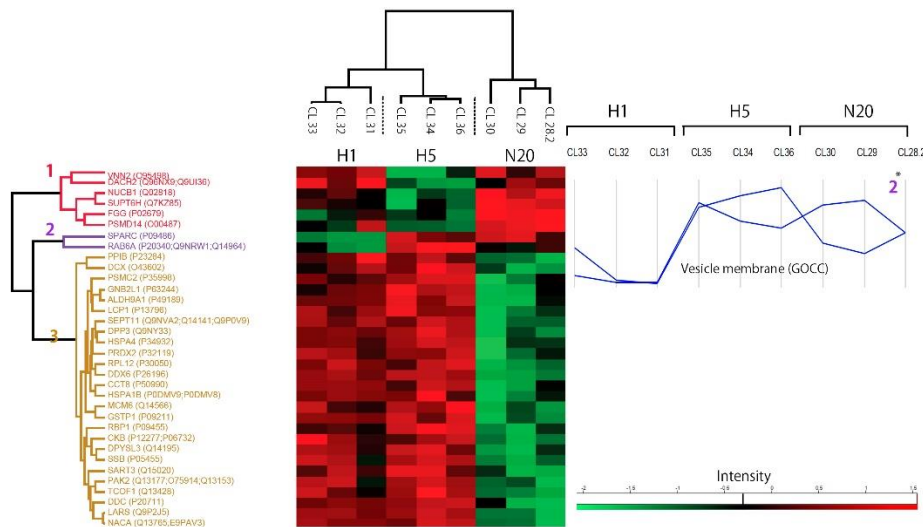


Figure 34. Hierarchical clustering analysis representing significant proteins extracted from ANOVA statistical analysis. Enrichment analysis of the clusters is attached. Protein profile of the enriched proteins within the Vesicle membrane (GOCC) (GSEA = 0.1) cluster is included.

The clusters were analysed by STRING (SEA). Different functional groups showed up (Appendix E.3.2., Table 13). STRING analysis suggests that there might be more pathways involved behind these proteins, including:

- In cluster two, enrichment of extracellular exosome, vesicle-mediated transport (GOBP) as well as cytoplasmic membrane-bound vesicle suggests an increased activity in EVs related pathways. Also, guanosine triphosphatase activity, myosin V binding and guanosine triphosphate-binding are found within GOMF, these are related to EVs biogenesis. These pathways were increased in hypoxic-physiologic conditions (H5).
- In cluster three, we found again the extracellular exosome, membrane-bound vesicle and extracellular region part (GOCC) enhanced in hypoxic conditions (H5 and H1) which is related to EVs biogenesis. Regarding EVs transport and cargo packing, we found the retrograde vesicle-mediated transport, Golgi to endoplasmic reticulum (GOBP) function. We could also see an enrichment of ribonucleotide and ribonucleoside bindings (GOMF) and symbiosis, encompassing mutualism through parasitism (GOBP).

Using STRING, protein-protein interaction (PPI) network of the different clusters was obtained, graphically representing the linkages between proteins of the three different clusters alone (Appendix E.3.3., Figure 6) as well as, all the significant proteins identified by ANOVA (Appendix E.3.3., Figure 7). The cluster with more interaction is the number three, which also contains a larger amount of proteins.

To further look at where the functional differences between groups were, independent samples T-test ( $p$ -value = 0.01,  $S0 = 0$ ) was performed. 62 proteins were found to be significant (Appendix E.3.4., Table 14). Analysis of the protein expression groups by STRING resulted in:

- Overexpression of the Ribosome (KEGG Pathways), nucleotide binding, poly(A)-RNA binding, myosin binding (GOMF) enrichment functions was found in H1 compared with N20. We can see an overexpression of the ribosome, which is the protein factory of the cell, therefore we could expect an increase in the number of proteins, as confirmed before in the Venn diagrams (Figure 31).
- When comparing N20 against H5, we could find that H5 overexpressed hypermethylation of CpG island and cellular response to interleukin-3 (IL-3) (GOBP). Hypermethylation of the CpG island is closely correlated with the onset of the pro-carcinogenic phenotype. Furthermore, interleukin 3



response is known to mediate in angiogenesis-related pathways. These findings suggest that when hypoxic conditions take place the cells might shift their behaviour towards a pro-carcinogenic phenotype.

Using DAVID, 11 clusters were found, of which only the first three were valid (DAVID Score = 2.87, 2.8 and 2.6, respectively). The following enrichments were obtained:

- In cluster one, smooth muscle contractile fiber (FDR =  $5.3E-2$ ), actin cytoskeleton (FDR =  $1.1E-1$ ) (GOCC). Indicating that overexpression of the actin proteins is found.
- In cluster two, nucleotide binding (FDR =  $2.0E-2$ ) (GOMF).
- In cluster three, RNA binding (FDR =  $2.0E-1$ ) (GOMF). Overexpression of proteins which interfere with RNA.

Hereafter, visualization with volcano plots (FDR = 0.05) was performed (Figure 35) (Appendix E.3.5.). The volcanos represent on the left side, in blue, the down-regulated proteins and on the right side, in red, the up-regulated proteins of N20 (Figure 35A against H1 and 35B against H5). By looking at the function of the significant proteins found in the volcano plots independently, further information could be extracted (Figure 35). Probable ATP-dependent RNA helicase DDX6 protein (DDX6) is highly expressed in both H1 and H5, this protein is an enzyme deeply implicated in many cellular processes related in RNA secondary structure alteration (Figure 35). We also found nebulin-related-anchoring protein (NRAP) and 26S proteasome non-ATPase regulatory subunit 14 or Rpn11 (PSMD14 or RPN11) proteins highly expressed in cells co-cultured with exosomes originated under normoxic conditions (N20). NRAP is fundamental in  $\alpha$ -actin filaments architecture organisation while PSMD14 (also known as 26S proteasome non-ATPase regulatory subunit 14) plays a critical role in maintaining the homeostasis of the cellular proteome.

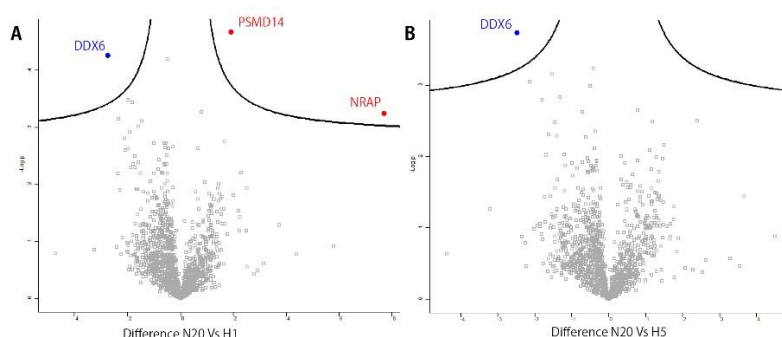


Figure 35. Volcano plots representing the significant proteins (A) N20 Vs H1 and (B) N20 Vs H5. Blue – up-regulated proteins of the main condition (first in the comparison). Red – down-regulated proteins of the main condition (first in the comparison). FDR = 0.05. FDR = 0.05.



## 5. DISCUSSION

In the last 40-years, a revolution in diagnostics and therapeutics within oncology has been started to shift the paradigm of cancer in society, from a mortal disease with less than 25% to 50% chances of survival<sup>15</sup>. However, some cancers have not denoted any prognostic improvements in all these decades, SCLC is a clear exemplification<sup>147</sup>. The clinical advance in SCLC is impeded by development of aggressiveness and chemoresistance during treatment resulting in a poor survival ratio. SCLC is characterized by a hypoxic core; therefore, hypoxia is thought to be an important external stressor and contributor in this disease. Many researchers have proven the pro-carcinogenic effect of hypoxia in different cancer lines, however the effect within SCLC has still not been broadly documented. Therefore, further understanding of this external stressor and how it might be driving the carcinogenic potential of SCLC is of great need. In this MSc thesis, it was investigated how oxygenation levels in SCLC affect the pro-carcinogenic potential worsening the prognosis of the patients. We did this by examining the involvement of the proteome, communication through EVs and their bystander effect in the arise of the pro-carcinogenic phenotype that SCLC cells acquire.

### 5.1. Hypoxia induces metabolic reprogramming increasing pro-carcinogenic pathways

When examining how hypoxia induce protein changes in SCLC H69 cell line, we found that when cells are cultured in hypoxic conditions, results in an increase in hypoxia-regulated proteins. This suggests that H69 SCLC cells are highly influenced by hypoxia. This findings are in accordance with previously reported data using other SCLC cell lines<sup>148</sup>. This protein up-regulation is amplified when oxygen conditions drop to 1%, however, this effect is also noticeable when oxygen levels fall from the normal *in vitro* settings (20% oxygen) to 5% oxygen. This protein shift is not only applicable to the hypoxia-related proteins as it has also been demonstrated in many other studies showing the reprogramming ability of hypoxia over cells<sup>149,150</sup>. The specific implications of the hypoxic shift in the SCLC cells proteome, might unveil some of the paradigms regarding the aggressive phenotype towards which SCLC cells shift. Therefore, we evaluated the link between hypoxia and the cell proteome shift to explain the poor prognosis of SCLC patients.

When comparing the proteins present in normoxia and hypoxia, an increase in the hypoxic proteome revealed angiogenesis, metastasis and invasiveness, motility and cell proliferation. This indicates that hypoxia alters the protein profile of SCLC cells towards a pro-carcinogenic phenotype. This carcinogenic potential portrayed by SCLC cells under hypoxia resemble previous findings<sup>37,42,151,152</sup>. This metabolic reprogramming of the cell caused by hypoxia has been under study in recent years<sup>43</sup>. The start of this idea known as the “Warburg hypothesis” which dates back to the early 20<sup>th</sup> century, kickstarted when Otto Warburg suggested that cancer cells might obtain their energy through fermentation, rather than aerobic pathways<sup>153</sup>. It is now evident that this fact is inaccurate, as research on this topic quickly showed the limitations of the theory. Nevertheless, it established a new concept in which cells can rewire their metabolic pathways to endure the hypoxic conditions. It is also known that HIF-1 $\alpha$  regulates the expression of enzymes implied in the cells metabolism, specifically the glucose metabolism, inducing a metabolic reprogramming of the cell as Maxwell., *et al* and Keith., *et al* describes<sup>154,155</sup>. Therefore, creating a linkage between hypoxia and cells metabolism<sup>154,155</sup>. The discoveries by these two research groups resemble our findings, in which, the glycolytic metabolic routes are enhanced under hypoxia, thereby, sustaining the pathways critical for cancer cell growth.

Additionally, we observed in hypoxic conditions an up-regulation of specific proteins like LDH implicated in catalysing L-lactate from pyruvate and PGK1 which is implicated in the glucose metabolism transferring phosphate groups. These proteins were previously reported by Maxwell., *et al* and Keith., *et al* to be promoted by HIF-1 $\alpha$ . Therefore, proving that exists a link between hypoxia and its metabolic reprogramming abilities over SCLC cells through HIF-1 $\alpha$ . Keith and co-workers also demonstrated an association between glucose

metabolic reprogramming and c-Myc, which implied that there is also an enhanced cell proliferation. C-Myc was not found as a significant protein in our samples, however, many proteins linked with c-Myc were found to be altered under hypoxic conditions. C-myc is a proto-oncogene normally up-regulated in cancer. Specifically, it is implicated in cell proliferation and metabolism by regulating many genes within these categories. For example, LDH is a c-myc responsive gene. Therefore, up-regulated LDH levels could be a feasible explanation that c-myc might be the driving force behind it. Shim., *et al* discovered <sup>156</sup> that C-myc induces LDH overexpression, resembling our results. Furthermore, Shim., *et al* also discovered that apoptosis is induced in lung carcinoma cells by glucose deprivation through LDH and c-Myc, supporting our findings <sup>157</sup>.

As observed, hypoxia induces glucose starvation in lung cancer cells due to the blockage of the aerobic glycolytic pathway, the cells increase their LDH levels to avoid apoptosis. This enables glycolysis through the alternative anaerobic pathway, ensuring the supply of energy and therefore avoiding natural apoptosis <sup>157</sup>. However, this route is less efficient, resulting in a higher consumption of glucose, emptying the reservoir of glucose of the cell. To solve this issue, cancer cells, display a fascinating mechanism, as described by Leij-Halfwerk., *et al*. They found that gluconeogenesis from alanine is enhanced in lung cancer patients <sup>158</sup>. This provides a feasible explanation of the found enrichment of this pathway (gluconeogenesis and alanine metabolism). This up-regulation ensures a never-ending supply of glucose, solving the lack of glucose availability. In our results, an enhanced gluconeogenesis, alanine, aspartate and glutamate metabolism and LDH overexpression were also found enriched in hypoxic cells, therefore resembling the conclusions obtained from Shim., *et al* and Leij-Halfwerk., *et al*. Therefore, hypoxic tumours will, through metabolic reprogramming, shift towards a more pro-carcinogenic phenotype worsening the prognosis of SCLC patients.

Regarding the previously mentioned alanine metabolism, aspartate and glutamate metabolism, recent research has found that glutamine and glutamate, are considered “conditionally essential” for biosynthesis and bioenergetic metabolic routes in cancer cells <sup>159,160</sup>. Cancer cells reside in a glutamine-limited environment, therefore, development of adaptive strategies seems essential to ensure the supply of this molecules to sustain their enhanced proliferation <sup>159</sup>. Enrichment of nicotinamide adenine dinucleotide metabolic processes was found in hypoxic SCLC cells. This pathway is essential in the bioenergetic generation and is enhanced in SCLC under hypoxic conditions as a requirement to sustain its highly metabolic profile. Additionally, Lewis., *et al* found that glycolysis and mitochondrial metabolism <sup>161</sup> are enhanced in cancer, therefore, a direct and natural consequence is that NAD metabolism will also be increased <sup>162</sup>. Moreover, this research group reported a correlation between the pentose metabolism and the NAD metabolic pathway in cancer cells, backing our findings.

Our results also show that other specific proteins were found to be highly increased in hypoxic conditions like P4HA1, which is an enzyme that synthesises collagen, being implicated in the synthesis and remodelling of the ECM, essential to ensure the survival and motility of SCLC cells, leading to chemoresistance. Additionally, GPI was also found overexpressed in hypoxia, which functions as an angiogenic, growth and motility factor and it has been used as a predictive biomarker for many cancer types <sup>163,164</sup>. GPI also regulates cell migration and metastasis and it is known to be secreted only by cancer cells <sup>163</sup>. Moreover, P4HA1 and GPI are found to be involved in EMT, therefore, being implicated in metastasis and cancer progression <sup>165,166</sup>. In addition, GPI has been known to drive receptor tyrosine-protein kinase erbB-2 resistance to chemotherapy in breast cancer, suggesting that up-regulation of this protein might also be potentially related to chemoresistance development in SCLC <sup>167</sup>.

Up-regulation of glycolysis and the transformation of mitochondria into biosynthesis factories backed by an increased glutaminolysis, gluconeogenesis through amino acids and lipids, and the enhanced pentose

phosphate metabolism occurs during hypoxia. Resulting in the production of large amounts of lactate instead of synthesizing ATP to sustain cancer cell growth and proliferation. This metabolic rewiring benefits SCLC cells survival, invasion, metastasis, growth, angiogenesis, proliferation and chemoresistance. Further understanding is needed regarding how hypoxia induces SCLC cells towards metabolic reprogramming to increase channelling of molecules into biosynthesis might also allow for the discovery of novel drug targets to treat SCLC. Many proteins of the metabolic pathways reprogrammed by hypoxia are also central to apoptosis. These proteins, like GPI, are also aberrantly regulated in SCLC and are essential mediators of the metabolic and cell proliferative pathways. Therefore, proving their importance regarding the metabolic shift to cell survival. Targeting these anti-apoptotic members might be a profitable way to selectively target SCLC cells and induce their apoptosis.

## 5.2. Cells under hypoxia shift their EV-packing and release-modifying its communication and reprogramming abilities

Communication of cancer cells with their tumor-microenvironment is essential and is performed in multiple ways. EVs are one of the most newly discovered mechanisms of cell-to-cell communication. EVs are attracting interest due to their promising pathological potential as they are capable of inducing cell reprogramming. This crosstalk between cells and EVs might be fundamental to the onset of the pro-carcinogenic phenotype in SCLC cells under normoxic conditions. Thereby, potentially increasing the survival, metastatic, angiogenic, invasive and proliferative potentials of SCLC cells even though they are located outside the hypoxic core.

We examined whether hypoxia might promote tumour progression through altered EV-release. A link between HIF-1 $\alpha$  and the production of EVs has long been debated, therefore, our desire to detect this elusive protein in the cell lysate by WB was of high importance<sup>168</sup>. Even though we were unable to detect HIF-1 $\alpha$ , a two-fold increase in the amount of hypoxic identified proteins by MS, most of them highly-controlled by HIF-1 $\alpha$ , were found in hypoxic conditions. This serves as a surrogate of HIF-1 $\alpha$  overexpression. According to other studies, under hypoxic conditions, EVs release is enhanced<sup>169,170</sup>. We found an increased exosome-release, suggesting that hypoxia actively regulates the secretion of exosomes, and we hypothesized that HIF-1 $\alpha$  might be behind this effect. Furthermore, increase in the exosome-release by cancer cells has been related to the chemoresistance development in lung cancer<sup>171</sup> and with worse prognosis of the patients<sup>86</sup>. Therefore, suggesting that exosome-release and poor prognosis in SCLC cells are intimately related. We also found that hypoxia is involved in the modification of particle size of MVs. The implication of these findings is unknown, as no research has been conducted regarding the size of MVs and its implication in carcinogenesis.

Regarding the cargo of EVs, we hypothesized that if the cell proteome shift towards a specific phenotype, probably the cargo contained within EVs might also be altered in a specific way, thereby, modifying the manner in which SCLC cells communicate with its microenvironment under hypoxic conditions. Our results indicate that the proteome of MVs is larger than that of the exosomes. These findings are similar to that of Sun and co-workers<sup>172</sup>. Furthermore, a high percentage of the exosomes proteome is contained within the MV proteome, suggesting that they might share a similar role. However, the unique proteins expressed in these two EV-subpopulations is 77% and 21% in MVs and exosomes, respectively. Therefore, even though they share a big part of their proteomes, many uniquely different proteins are expressed within each EV-subpopulation, probably portraying a different role. We observed that even though the hypoxic cells produce EVs with a distinct proteome, the content of proteins in each proteome driving angiogenesis, metastasis and invasiveness and motility is the same in both MVs and exosomes. Nevertheless, when comparing angiogenic, metastatic and invasiveness and motility protein profiles of normoxic against hypoxic originated-MVs, enrichment in proteins driving these pro-carcinogenic profiles are found in hypoxic MVs. The proteome of MVs under hypoxic

conditions is greatly reduced, however, the proteins involved in the pro-carcinogenic pathways are preserved within the MV-proteome. These results indicate that there is selective packaging, where the enriched-MV cargo contained a higher percentage of pro-carcinogenic proteins. Therefore, we suggest that the pro-carcinogenic effect of MVs originated under hypoxic conditions might be enhanced compared to the normoxic counterpart.

When investigating the enriched functional pathways and specific proteins within MVs under hypoxic conditions, we found that EPH proteins were over-expressed. EPH proteins are implicated in cancer, and its overexpression is linked with cancer proliferation, angiogenesis, metastasis and cell movement <sup>173–175</sup>. Furthermore, EPH proteins are also released in vesicles, and have pro-carcinogenic properties, as investigated by Takasugi., *et al* <sup>176</sup>. Regarding exosomes, overexpression of positive regulation of apoptosis was found in the proteins contained within normoxic cell-derived exosomes, while exosomes originated under hypoxic conditions under-expressed these sets of proteins. This under-expression of positive apoptotic regulation in hypoxic exosomes might induce a survival signal over other cells by avoiding apoptosis, opposed to the normal apoptotic response that exosomes under normoxic conditions undergo.

We found that proteins significantly over-expressed in MVs originated under normoxic conditions like Receptor-like protein 2 and fatty acid binding protein 7 are correlated with benign tumours and improved patient outcome, while proteins found highly expressed in hypoxic conditions like collagen 5 alpha-1, cysteine and glycine-rich protein 1 and HMGA1 are correlated with carcinogenesis and therefore a poor patient prognosis <sup>177,178</sup>. Overall, a tendency in the packing of MVs towards a benign response when originated under normoxia and towards the pro-carcinogenic phenotype when originated under hypoxia is noticeable. Furthermore, HMGA1 portrays the role as a master regulator of tumour progression and its expression is associated with malignant prognosis in lung cancer patients <sup>178</sup>. HMGA1 knock-down was correlated with a blockage of the aggressive pro-carcinogenic phenotype, reducing its proliferative, metastatic, invasive and tumorigenic properties in a research performed in breast cancer cells by Shah., *et al* <sup>179</sup>. Therefore, HMGA1 up-regulation under hypoxic conditions suggests that hypoxia might also enhance the pro-carcinogenic phenotype through this master regulator in cancer. Furthermore, a link between HMGA1 and HIF-1 has been found to induce VEGF overexpression under hypoxic conditions. This might have implications contributing towards an enhanced angiogenic potential which is characteristic of hypoxic SCLC cells <sup>180</sup>.

When EVs were originated under hypoxic conditions, they seem to resemble their parent cell of origin, containing a cargo with a high pro-carcinogenic content, mimicking the response that the progenitor cell obtained under the hypoxic environment. This discovery was previously described by Théry., *et al* who demonstrated that EVs resemble their parental cell <sup>181</sup>. Furthermore, these results described of hypoxic-EVs containing pro-carcinogenic proteins, suggest their potential as reprogramming entities, an ability proposed by Ratajczak., *et al* <sup>182</sup>.

### 5.3. Hypoxic exosomes have an enhanced pro-carcinogenic bystander effect

The ability of EVs to re-programme other cells was discovered a decade ago by Ratajczak., *et al* <sup>182</sup>. As previously discussed, SCLC hypoxic tumours increase exosome release with a very particular cargo containing a set of unique proteins and overexpression of certain pro-carcinogenic proteins. Therefore, these SCLC cell-derived exosomes originated under hypoxic conditions might induce in the recipient cells a shift of its phenotype towards an enhanced pro-carcinogenic phenotype.

Investigation of cells co-cultured with exosomes originated under different oxygenation conditions was performed to examine the different effects of the exosomes over the H69 SCLC cells. The cells co-cultured

with hypoxic exosomes showed a larger proteome when compared with cells co-cultured with normoxic exosomes. It seems that hypoxic exosomes induce a larger proteome expression in SCLC cells, mimicking a hypoxia-like effect similar to the one observed in the parental cells. Furthermore, examination of the specific protein profiles driving motility and proliferation, resulted in a higher number of proteins identified in the cells co-cultured with exosomes originated under hypoxic conditions. Therefore, we suggest that the hypoxic exosomes might also be responsible for this proteome shift towards a pro-carcinogenic phenotype. These results follow the same tendency as the results obtained from the proteome comparison of cell lysates from the hypoxia experiment. This reprogramming ability mimicking their parental cell response under the influence of hypoxia that exosomes portray over other SCLC cells when co-cultured, has not yet been reported. We hypothesized that this pro-carcinogenic reprogramming ability exerted by hypoxic-derived exosomes might aid other SCLC cells to endure adverse conditions towards survival.

The specific enriched pathways in the cells co-cultured with exosomes from different origins, we observe an overall negative regulation of apoptosis and programmed cell death, therefore, confirming our hypothesis that exosomes reprogramme the recipient cells to survive and avoid cell death. Furthermore, up-regulation of tyrosine kinase activity and histidine metabolism are present. Tyrosine kinase activity is found rooted in carcinogenesis and it has been closely studied in non-small cell lung cancer <sup>183</sup> and has implications in the enhancement of the aggressiveness of the pro-carcinogenic phenotype <sup>184,185</sup>. For example, tyrosine kinases are involved in cell growth, and in lung cancer has been found that their aberrant functionality leads to an increased release of growth factors, contributing to the malignant pro-carcinogenic phenotype <sup>186</sup>. This finding supports our theory on exosomes reprogramming cells towards an enhanced survival and a more aggressive phenotype.

When investigating the specific functions in cells cultured with exosomes originated under a specific condition, we observed an up-regulation of some functions directly related to exosome biogenesis in the hypoxic conditions. Therefore, the whole EVs machinery of the cell is over-activated, producing an increasing number of EVs compared with cells cultured with normoxic exosomes. Additionally, findings of ribonucleotide and ribonucleoside binding, ribosome, poly(A)-RNA binding, specifically up-regulated in H1, suggesting that the machinery responsible for transcription and protein synthesis is upregulated. We hypothesize that this might be the results of some sort of reprogramming implications in the recipient cell towards an increased survival. Therefore, linking the hypoxic-exosomes with the pro-carcinogenic phenotype reprogramming of H69 SCLC cells.

When comparing N20 and H5 conditions, we found that hypermethylation of CpG islands was upregulated in the hypoxic condition compared with the normoxic one. Hypermethylation of CpG islands has long been proposed as a lung cancer biomarker <sup>187,188</sup> and its association with worse prognosis was first described in colorectal cancer patients. Furthermore, a link between an increase in hypermethylation of CpG islands is directly correlated with poor prognosis of the patient <sup>188</sup>. These findings suggest that these hypoxic-exosomes might be contributing to the poor prognosis of the cancer patient by inducing a proteome shift and reprogramming the cell towards a more pro-carcinogenic phenotype by hypermethylation of the CpG islands.

When investigating specific proteins highly expressed in hypoxic conditions we observed that overexpression of DDX6 was found in both H5 and H1 when compared with N20 conditions. DDX is a group of proteins known for their implications in carcinogenesis <sup>189</sup> and chemoresistance <sup>190</sup>. Additionally, NRAP and PSMD14 were found to be up-regulated in normoxia when compared with hypoxia. The PSMD14 encoded protein is the 26S proteasome subunit 14 or subunit RPN11. The 26S proteasome is an enzyme responsible for catalysing around 70% of the intracellular proteolysis, normally misfolded or damaged proteins <sup>191</sup>, therefore playing a

fundamental role in cell homeostasis. Furthermore, proteins degraded by the proteasome are presented as antigens by the major histocompatibility complex class I, having an essential function in the immune signalling process. Therefore, a reduction in RPN11 protein in cells co-cultured with hypoxic exosomes might mask cancer cells, avoiding immune-cell surveillance by not presenting antigens. This remarkable strategy performed by SCLC cells was reported two-decades ago by the research group of Johnsen., *et al*<sup>192</sup>, confirming our hypothesis. In addition to these functions, RPN11 also has the ability to hydrolyse the ubiquitin molecules before the protein is degraded<sup>193</sup>. This system of protein ubiquitin degradation is known as the ubiquitin-proteasome system (UPS), which has profound implications on the cell cycle, growth, proliferation, communication and apoptosis<sup>193</sup>. On one side, UPS plays a fundamental role in carcinogenesis, by degrading transcription factors (tumour protein 53, nuclear factor kappa beta, c-Myc and HIF-1 $\alpha$ ) and a big number of proto-oncogenes (serine/threonine kinases like Raf, Myc, Myb, Src, Mos)<sup>194</sup>. We could observe, upregulation or normal expression is found in cells co-cultured with normoxic-exosomes, however, hypoxic-exosome co-culture with cells showed a downregulation of the 26S proteasome, this suggests that these cells will be unable to degrade the pro-carcinogenic transcription factors, proto-oncogenes and the resulting proteins. As a result, this might translate into an enhanced pro-carcinogenic potential of these cells. On the other hand, UPS also regulates cell growth, proliferation and its inhibition induces apoptosis, therefore, inhibition of the proteasome has been targeted for cancer therapy in the last years. However, primary and resistance development to this therapeutic strategy remains a challenge<sup>195,196</sup>.

Overall, hypoxia can drive cell reprogramming at many levels. Hypoxia's reprogramming ability over SCLC cells can shift the communication of the cells through EVs, changing its release and their cargo, therefore re-shaping the way cancer cells communicate with their tumour-microenvironment. These EVs are capable of reprogramming the SCLC cells proteome when co-cultured with hypoxic exosomes by enhancing the pro-carcinogenic phenotype.

#### 5.4. Study limitations

In this study, we found several limitations. First, the amount of EVs obtained was below expected, which limited the amount of protein available to perform WB and detect HIF-1 $\alpha$  and CD9. Moreover, it also narrowed the protein identification and quantification in the MS-analysis of the EV-samples. Additionally, EV-scarcity also delimited the number of exosomes available to perform the co-culture experiment. As a result, a low number of cells were seeded, therefore obtaining a low protein content for WB, resulting in the impossibility of detecting HIF-1 $\alpha$ . Therefore, for future research a larger population of cells is required to perform the same amount of analysis and experiments, this will provide a higher protein content, required to detect HIF-1 $\alpha$  and CD9. Regarding HIF-1 $\alpha$ , further precautions need to be taken during sample handling to ensure it is not degraded.

The second limitation we encountered was the isolation method for the EV-subpopulations. Ultracentrifugation does not provide a clean isolation of the EV-subpopulations making it difficult to uncover the effects of hypoxia over each subpopulation and the bystander effect when the "exosomes" were co-cultured with H69 SCLC cells. Nowadays, no gold standard for EV-isolation exist, therefore, a more precise comparison of MVs against exosomes protein cargo composition and function was inconceivable.

## 6. Conclusion

In this MSc thesis, we investigated the effects of hypoxia on H69 cells. We evaluated: 1) the proteome changes induced by hypoxia and their implications in the carcinogenesis of SCLC, 2) how hypoxia affects EV-release and 3) EV-proteome composition as well as the bystander effect that hypoxic-exosomes have on SCLC cells.

We showed that cells grown under hypoxic conditions has many of the proteins which mandates the main pro-carcinogenic functions like metastasis, angiogenesis, invasiveness, motility and proliferation. Furthermore, we demonstrated that hypoxia-induced metabolic reprogramming of the cell to sustain their pro-metastatic potential by increasing their glycolysis, gluconeogenesis, alanine, aspartate and glutamate, protein and bioenergetic metabolism. Additionally, the over-expression of GPI and P4HA1 proteins indicates that role of hypoxia in metastasis, ECM remodelling, motility, proliferation, progression and chemoresistance. Therefore, hypoxia has profound implications in the pro-carcinogenic phenotype which can be directly linked with a worse patient prognosis. The metabolic reprogramming of the cell affects a multitude of pathways. Some of these pathways are also involved in cell death by regulating apoptosis and proliferation, therefore, targeting specific molecules that play a role in both pathways, can bring a solution to the therapeutic arsenal against SCLC. From our study, GPI was found to be over-expressed in SCLC cells and has implications in metabolic routes as well as in angiogenesis, growth, motility, cell migration, metastasis, EMT and the development of resistance to chemotherapy. GPI is also only found in cancer cells, therefore, making it an ideal candidate for therapeutic targeting.

The role of hypoxia in EV-release and cargo composition resulted in changes in the biogenesis of EVs, by shifting their packing towards a more pro-carcinogenic proteome, as well as an enhanced release of exosomes. The modification on the EV-proteome that hypoxia-induced have direct implications in the way cells communicate with their microenvironment. We also discovered that MVs and exosomes share part of their proteomes, and this might imply a similar functionality, however, also unique proteins were found in both EV-subpopulations, highlighting the different roles they might have in carcinogenesis. Hypoxic-EVs expressed an up-regulation of the EPH proteins, related to proliferation, angiogenesis, metastasis and cell movement. Additionally, an over-expression of HMGA1 which is a master regulator of tumour progression in SCLC cells. All of this confirms that hypoxic EVs contains a more pro-carcinogenic cargo resembling the parent cell.

We discovered that exosomes cultured under hypoxic conditions can reprogramme other SCLC cells towards an enhanced pro-carcinogenic phenotype by changing composition. Cells co-cultured with hypoxic exosomes portrayed a decrease in apoptosis and programmed cell death. Additionally, up-regulation of transcription, translation and tyrosine kinase activity results in cell growth, proliferation and survival of cells co-cultured with hypoxic-derived exosomes. Moreover, hypermethylation of the CpG islands suggests a pro-carcinogenic effect probably contributing to the poor prognosis of the patients, also induced by hypoxic exosomes. DDX6 up-regulation is linked with carcinogenesis and chemoresistance while PSMD14 down-regulation translate into a reduced 26S proteasome synthesis. The decrease in the proteasome levels allows SCLC cells co-cultured with hypoxic-exosomes to avoid immune-cell surveillance and apoptosis while increasing their proliferation and growth.

Lastly, we can confirm that hypoxia induces carcinogenesis and tumour progression in SCLC cells. Its effects can be mapped as direct impact over cells by altering cell communication ability through EVs. Furthermore, induction of cell reprogramming towards a pro-carcinogenic phenotype was associated with the bystander effect induced by hypoxic-exosomes.



## 7. Future directions

After the completion of the project, we speculate on how different incubation times for hypoxia and co-culture experiment might affect the results. A more complex overview of the effect of different hypoxia environments like acute and chronic might induce different cell responses, providing a wider and more complete scope within this area of research. Additionally, the exosomes originated under these different hypoxic conditions might induce distinct responses when co-cultured with cells. Furthermore, an alternative investigation of the bystander effect induced by MVs in SCLC cells was also of great interest, however, due to the scarcity of analyte and time, only exosomes could be tested for co-culture with SCLC cells, narrowing the results output.

Repetition of the experiments including also healthy lung cells as a control could have been of great interest towards biomarker discovery. Furthermore, allowing for a more detailed understanding of the pathways involved in SCLC. It can also shed light on possible molecule targets for SCLC therapy, thereby improving outcome and prognosis for patients with SCLC in the future.

A direct application of the findings into current research is further investigation of the enriched functional pathways and up-regulated proteins found to be mediators between the interplay of hypoxia, EV-communication and SCLC cells. This might hit the nail of a specific targetable protein which might bring better therapeutic and diagnostic tools, bringing a better future for SCLC patients.

## 8. Bibliography

1. Siegel, R. Cancer Statistics. *Cancer J.* 67, 7–30 (2017).
2. Byers, L. A. & Rudin, C. M. Small cell lung cancer: Where do we go from here? *Cancer* 121, 664–672 (2015).
3. Paglialunga, L., Salih, Z., Ricciuti, B. & Califano, R. Immune checkpoint blockade in small cell lung cancer: is there a light at the end of the tunnel? *ESMO Open* 1, e000022 (2016).
4. Morabito, A. et al. Treatment of small cell lung cancer. *Crit. Rev. Oncol. Hematol.* 91, 257–270 (2014).
5. Miller, K. D. et al. Cancer treatment and survivorship statistics, 2016. *CA. Cancer J. Clin.* 66, 271–289 (2016).
6. Yamada, T. et al. Genetically engineered humanized anti-ganglioside GM2 antibody against multiple organ metastasis produced by GM2-expressing small-cell lung cancer cells. *Cancer Sci.* 102, 2157–2163 (2011).
7. Minami, T. et al. Overcoming chemoresistance of small-cell lung cancer through stepwise HER2-targeted antibody-dependent cell-mediated cytotoxicity and VEGF-targeted antiangiogenesis. *Sci. Rep.* 3, 2669 (2013).
8. Rekhtman, N. Neuroendocrine tumors of the lung: an update. *Arch. Pathol. Lab. Med.* 134, 1628–38 (2010).
9. Oze, I. et al. Twenty-Seven Years of Phase III Trials for Patients with Extensive Disease Small-Cell Lung Cancer: Disappointing Results. *PLoS One* 4, e7835 (2009).
10. Kang, H. C. et al. FAIM2, as a novel diagnostic maker and a potential therapeutic target for small-cell lung cancer and atypical carcinoid. *Sci. Rep.* 6, 1–9 (2016).
11. Hande, K. R. & Des Prez, R. M. Current perspectives in small cell lung cancer. *Chest* 85, 669–677 (1984).
12. Bunn, P. A. et al. Small Cell Lung Cancer: Can Recent Advances in Biology and Molecular Biology Be Translated into Improved Outcomes? *J. Thorac. Oncol.* 11, 453–474 (2016).
13. Gazdar, A. F., Bunn, P. A. & Minna, J. D. Small-cell lung cancer: what we know, what we need to know and the path forward. *Nat. Rev. Cancer* 17, 725–737 (2017).
14. Ferlay, J. et al. Cancer incidence and mortality worldwide: Sources, methods and major patterns in GLOBOCAN 2012. *Int. J. Cancer* 136, E359–E386 (2015).
15. Quaresma, M., Coleman, M. P. & Rachet, B. 40-year trends in an index of survival for all cancers combined and survival adjusted for age and sex for each cancer in England and Wales, 1971–2011: a population-based study. *Lancet* 385, 1206–1218 (2015).
16. Joshi, M., Ayoola, A. & Belani, C. P. in *Advances in experimental medicine and biology* 779, 385–404 (2013).
17. Orlow, I. et al. DNA damage and repair capacity in patients with lung cancer: prediction of multiple primary tumors. *J. Clin. Oncol.* 26, 3560–6 (2008).
18. Bonanno, L., Favaretto, A. & Rosell, R. Platinum drugs and DNA repair mechanisms in lung cancer. *Anticancer Res.* 34, 493–501 (2014).
19. Foster, N. R. et al. Prognostic Factors Differ by Tumor Stage for Small Cell Lung Cancer. doi:10.1002/cncr.24314

20. Hamilton, G. & Rath, B. Combination chemotherapy for relapsed small-cell lung cancer—perspective on mechanisms of chemoresistance. *Transl. Cancer Res.* 5, S1255–S1261 (2016).
21. Bernhardt, E. B. & Jalal, S. I. in 301–322 (Springer, Cham, 2016). doi:10.1007/978-3-319-40389-2\_14
22. Bryant, J. L., Meredith, S. L., Williams, K. J. & White, A. Targeting hypoxia in the treatment of small cell lung cancer. *Lung Cancer* 86, 126–132 (2014).
23. Maxwell, P. H. et al. The tumour suppressor protein VHL targets hypoxia-inducible factors for oxygen-dependent proteolysis. *Nature* 399, 271–275 (1999).
24. Bruick, R. K. & McKnight, S. L. A Conserved Family of Prolyl-4-Hydroxylases That Modify HIF. *Science* (80-. ). 294, 1337–1340 (2001).
25. Liao, D., Corle, C., Seagroves, T. N. & Johnson, R. S. Hypoxia-Inducible Factor-1 $\alpha$  Is a Key Regulator of Metastasis in a Transgenic Model of Cancer Initiation and Progression. *Cancer Res.* 67, 563–572 (2007).
26. Muz, B., de la Puente, P., Azab, F. & Azab, A. K. The role of hypoxia in cancer progression, angiogenesis, metastasis, and resistance to therapy. *Hypoxia* 83 (2015). doi:10.2147/HP.S93413
27. Sullivan, R., Pare, G. C., Frederiksen, L. J., Semenza, G. L. & Graham, C. H. Hypoxia-induced resistance to anticancer drugs is associated with decreased senescence and requires hypoxia-inducible factor-1 activity. *Mol. Cancer Ther.* 7, 1961–1973 (2008).
28. Hao, J. et al. Effects of lentivirus-mediated HIF-1 $\alpha$  knockdown on hypoxia-related cisplatin resistance and their dependence on p53 status in fibrosarcoma cells. *Cancer Gene Ther.* 15, 449–455 (2008).
29. Roberts, D. L. et al. Contribution of HIF-1 and drug penetrance to oxaliplatin resistance in hypoxic colorectal cancer cells. *Br. J. Cancer* 101, 1290–7 (2009).
30. Rohwer, N. & Cramer, T. Hypoxia-mediated drug resistance: Novel insights on the functional interaction of HIFs and cell death pathways. *Drug Resist. Updat.* 14, 191–201 (2011).
31. Ito, T. et al. Small cell lung cancer, an epithelial to mesenchymal transition (EMT)-like cancer: significance of inactive Notch signaling and expression of achaete-scute complex homologue 1. *Hum. Cell* 30, 1–10 (2017).
32. Song, X. et al. Hypoxia-induced resistance to cisplatin and doxorubicin in non-small cell lung cancer is inhibited by silencing of HIF-1 $\alpha$  gene. *Cancer Chemother. Pharmacol.* 58, 776–784 (2006).
33. Suzuki, M., Suzuki, M., Goitsuka, R. & Ueno, H. Hypoxia induces CD133 expression in human lung cancer cells by up-regulation of OCT3/4 and SOX2. *Int. J. Oncol.* 40, 71–9 (2011).
34. Li, C. et al. Prognostic Role of Hypoxic Inducible Factor Expression in Non-small Cell Lung Cancer: A Meta-analysis. *Asian Pacific J. Cancer Prev.* 14, 3607–3612 (2013).
35. Yang, S., Ren, Q., Wen, L. & Hu, J. Clinicopathological and prognostic significance of hypoxia-inducible factor-1 alpha in lung cancer: a systematic review with meta-analysis. *J. Huazhong Univ. Sci. Technol. [Medical Sci.* 36, 321–327 (2016).
36. Ren, W. et al. The expression of hypoxia-inducible factor-1 $\alpha$  and its clinical significance in lung cancer: a systematic review and meta-analysis. *Swiss Med. Wkly.* (2013). doi:10.4414/smw.2013.13855
37. Lin, C.-S., Liu, T.-C., Lee, M.-T., Yang, S.-F. & Tsao, T. C.-Y. Independent Prognostic Value of Hypoxia-inducible Factor 1-alpha Expression in Small Cell Lung Cancer. *Int. J. Med. Sci.* 14, 785–790 (2017).
38. Zhong, H. et al. Overexpression of hypoxia-inducible factor 1alpha in common human cancers and their metastases. *Cancer Res.* 59, 5830–5 (1999).

39. Talks, K. L. et al. The expression and distribution of the hypoxia-inducible factors HIF-1 $\alpha$  and HIF-2 $\alpha$  in normal human tissues, cancers, and tumor-associated macrophages. *Am. J. Pathol.* 157, 411–21 (2000).
40. Huang, H. et al. Prostate cancer cell malignancy via modulation of HIF-1 $\alpha$  pathway with isoflurane and propofol alone and in combination. *Br. J. Cancer* 111, 1338–1349 (2014).
41. Brizel, D. M., Sibley, G. S., Prosnitz, L. R., Scher, R. L. & Dewhirst, M. W. Tumor hypoxia adversely affects the prognosis of carcinoma of the head and neck. *Int. J. Radiat. Oncol. Biol. Phys.* 38, 285–9 (1997).
42. Wan, J. et al. HIF-1 $\alpha$  effects on angiogenic potential in human small cell lung carcinoma. *J. Exp. Clin. Cancer Res.* 30, 77 (2011).
43. Zhao, T. et al. HIF-1-mediated metabolic reprogramming reduces ROS levels and facilitates the metastatic colonization of cancers in lungs. *Sci. Rep.* 4, 3793 (2015).
44. Yang, M.-H. et al. Direct regulation of TWIST by HIF-1 $\alpha$  promotes metastasis. *Nat. Cell Biol.* 10, 295–305 (2008).
45. Sowa, T. et al. Hypoxia-inducible factor 1 promotes chemoresistance of lung cancer by inducing carbonic anhydrase IX expression. *Cancer Med.* 6, 288–297 (2017).
46. Lucchi, M. et al. Small cell lung carcinoma (SCLC): the angiogenic phenomenon. *Eur. J. Cardiothorac. Surg.* 21, 1105–10 (2002).
47. Choi, J. Y., Jang, Y. S., Min, S. Y. & Song, J. Y. Overexpression of MMP-9 and HIF-1 $\alpha$  in Breast Cancer Cells under Hypoxic Conditions. *J. Breast Cancer* 14, 88–95 (2011).
48. Zheng, S. et al. Expression of KISS1 and MMP-9 in non-small cell lung cancer and their relations to metastasis and survival. *Anticancer Res.* 30, 713–8 (2010).
49. Gilkes, D. M., Bajpai, S., Chaturvedi, P., Wirtz, D. & Semenza, G. L. Hypoxia-inducible factor 1 (HIF-1) promotes extracellular matrix remodeling under hypoxic conditions by inducing P4HA1, P4HA2, and PLOD2 expression in fibroblasts. *J. Biol. Chem.* 288, 10819–29 (2013).
50. Gilkes, D. M., Semenza, G. L. & Wirtz, D. Hypoxia and the extracellular matrix: drivers of tumour metastasis. *Nat. Rev. Cancer* 14, 430–439 (2014).
51. Rohwer, N. et al. HIF-1 $\alpha$  determines the metastatic potential of gastric cancer cells. *Br. J. Cancer* 100, 772–781 (2009).
52. Kucharzewska, P. & Belting, M. Emerging roles of extracellular vesicles in the adaptive response of tumour cells to microenvironmental stress. *J. Extracell. Vesicles* 2, (2013).
53. Gunaratnam, L. et al. Hypoxia Inducible Factor Activates the Transforming Growth Factor- $\alpha$ /Epidermal Growth Factor Receptor Growth Stimulatory Pathway in VHL-/- Renal Cell Carcinoma Cells. *J. Biol. Chem.* 278, 44966–44974 (2003).
54. Cao, D. et al. Expression of HIF-1 $\alpha$  and VEGF in colorectal cancer: association with clinical outcomes and prognostic implications. *BMC Cancer* 9, 432 (2009).
55. Zhang, Y., Xu, Y., Ma, J., Pang, X. & Dong, M. Adrenomedullin promotes angiogenesis in epithelial ovarian cancer through upregulating hypoxia-inducible factor-1 $\alpha$  and vascular endothelial growth factor. *Sci. Rep.* 7, 40524 (2017).
56. Baltaziak, M. et al. The relationships between hypoxia-dependent markers: HIF-1 $\alpha$ , EPO and EPOR in colorectal cancer. *Folia Histochem. Cytobiol.* 51, 320–325 (2014).

57. Labak, C. M. et al. Glucose transport: meeting the metabolic demands of cancer, and applications in glioblastoma treatment. *Am. J. Cancer Res.* 6, 1599–608 (2016).
58. Fulda, S. & Debatin, K.-M. HIF-1-Regulated Glucose Metabolism: A Key to Apoptosis Resistance? *Cell Cycle* 6, 790–792 (2007).
59. Li, L. et al. Integrated Omic analysis of lung cancer reveals metabolism proteome signatures with prognostic impact. *Nat. Commun.* 5, 5469 (2014).
60. Pap, E., Pállinger, É. & Falus, A. The role of membrane vesicles in tumorigenesis. *Crit. Rev. Oncol. Hematol.* 79, 213–223 (2011).
61. Linē, A. et al. Hypoxic conditions regulate the molecular content, release and uptake rates of extracellular vesicles produced by colorectal cancer cells. *Eur. J. Cancer* 61, S96 (2016).
62. Valadi, H. et al. Exosome-mediated transfer of mRNAs and microRNAs is a novel mechanism of genetic exchange between cells. *Nat. Cell Biol.* 9, 654–659 (2007).
63. Ratajczak, J., Wysoczynski, M., Hayek, F., Janowska-Wieczorek, A. & Ratajczak, M. Z. Membrane-derived microvesicles: important and underappreciated mediators of cell-to-cell communication. *Leukemia* 20, 1487–1495 (2006).
64. Deregibus, M. C. et al. Endothelial progenitor cell derived microvesicles activate an angiogenic program in endothelial cells by a horizontal transfer of mRNA. *Blood* 110, 2440–2448 (2007).
65. Raposo, G. & Stoorvogel, W. Extracellular vesicles: Exosomes, microvesicles, and friends. *J. Cell Biol.* 200, 373–383 (2013).
66. Simons, M. & Raposo, G. Exosomes – vesicular carriers for intercellular communication. *Curr. Opin. Cell Biol.* 21, 575–581 (2009).
67. Lässer, C. et al. Human saliva, plasma and breast milk exosomes contain RNA: uptake by macrophages. *J. Transl. Med.* 9, 9 (2011).
68. Théry, C., Zitvogel, L. & Amigorena, S. Exosomes: composition, biogenesis and function. *Nat. Rev. Immunol.* 2, 569–579 (2002).
69. Gangoda, L., Boukouris, S., Liem, M., Kalra, H. & Mathivanan, S. Extracellular vesicles including exosomes are mediators of signal transduction: Are they protective or pathogenic? *Proteomics* 15, 260–271 (2015).
70. Yuana, Y., Sturk, A. & Nieuwland, R. Extracellular vesicles in physiological and pathological conditions. *Blood Rev.* 27, 31–39 (2013).
71. Kowal, J. et al. Proteomic comparison defines novel markers to characterize heterogeneous populations of extracellular vesicle subtypes. *Proc. Natl. Acad. Sci.* 113, E968–E977 (2016).
72. Gruenberg, J. & Stenmark, H. The biogenesis of multivesicular endosomes. *Nat. Rev. Mol. Cell Biol.* 5, 317–323 (2004).
73. Akers, J. C., Gonda, D., Kim, R., Carter, B. S. & Chen, C. C. Biogenesis of extracellular vesicles (EV): exosomes, microvesicles, retrovirus-like vesicles, and apoptotic bodies. *J. Neurooncol.* 113, 1–11 (2013).
74. Choi, D.-S., Kim, D.-K., Kim, Y.-K. & Gho, Y. S. Proteomics of extracellular vesicles: Exosomes and ectosomes. *Mass Spectrom. Rev.* 34, 474–490 (2015).
75. Yáñez-Mó, M. et al. Biological properties of extracellular vesicles and their physiological functions. *J. Extracell. vesicles* 4, 27066 (2015).

76. Mathivanan, S. et al. Proteomics Analysis of A33 Immunoaffinity-purified Exosomes Released from the Human Colon Tumor Cell Line LIM1215 Reveals a Tissue-specific Protein Signature. *Mol. Cell. Proteomics* 9, 197–208 (2010).
77. Skog, J. et al. Glioblastoma microvesicles transport RNA and proteins that promote tumour growth and provide diagnostic biomarkers. *Nat. Cell Biol.* 10, 1470–1476 (2008).
78. Denzer, K., Kleijmeer, M. J., Heijnen, H. F., Stoorvogel, W. & Geuze, H. J. Exosome: from internal vesicle of the multivesicular body to intercellular signaling device. *J. Cell Sci.* 113 Pt 19, 3365–74 (2000).
79. Corrado, C. et al. Exosome-mediated crosstalk between chronic myelogenous leukemia cells and human bone marrow stromal cells triggers an Interleukin 8-dependent survival of leukemia cells. *Cancer Lett.* 348, 71–76 (2014).
80. Foster, B. P. et al. Extracellular vesicles in blood, milk and body fluids of the female and male urogenital tract and with special regard to reproduction. *Crit. Rev. Clin. Lab. Sci.* 53, 379–395 (2016).
81. Logozzi, M. et al. High Levels of Exosomes Expressing CD63 and Caveolin-1 in Plasma of Melanoma Patients. *PLoS One* 4, e5219 (2009).
82. Théry, C. et al. in *Current Protocols in Cell Biology* 3.22.1–3.22.29 (John Wiley & Sons, Inc., 2006). doi:10.1002/0471143030.cb0322s30
83. Gardiner, C. et al. Techniques used for the isolation and characterization of extracellular vesicles: results of a worldwide survey. *J. Extracell. vesicles* 5, 32945 (2016).
84. Witwer, K. W. et al. Standardization of sample collection, isolation and analysis methods in extracellular vesicle research. *J. Extracell. Vesicles* 2, 20360 (2013).
85. Whiteside, T. L. Extracellular vesicles isolation and their biomarker potential: are we ready for testing? *Ann. Transl. Med.* 5, 54 (2017).
86. Kim, H. . et al. Elevated levels of circulating platelet microparticles, VEGF, IL-6 and RANTES in patients with gastric cancer: possible role of a metastasis predictor. *Eur. J. Cancer* 39, 184–191 (2003).
87. Peinado, H. et al. Melanoma exosomes educate bone marrow progenitor cells toward a pro-metastatic phenotype through MET. *Nat. Med.* 18, 883–891 (2012).
88. Costa-Silva, B. et al. Pancreatic cancer exosomes initiate pre-metastatic niche formation in the liver. *Nat. Cell Biol.* 17, 816–826 (2015).
89. Al-Nedawi, K. et al. Intercellular transfer of the oncogenic receptor EGFRvIII by microvesicles derived from tumour cells. *Nat. Cell Biol.* 10, 619–624 (2008).
90. Hood, J. L., Pan, H., Lanza, G. M. & Wickline, S. A. Paracrine induction of endothelium by tumor exosomes. *Lab. Investig.* 89, 1317–1328 (2009).
91. Al-Nedawi, K., Meehan, B., Kerbel, R. S., Allison, A. C. & Rak, J. Endothelial expression of autocrine VEGF upon the uptake of tumor-derived microvesicles containing oncogenic EGFR. *Proc. Natl. Acad. Sci.* 106, 3794–3799 (2009).
92. Webber, J. P. et al. Differentiation of tumour-promoting stromal myofibroblasts by cancer exosomes. *Oncogene* 34, 290–302 (2015).
93. Baglio, S. R. et al. Blocking Tumor-Educated MSC Paracrine Activity Halts Osteosarcoma Progression. *Clin. Cancer Res.* 23, 3721–3733 (2017).
94. Hoshino, A. et al. Tumour exosome integrins determine organotropic metastasis. *Nature* 527, 329–

335 (2015).

95. Fidler, I. J. & Poste, G. The "seed and soil" hypothesis revisited. *Lancet. Oncol.* 9, 808 (2008).
96. Hakulinen, J., Sankkila, L., Sugiyama, N., Lehti, K. & Keski-Oja, J. Secretion of active membrane type 1 matrix metalloproteinase (MMP-14) into extracellular space in microvesicular exosomes. *J. Cell. Biochem.* 105, 1211–1218 (2008).
97. Vella, L. J. The Emerging Role of Exosomes in Epithelial Mesenchymal-Transition in Cancer. *Front. Oncol.* 4, 361 (2014).
98. Bandari, S. K. et al. Chemotherapy induces secretion of exosomes loaded with heparanase that degrades extracellular matrix and impacts tumor and host cell behavior. *Matrix Biol.* 65, 104–118 (2018).
99. Clayton, A. et al. Human tumor-derived exosomes down-modulate NKG2D expression. *J. Immunol.* 180, 7249–58 (2008).
100. Wieckowski, E. U. et al. Tumor-derived microvesicles promote regulatory T cell expansion and induce apoptosis in tumor-reactive activated CD8<sup>+</sup> T lymphocytes. *J. Immunol.* 183, 3720–30 (2009).
101. Bergmann, C. et al. Tumor-derived microvesicles in sera of patients with head and neck cancer and their role in tumor progression. *Head Neck* 31, 371–380 (2009).
102. Chalmin, F. et al. Membrane-associated Hsp72 from tumor-derived exosomes mediates STAT3-dependent immunosuppressive function of mouse and human myeloid-derived suppressor cells. *J. Clin. Invest.* 120, 457–71 (2010).
103. Shinohara, H. et al. Regulated Polarization of Tumor-Associated Macrophages by miR-145 via Colorectal Cancer-Derived Extracellular Vesicles. *J. Immunol.* 199, 1505–1515 (2017).
104. Lopes-Rodrigues, V. et al. Multidrug resistant tumour cells shed more microvesicle-like EVs and less exosomes than their drug-sensitive counterpart cells. *Biochim. Biophys. Acta - Gen. Subj.* 1860, 618–627 (2016).
105. Lopes-Rodrigues, V. et al. Identification of the metabolic alterations associated with the multidrug resistant phenotype in cancer and their intercellular transfer mediated by extracellular vesicles. *Sci. Rep.* 7, 44541 (2017).
106. Aung, T. et al. Exosomal evasion of humoral immunotherapy in aggressive B-cell lymphoma modulated by ATP-binding cassette transporter A3. *Proc. Natl. Acad. Sci.* 108, 15336–15341 (2011).
107. Safaei, R. et al. Abnormal lysosomal trafficking and enhanced exosomal export of cisplatin in drug-resistant human ovarian carcinoma cells. *Mol. Cancer Ther.* 4, 1595–604 (2005).
108. Qin, X. et al. Cisplatin-resistant lung cancer cell-derived exosomes increase cisplatin resistance of recipient cells in exosomal miR-100–5p-dependent manner. *Int. J. Nanomedicine* 12, 3721–3733 (2017).
109. Xiao, X. et al. Exosomes: Decreased sensitivity of lung cancer A549 cells to cisplatin. *PLoS One* 9, 1–6 (2014).
110. Shedden, K., Xie, X. T., Chandaroy, P., Chang, Y. T. & Rosania, G. R. Expulsion of small molecules in vesicles shed by cancer cells: association with gene expression and chemosensitivity profiles. *Cancer Res.* 63, 4331–7 (2003).
111. Bebawy, M. et al. Membrane microparticles mediate transfer of P-glycoprotein to drug sensitive cancer cells. *Leukemia* 23, 1643–1649 (2009).



112. Hsu, Y.-L. et al. Hypoxic lung cancer-secreted exosomal miR-23a increased angiogenesis and vascular permeability by targeting prolyl hydroxylase and tight junction protein ZO-1. *Oncogene* 36, 4929–4942 (2017).
113. Kucharzewska, P. et al. Exosomes reflect the hypoxic status of glioma cells and mediate hypoxia-dependent activation of vascular cells during tumor development. *Proc. Natl. Acad. Sci. U. S. A.* 110, 7312–7 (2013).
114. Han, S. et al. Stroma-derived extracellular vesicles deliver tumor-suppressive miRNAs to pancreatic cancer cells. *Oncotarget* 9, 5764–5777 (2018).
115. de Jong, O. G. et al. Cellular stress conditions are reflected in the protein and RNA content of endothelial cell-derived exosomes. *J. Extracell. Vesicles* 1, 18396 (2012).
116. Muralidharan-Chari, V., Clancy, J. W., Sedgwick, A. & D'Souza-Schorey, C. Microvesicles: mediators of extracellular communication during cancer progression. *J. Cell Sci.* 123, 1603–1611 (2010).
117. Stroncek, D. F. et al. Advancing cancer biotherapy with proteomics. *J. Immunother.* 28, 183–92
118. Sung, H.-J. & Cho, J.-Y. Biomarkers for the lung cancer diagnosis and their advances in proteomics. *BMB Rep.* 41, 615–25 (2008).
119. Han, X., Aslanian, A., Yates, J. R. & III. Mass spectrometry for proteomics. *Curr. Opin. Chem. Biol.* 12, 483–90 (2008).
120. Krieg, R. C., Paweletz, C. P., Liotta, L. A. & Petricoin, E. F. Clinical Proteomics for Cancer Biomarker Discovery and Therapeutic Targeting. *Technol. Cancer Res. Treat.* 1, 263–272 (2002).
121. Cho, W. C. Contribution of oncoproteomics to cancer biomarker discovery. *Mol. Cancer* 6, 25 (2007).
122. Posadas, E. M., Simpkins, F., Liotta, L. A., MacDonald, C. & Kohn, E. C. Proteomic analysis for the early detection and rational treatment of cancer—realistic hope? *Ann. Oncol.* 16, 16–22 (2005).
123. Mathivanan, S. & Simpson, R. J. ExoCarta: A compendium of exosomal proteins and RNA. *Proteomics* 9, 4997–5000 (2009).
124. Keerthikumar, S. et al. ExoCarta: A Web-Based Compendium of Exosomal Cargo. *J. Mol. Biol.* 428, 688–692 (2016).
125. Kalra, H. et al. Vesiclepedia: a compendium for extracellular vesicles with continuous community annotation. *PLoS Biol.* 10, e1001450 (2012).
126. Kim, D.-K., Lee, J., Simpson, R. J., Lötvall, J. & Gho, Y. S. EVpedia: A community web resource for prokaryotic and eukaryotic extracellular vesicles research. *Semin. Cell Dev. Biol.* 40, 4–7 (2015).
127. Kim, D.-K. et al. EVpedia: an integrated database of high-throughput data for systemic analyses of extracellular vesicles. *J. Extracell. Vesicles* 2, 20384 (2013).
128. World Medical Association Declaration of Helsinki. *JAMA* 310, 2191 (2013).
129. Jin, Y. et al. DNA in serum extracellular vesicles is stable under different storage conditions. *BMC Cancer* 16, 753 (2016).
130. Cox, J. & Mann, M. MaxQuant enables high peptide identification rates, individualized p.p.b.-range mass accuracies and proteome-wide protein quantification. *Nat. Biotechnol.* 26, 1367–1372 (2008).
131. Cox, J. et al. Andromeda: A Peptide Search Engine Integrated into the MaxQuant Environment. *J. Proteome Res.* 10, 1794–1805 (2011).
132. Elias, J. E. & Gygi, S. P. Target-decoy search strategy for increased confidence in large-scale protein

identifications by mass spectrometry. *Nat. Methods* 4, 207–214 (2007).

133. Webb-Robertson, B.-J. M. et al. Review, Evaluation, and Discussion of the Challenges of Missing Value Imputation for Mass Spectrometry-Based Label-Free Global Proteomics. *J. Proteome Res.* 14, 1993–2001 (2015).
134. Lazar, C., Gatto, L., Ferro, M., Bruley, C. & Burger, T. Accounting for the Multiple Natures of Missing Values in Label-Free Quantitative Proteomics Data Sets to Compare Imputation Strategies. doi:10.1021/acs.jproteome.5b00981
135. Snel, B., Lehmann, G., Bork, P. & Huynen, M. A. STRING: a web-server to retrieve and display the repeatedly occurring neighbourhood of a gene. *Nucleic Acids Res.* 28, 3442–4 (2000).
136. Pathan, M. et al. FunRich: An open access standalone functional enrichment and interaction network analysis tool. *Proteomics* 15, 2597–2601 (2015).
137. Tyanova, S. et al. The Perseus computational platform for comprehensive analysis of (prote)omics data. *Nat. Methods* 13, 731–740 (2016).
138. Cox, J. & Mann, M. 1D and 2D annotation enrichment: a statistical method integrating quantitative proteomics with complementary high-throughput data. *BMC Bioinformatics* 13 Suppl 16, S12 (2012).
139. Huang, D. W., Sherman, B. T. & Lempicki, R. A. Bioinformatics enrichment tools: paths toward the comprehensive functional analysis of large gene lists. *Nucleic Acids Res.* 37, 1–13 (2009).
140. Huang, D. W., Sherman, B. T. & Lempicki, R. A. Systematic and integrative analysis of large gene lists using DAVID bioinformatics resources. *Nat. Protoc.* 4, 44–57 (2009).
141. Kim, D.-K. et al. EVpedia: a community web portal for extracellular vesicles research. *Bioinformatics* 31, 933–939 (2015).
142. Khurana, P., Sugadev, R., Jain, J. & Singh, S. B. HypoxiaDB: a database of hypoxia-regulated proteins. *Database* 2013, bat074-bat074 (2013).
143. Zheng, G. et al. HCMDDB: the human cancer metastasis database. *Nucleic Acids Res.* 46, D950–D955 (2018).
144. Ashburner, M. et al. Gene Ontology: tool for the unification of biology. *Nat. Genet.* 25, 25–29 (2000).
145. Kanehisa, M. & Goto, S. KEGG: kyoto encyclopedia of genes and genomes. *Nucleic Acids Res.* 28, 27–30 (2000).
146. Kong, X., Alvarez-Castelao, B., Lin, Z., Castaño, J. G. & Caro, J. Constitutive/Hypoxic Degradation of HIF- $\alpha$  Proteins by the Proteasome Is Independent of von Hippel Lindau Protein Ubiquitylation and the Transactivation Activity of the Protein. *J. Biol. Chem.* 282, 15498–15505 (2007).
147. Wang, S. et al. Survival changes in patients with small cell lung cancer and disparities between different sexes, socioeconomic statuses and ages. *Sci. Rep.* 7, 1339 (2017).
148. Ioannou, M. et al. Hypoxia Inducible Factor-1 $\alpha$  and Vascular Endothelial Growth Factor in Biopsies of Small Cell Lung Carcinoma. *Lung* 187, 321–329 (2009).
149. Qiu, G.-Z. et al. Reprogramming of the Tumor in the Hypoxic Niche: The Emerging Concept and Associated Therapeutic Strategies. *Trends Pharmacol. Sci.* 38, 669–686 (2017).
150. Mathieu, J. et al. Hypoxia induces re-entry of committed cells into pluripotency. *Stem Cells* 31, 1737–48 (2013).
151. Wan, J., Ma, J., Mei, J. & Shan, G. The effects of HIF-1 $\alpha$  on gene expression profiles of NCI-H446

- human small cell lung cancer cells. *J. Exp. Clin. Cancer Res.* 28, 150 (2009).
152. Thorén, M. M. et al. Myc-induced glutaminolysis bypasses HIF-driven glycolysis in hypoxic small cell lung carcinoma cells. *Oncotarget* 8, 48983–48995 (2017).
  153. Warburg, O., Wind, F. & Negelein, E. The metabolism of tumors in the body. *J. Gen. Physiol.* 8, 519–30 (1927).
  154. Maxwell, P. H. et al. Hypoxia-inducible factor-1 modulates gene expression in solid tumors and influences both angiogenesis and tumor growth. *Proc. Natl. Acad. Sci. U. S. A.* 94, 8104–9 (1997).
  155. Keith, B., Johnson, R. S. & Simon, M. C. HIF1 $\alpha$  and HIF2 $\alpha$ : sibling rivalry in hypoxic tumour growth and progression. *Nat. Rev. Cancer* 12, 9–22 (2012).
  156. Shim, H. et al. c-Myc transactivation of LDH-A: implications for tumor metabolism and growth. *Proc. Natl. Acad. Sci. U. S. A.* 94, 6658–63 (1997).
  157. Shim, H., Chun, Y. S., Lewis, B. C. & Dang, C. V. A unique glucose-dependent apoptotic pathway induced by c-Myc. *Proc. Natl. Acad. Sci. U. S. A.* 95, 1511–6 (1998).
  158. Leij-Halfwerk, S. et al. Weight loss and elevated gluconeogenesis from alanine in lung cancer patients. *Am. J. Clin. Nutr.* 71, 583–589 (2000).
  159. Zhang, J., Pavlova, N. N. & Thompson, C. B. Cancer cell metabolism: the essential role of the nonessential amino acid, glutamine. *EMBO J.* 36, 1302–1315 (2017).
  160. Watford, M. Glutamine and glutamate: Nonessential or essential amino acids? *Anim. Nutr.* 1, 119–122 (2015).
  161. Ahn, C. S. & Metallo, C. M. Mitochondria as biosynthetic factories for cancer proliferation. *Cancer Metab.* 3, 1 (2015).
  162. Lewis, C. A. et al. Tracing compartmentalized NADPH metabolism in the cytosol and mitochondria of mammalian cells. *Mol. Cell* 55, 253–63 (2014).
  163. Haga, A., Niinaka, Y. & Raz, A. Phosphohexose isomerase/autocrine motility factor/neuroleukin/maturation factor is a multifunctional phosphoprotein. *Biochim. Biophys. Acta - Protein Struct. Mol. Enzymol.* 1480, 235–244 (2000).
  164. Somarowthu, S. et al. A Tale of Two Isomerases: Compact versus Extended Active Sites in Ketosteroid Isomerase and Phosphoglucose Isomerase. *Biochemistry* 50, 9283–9295 (2011).
  165. Gilkes, D. M., Bajpai, S., Chaturvedi, P., Wirtz, D. & Semenza, G. L. Hypoxia-inducible Factor 1 (HIF-1) Promotes Extracellular Matrix Remodeling under Hypoxic Conditions by Inducing P4HA1, P4HA2, and PLOD2 Expression in Fibroblasts. *J. Biol. Chem.* 288, 10819–10829 (2013).
  166. Zhao, Q. et al. Effects of YC-1 on Hypoxia-Inducible Factor 1-Driven Transcription Activity, Cell Proliferative Vitality, and Apoptosis in Hypoxic Human Pancreatic Cancer Cells. *Pancreas* 34, 242–247 (2007).
  167. Molina, M. A. et al. Trastuzumab (herceptin), a humanized anti-Her2 receptor monoclonal antibody, inhibits basal and activated Her2 ectodomain cleavage in breast cancer cells. *Cancer Res.* 61, 4744–9 (2001).
  168. Burnley-Hall, N., Willis, G., Davis, J., Rees, D. A. & James, P. E. Nitrite-derived nitric oxide reduces hypoxia-inducible factor 1 $\alpha$ -mediated extracellular vesicle production by endothelial cells. *Nitric Oxide* 63, 1–12 (2017).
  169. Wysoczynski, M. & Ratajczak, M. Z. Lung cancer secreted microvesicles: Underappreciated

- modulators of microenvironment in expanding tumors. *Int. J. Cancer* 125, 1595–1603 (2009).
170. Orriss, I. R. et al. Hypoxia stimulates vesicular ATP release from rat osteoblasts. *J. Cell. Physiol.* 220, 155–162 (2009).
  171. Lobb, R. J. et al. Exosomes derived from mesenchymal non-small cell lung cancer cells promote chemoresistance. *Int. J. Cancer* 141, 614–620 (2017).
  172. Sun, Y. et al. Comparative Proteomic Analysis of Exosomes and Microvesicles in Human Saliva for Lung Cancer. *J. Proteome Res.* 17, 1101–1107 (2018).
  173. Surawska, H., Ma, P. C. & Salgia, R. The role of ephrins and Eph receptors in cancer. *Cytokine Growth Factor Rev.* 15, 419–433 (2004).
  174. Mosch, B., Reissenweber, B., Neuber, C. & Pietzsch, J. Eph receptors and ephrin ligands: important players in angiogenesis and tumor angiogenesis. *J. Oncol.* 2010, 135285 (2010).
  175. Cheng, N., Brantley, D. M. & Chen, J. The ephrins and Eph receptors in angiogenesis. *Cytokine Growth Factor Rev.* 13, 75–85 (2002).
  176. Takasugi, M. et al. Small extracellular vesicles secreted from senescent cells promote cancer cell proliferation through EphA2. *Nat. Commun.* 8, 15729 (2017).
  177. Vanaja, D. K., Cheville, J. C., Iturria, S. J. & Young, C. Y. F. Transcriptional silencing of zinc finger protein 185 identified by expression profiling is associated with prostate cancer progression. *Cancer Res.* 63, 3877–82 (2003).
  178. Zhang, Z., Wang, Q., Chen, F. & Liu, J. Elevated expression of HMGA1 correlates with the malignant status and prognosis of non-small cell lung cancer. *Tumor Biol.* 36, 1213–1219 (2015).
  179. Shah, S. N. et al. HMGA1: A Master Regulator of Tumor Progression in Triple-Negative Breast Cancer Cells. *PLoS One* 8, e63419 (2013).
  180. Messineo, S. et al. Cooperation between HMGA1 and HIF-1 Contributes to Hypoxia-Induced VEGF and Visfatin Gene Expression in 3T3-L1 Adipocytes. *Front. Endocrinol. (Lausanne)*. 7, 73 (2016).
  181. Théry, C., Ostrowski, M. & Segura, E. Membrane vesicles as conveyors of immune responses. *Nat. Rev. Immunol.* 9, 581–593 (2009).
  182. Ratajczak, J. et al. Embryonic stem cell-derived microvesicles reprogram hematopoietic progenitors: evidence for horizontal transfer of mRNA and protein delivery. *Leukemia* 20, 847–856 (2006).
  183. Kris, M. G. et al. Efficacy of Gefitinib, an Inhibitor of the Epidermal Growth Factor Receptor Tyrosine Kinase, in Symptomatic Patients With Non–Small Cell Lung Cancer. *JAMA* 290, 2149 (2003).
  184. Sangwan, V. & Park, M. Receptor tyrosine kinases: role in cancer progression. *Curr. Oncol.* 13, 191–3 (2006).
  185. Paul, M. K. & Mukhopadhyay, A. K. Tyrosine kinase - Role and significance in Cancer. *Int. J. Med. Sci.* 1, 101–115 (2004).
  186. Maulik, G., Kijima, T. & Salgia, R. Role of receptor tyrosine kinases in lung cancer. *Methods Mol. Med.* 74, 113–25 (2003).
  187. Rauch, T. A. et al. DNA methylation biomarkers for lung cancer. *Tumor Biol.* 33, 287–296 (2012).
  188. Kim, Y. & Kim, D.-H. in *Methods in molecular biology* (Clifton, N.J.) 1238, 141–171 (2015).
  189. Taniguchi, K. et al. Oncogene RNA helicase DDX6 promotes the process of c-Myc expression in gastric cancer cells. *Mol. Carcinog.* 57, 579–589 (2018).

190. CHO, Y. J. et al. Involvement of DDX6 gene in radio- and chemoresistance in glioblastoma. *Int. J. Oncol.* 48, 1053–1062 (2016).
191. Rock, K. L. et al. Inhibitors of the proteasome block the degradation of most cell proteins and the generation of peptides presented on MHC class I molecules. *Cell* 78, 761–771 (1994).
192. Johnsen, A., France, J., Sy, M. S. & Harding, C. V. Down-regulation of the transporter for antigen presentation, proteasome subunits, and class I major histocompatibility complex in tumor cell lines. *Cancer Res.* 58, 3660–7 (1998).
193. Conaway, R. C. et al. Emerging Roles of Ubiquitin in Transcription Regulation. *Science* (80-. ). 296, 1254–1258 (2002).
194. Jara, J. H., Frank, D. D. & Özdinler, P. H. Could Dysregulation of UPS be a Common Underlying Mechanism for Cancer and Neurodegeneration? Lessons from UCHL1. *Cell Biochem. Biophys.* 67, 45–53 (2013).
195. Almond, J. B. & Cohen, G. M. The proteasome: a novel target for cancer chemotherapy. *Leukemia* 16, 433–443 (2002).
196. Manasanch, E. E. & Orlowski, R. Z. Proteasome inhibitors in cancer therapy. *Nat. Rev. Clin. Oncol.* 14, 417–433 (2017).